

Northumbria Research Link

Citation: Shi, Yuan (2013) Investigation of a Novel Air Source Heat Pump Test Platform. Doctoral thesis, Northumbria University.

This version was downloaded from Northumbria Research Link:
<https://nrl.northumbria.ac.uk/id/eprint/11372/>

Northumbria University has developed Northumbria Research Link (NRL) to enable users to access the University's research output. Copyright © and moral rights for items on NRL are retained by the individual author(s) and/or other copyright owners. Single copies of full items can be reproduced, displayed or performed, and given to third parties in any format or medium for personal research or study, educational, or not-for-profit purposes without prior permission or charge, provided the authors, title and full bibliographic details are given, as well as a hyperlink and/or URL to the original metadata page. The content must not be changed in any way. Full items must not be sold commercially in any format or medium without formal permission of the copyright holder. The full policy is available online: <http://nrl.northumbria.ac.uk/policies.html>

Northumbria Research Link

Citation: Shi, Yuan (2013) Investigation of a Novel Air Source Heat Pump Test Platform. Doctoral thesis, Northumbria University.

This version was downloaded from Northumbria Research Link:
<http://nrl.northumbria.ac.uk/id/eprint/11372/>

Northumbria University has developed Northumbria Research Link (NRL) to enable users to access the University's research output. Copyright © and moral rights for items on NRL are retained by the individual author(s) and/or other copyright owners. Single copies of full items can be reproduced, displayed or performed, and given to third parties in any format or medium for personal research or study, educational, or not-for-profit purposes without prior permission or charge, provided the authors, title and full bibliographic details are given, as well as a hyperlink and/or URL to the original metadata page. The content must not be changed in any way. Full items must not be sold commercially in any format or medium without formal permission of the copyright holder. The full policy is available online: <http://nrl.northumbria.ac.uk/policies.html>



School of Computing Engineering and
Information Sciences

MPhil Dissertation

Project Title:

Investigation of a Novel Air Source Heat Pump Test
Platform

Student Name: Yuan Shi (09025185)

Company Supervisor: Alex Savidis

University Supervisor: Dr Neil Beattie

Second University Supervisor: Prof. Sean Danaher



Acknowledgement

I would like to thank Northumbria University and Narec for their funding and support to make this project and study possible.

Declaration

I declare that the work contained in this thesis has not been submitted for any other award and that it is all my own work. I also confirm that this work fully acknowledges opinions, ideas and contributions from the work of others. The work was done in collaboration with Narec.

Any ethical clearance for the research presented in this thesis has been approved. Approval has been sought and granted by the School Ethics Committee.

Name: Yuan Shi

Signature:

Date: 13/11/2012

Contents

Abstract	1
1. Introduction and Context	
1.1 Types of Heat Pumps	2
1.2 Motivations for this project and Objectives	7
2. Literature Review	
2.1 Chapter Introduction	10
2.2 The case for Heat Pumps	11
2.3 Air Source Heat Pump testing standards	12
2.4 Renewable Energy Targets for Heating and Heat Pumps	16
2.5 Renewable Heat Incentive	16
2.6 UK Heat Demand and Domestic Hot Water usage	19
2.7 The Energy Saving Trust Field Trial and user behaviour in the UK	23
2.8 Field trials in Germany, Sweden and Japan	24
2.9 More on Test Methods	29
2.10 Chapter Conclusion	31
3. Theory	
3.1 Chapter Introduction	34
3.2 SCOP	34
3.3 Seasonal Performance Factor	34
3.4 Carnot Efficiency	35
3.5 Basic and Generalised Heat Pump Operation	37
3.6 Radiator Sizing in the UK	37
3.7 The CO₂ Transcritical Cycle	39
3.8 Fixed Speed vs Variable Speed Heat Pumps	41

4. Test Platform	43
4.1 System Components	43
4.2 Sensors	44
4.3 Data Acquisition and Control	46
4.4 Heating Circuit 1	47
4.5 Radiator Model	48
4.6 Simulink Model	49
4.7 Test method and procedures	53
5. Initial Experimental Results	
5.1 Chapter Introduction	54
5.2 Heating Circuit 1 control	55
5.3 Cooling Tank dynamics	61
6. Heating Circuit 2 and Control	65
7. Results 2	
7.1 Chapter Introduction	68
7.2 Daily and Night-time operating COPs	69
7.3 Heat pump Buffer Tank heat up test	71
8. Discussion and Analysis	73
9. Conclusions and Recommendations for Future Work	76
References	79

List of Tables

Table 1. Projections of Carbon Intensity of Electricity, UK, 2020 – 2050 [4].	12
Table 2. EN14511 test conditions for air to water heat pump space heating.	13
Table 3. System boundaries for different heat pump test standards [11].	15
Table 4. Renewable Heat Premium Payment amounts [12].	19
Table 5. Degree Days for 3 locations in the UK.	20
Table 6. An example of the table lookup control.	58

List of Figures

Fig. 1. Illustration of how a heat pump works and its main components.	2
Fig. 2. Air to Air one piece packaged system [1].	3
Fig. 3. Air to Air one piece packaged system on roof [1].	3
Fig. 4. Air to Air split system [1].	4
Fig. 5. Water to Water Heat Pump system [1].	4
Fig. 6 Water to Air Heat Pump [1].	5
Fig. 7. Air to Water Heat Pump system [1].	6
Fig. 8. Ground Source Heat Pump system [1].	6
Fig. 9. An example of Inlet and Outlet of an Air to Water heat pump.	12
Fig. 10. Average monthly heat demands for defined cluster scenarios [13].	19
Fig. 11. Annual Degree Days for 3 locations in the UK.	20
Fig. 12. Hot water usage volumes for each of the destinations for a sample dwelling over a 24hrs period [14].	21
Fig. 13. Proportion of heat energy used amongst the hot water usage destinations [14].	22
Fig. 14. Mean hot water usage volumes for Regular and Combi boilers at different destinations [14].	22
Fig. 15. Monthly SPF and annual SPF obtained for the air source heat pump [18].	25
Fig. 16. Monthly and annual SPF for the ground source heat pump [18].	27
Fig. 17. Monthly system efficiencies of the field trial unit and modelled efficiencies [20].	28
Fig. 18. COP and System COP (SCOP) for the Hokkaido University field trial [21].	28
Fig. 19. Heating output and various operating temperatures for the first GSHP [21].	29
Fig. 20. Carnot model for a heat pump.	35
Fig. 21. COP variation with heat sink and outdoor temperature [28].	36
Fig. 22. Vapour Compression Cycle for a heat pump.	37
Fig. 23. Radiator flow temperatures and ambient room temperature.	38
Fig. 24. Rating performance of heating system using the Oversize Factor [30].	39
Fig. 25. Phase Diagram for CO ₂ [31].	40
Fig. 26. Transcritical Heat Pump with respect to pressure-enthalpy diagram [31].	40

Fig. 27. Test platform setup as shown on the Labview user interface.	45
Fig. 28. Heating Circuit 1.	47
Fig. 29. Diagram of radiator model.	48
Fig. 30. Interaction between model, weather station and heat pump [38].	50
Fig. 31. Simulink thermal model [38].	51
Fig. 32. Incorporating the radiator model with Simulink.	52
Fig. 33. Showing 2 periods of controlling heating against demand.	55
Fig. 34. Control resonances for 2 one hour periods.	56
Fig. 35. An example of using the 3-band control.	57
Fig. 36. (a) and (c) shows how far the turbulence travel in pipe diameters for injection amplitudes of 0.1 and 0.01 respectively. P is the probability of a particular travel length happening. The coloured lines are for different Reynolds numbers. (b) and (d) shows the half life of the turbulences for different Reynolds numbers for the two injection amplitudes [39].	59
Fig. 37. (a) to (f) shows the onset of turbulence when a small amount of fluid was injected into the laminar flow. (g) to (l) shows that a 'puff' was created when a larger amount of liquid was injected [39].	60
Fig. 38. Cooling Tank Vertical Temperatures for 3kW heating.	61
Fig. 39. Cooling Tank Vertical Temperatures for 7-8kW heating.	61
Fig. 40. Illustrating instances of the temperature and width of the plumes and the warming up of surrounding liquid. The patches show the resulting secondary plumes formed.	63
Fig. 41. The photographs from [15] show the collision of hot and cold plumes. Time frame is: (a) 0s, (b) 5s, (c) 10s, (d) 15s, (e) 17s, (f) 19s, (g) 22s, (h) 25s [41].	64
Fig. 42. Heating Circuit 2.	65
Fig. 43. Flow diagram for the combined temperature and flow control scheme.	67
Fig. 44. (a) is daily 24 hour COP against heating for month in April. (b) is corresponding night time COPs from 7pm to 7am.	70
Fig. 45. Logged outdoor temperatures for sensor at different locations in the vicinity of the heat pump unit.	71
Fig. 46. COP against Tank Temperature.	72
Fig. 47. COP against compressor frequency at different water temperatures [42].	73
Fig. 48. Effect of gas cooler pressure on refrigerating capacity and COP [31].	74

List of Abbreviations

COP	Coefficient of Performance
SCOP	System Coefficient of Performance
EST	Energy Saving Trust
SPF	Seasonal Performance Factor
TTD	Time Temperature Difference
PID	Proportional Integral Derivative
EER	Energy Efficiency Ratio
ASHP	Air Source Heat Pump
GSHP	Ground Source Heat Pump
DHW	Domestic Hot Water
RHI	Renewable Heat Incentive
MCS	Microgeneration Certification Scheme

Abstract

A flexible air source heat pump testing platform is being developed at the National Renewable Energy Centre that will have the advantages of both a field trial and a laboratory test. It may be considered as a “black box” testing method that will be able to produce performance data that reflects the actual operating performance of the heat pump. At the same time it will also enable more experimental investigations to be carried out to understand the parameters that influence a heat pump’s coefficient of performance.

The testing platform is controlled by automated instruments programmed in NI Labview software that enables customised tests to be carried out. The heat pump is installed normally as it would in operating condition. The heat pump under investigation in this study is a transcritical CO₂ inverter controlled heat pump. It is installed with a 220 litre buffer tank that provides combined hot water and space heating and is supported by an optional solar pre-heat system.

The characteristics of two alternative heating circuits for controlling heating in the test platform are compared based on experimental and theoretical findings. The first heating circuit is based on standard radiator installation and it is entirely controlled by flow rate. The second heating circuit combines both water temperature and flow rate control. The first heating circuit required a complex multi-band variable step control strategy, partly to overcome resonances and slow valve traverse. The second heating circuit required a much simpler control algorithm and achieved more responsive heating control.

Dynamic behaviour of the cooling tank in the test platform for heat transfer from the first heating circuit was investigated using vertical tank temperatures and theory. At low level heating of 3kW, long duration (12 minutes) temperature fluctuations were observed due to on/off cycling of chiller. Short duration (1-2 minutes) temperature fluctuations were also observed and attributed to natural convection. At high levels of heating of 7-8kW, only short duration (1-3 minutes) temperature fluctuations with larger amplitudes were seen with fluctuations due to chiller cycling masked by these fluctuations. According to theory and published experimental work on turbulence, the conclusion can be drawn that the temperature fluctuations are primarily due to laminar convection in the cooling tank.

Daily and night-time COPs were obtained using the second heating circuit continuously for a month in the winter season. Daily COPs showed an unexpected positive linear correlation with average daily heating. The COP varied from 1.8 to 2.6 for heating between 3 and 7kW. Based on the theory of CO₂ as a heat pump refrigerant and published experimental work, it is suggested that the rise in COP with higher heat output can be explained by the rise in refrigerant pressure as the heat pump tries to output more heat.

1. Introduction and Context

1.1 Types of Heat Pumps

Heat pump systems transfer heat from a source (air, ground, water) to a sink (domestic hot water, radiators) using a working refrigerant as the heat transfer medium. It works on the principle of heat absorption via evaporation, and heat rejection via condensation. Hence the terminology of “evaporator” for the part of the heat pump that absorbs heat from the source, and “condenser” for the part of the heat pump that rejects heat to the sink. Fig. 1 illustrates this. T_{amb} is the refrigerant temperature at the evaporator in ambient, T_{in} is the radiator in flow water temperature in to the condenser and T_{out} is the radiator out flow water temperature out of the condenser. W is the work required by the compressor. The Coefficient of Performance or COP is the performance ratio of total heat out divided by the work done by the compressor to deliver this heat. Please refer to sections 3.3, 3.4 and 3.6 for more detailed explanation of the thermodynamics and operation of a heat pump.

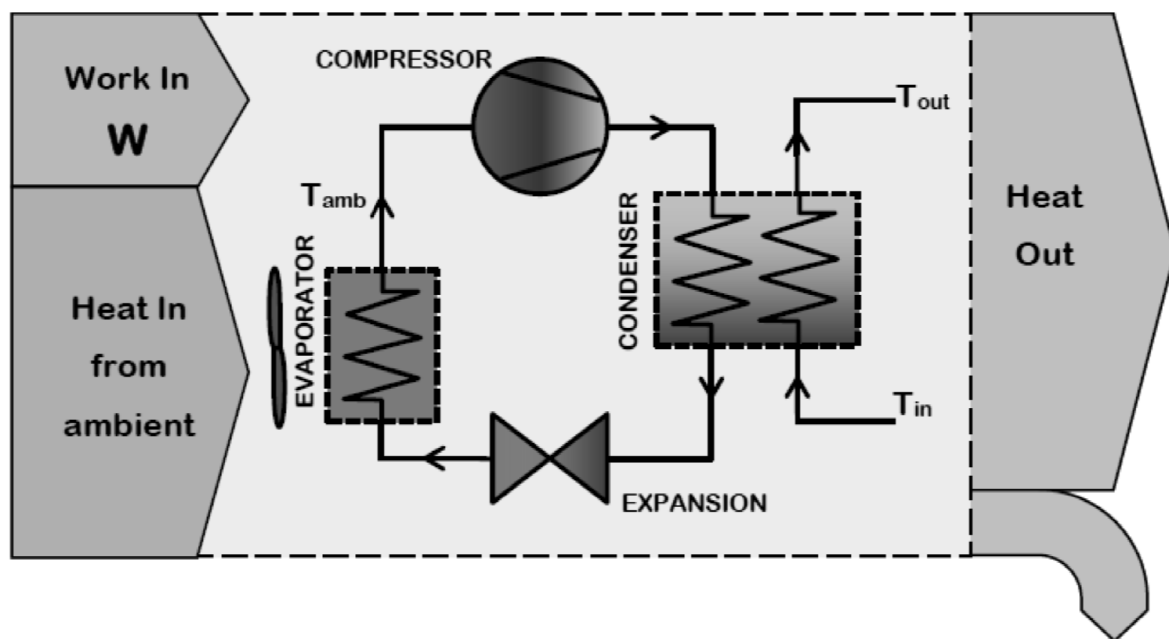


Fig. 1. Illustration of how a heat pump works and its main components.

Heat pump systems can be divided into basic types based on the heat medium at the source and the destination or sink. Heat is absorbed at the source and rejected at the sink via their respective heat exchangers. At either of the heat exchangers the heat transfer medium can be either liquid (water and often a glycol mixture) or air. Sometimes it is a combination of the two. In describing the types of heat pumps, generally the heat medium of the heat source is provided first, followed by that of the heat sink.

The main types in common use are:

- Air to Air
- Water to Water
- Water to Air
- Air to Water
- Ground to Water
- Ground to Air

The following gives an account of the main types of heat pumps as in [1].

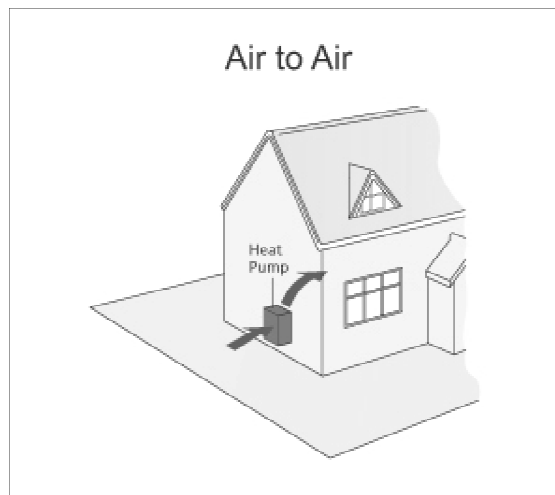


Fig. 2. Air to Air one piece packaged system [1].

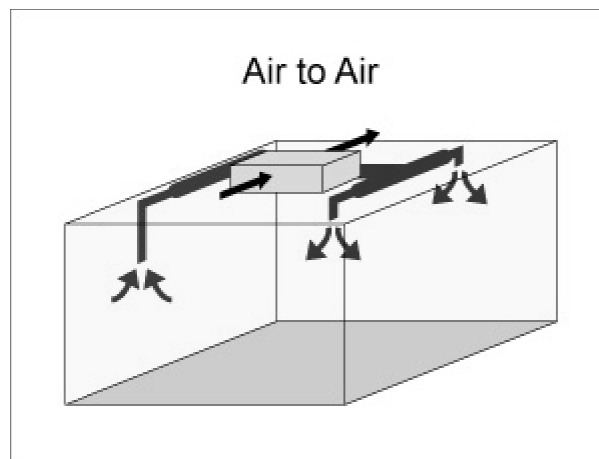


Fig. 3. Air to Air one piece packaged system on roof [1].

Air to Air

Air to Air Heat Pumps absorb heat energy contained in outside air and its vapour and reject this into indoor air by fan assisted units.

They are the largest single group of heat pump systems marketed in the UK today and can range in capacity from 3kW to over 100kW and from one piece packaged units to multiple split units (Fig. 2 and 3). Many of these are installed in offices and retail outlets, and can

heat and cool the building simultaneously by removing unwanted heat from one part of the premises where cooling is required and delivering it to another part as useful warmth.

Split units have one outdoor unit (normally the heat pump unit) and one or more indoor units. The indoor and outdoor units are connected by a pipe and electrical connections. Each indoor unit is capable of controlling its own space or zone (Fig. 4).

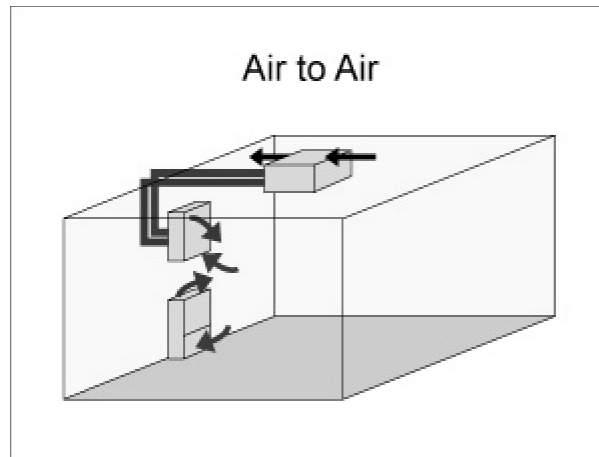


Fig. 4. Air to Air split system [1].

Water to Water

Water to Water systems operate in the same way, as Air to Air systems except that the heat source is water, generally ground water, river or pond water or even waste heat from factory processes. The heat is then delivered to either radiators or fan-coil units within the indoor space. In the case of river or lake water the source liquid is seldom circulated, due to fouling of pipes, a continuous pipe heat exchanger is submerged at the source to absorb the

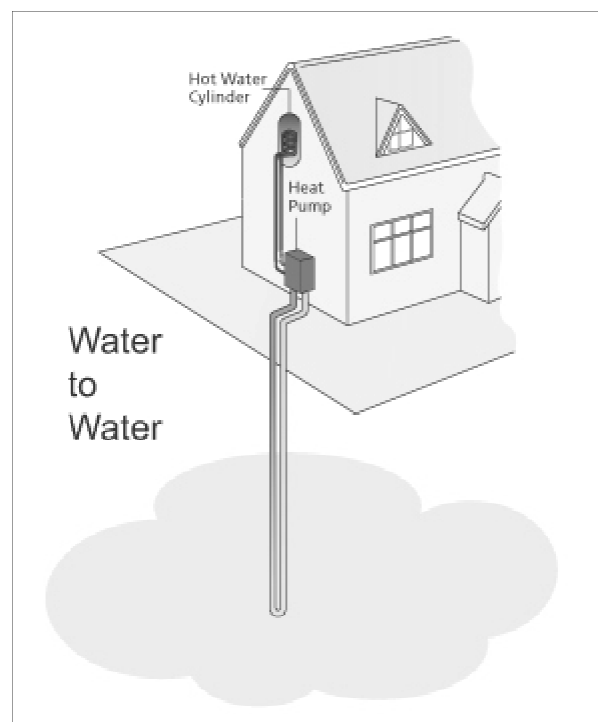


Fig. 5. Water to Water Heat Pump system [1].

heat from the water (Fig. 5). Approvals are needed for this type of installation and restrictions exist on the type of anti-freeze solution used. Water to Water systems can be configured as heating only or they are available as Heating/Cooling reversible systems.

Water to Air

The heat source is as described in the Water to Water Heat Pump, the heat in this case is rejected to the indoor room air rather than to water (Fig. 6). This system is available in a similar range of sizes as air to air heat pumps in the UK.

Air to Water (Air Source Heat Pump - ASHP)

Heat is absorbed from outside air and transferred to a water based indoor system of radiators or fan coils (Fig. 7).

Ground Source Heat Pump (GSHP)

Heat energy is extracted from the ground using closed pipe loops buried horizontally in trenches or in vertical boreholes that are connected back to the GSHP (Fig. 8). The fluid circulating in the closed loop will normally be a water/propylene glycol or acceptable equivalent antifreeze mixture, however, some direct acting GSHPs will use refrigerant in the closed loops. Direct acting heat pumps are ones that have the refrigerant in direct contact with the heat source and heat sink such as for most air source heat pumps with a non-toxic refrigerant. Open loops may also be used to collect water from an aquifer and discharge via

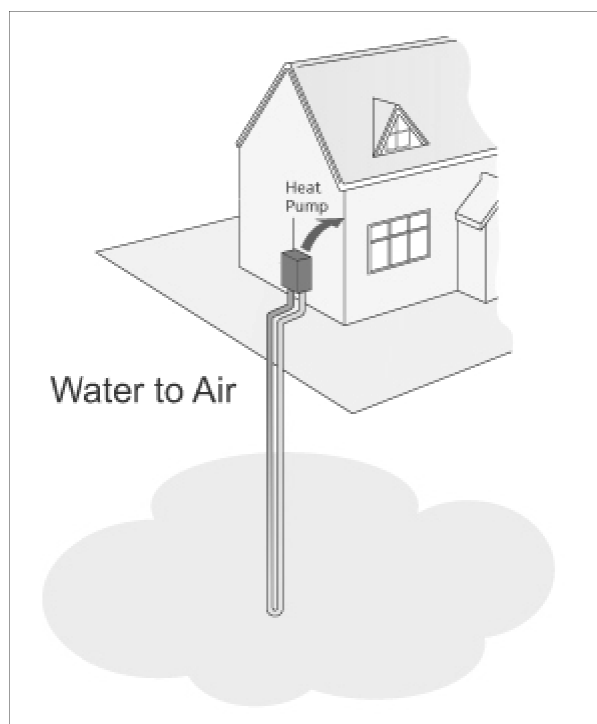


Fig. 6 Water to Air Heat Pump [1].

a separate aquifer downstream of the water table flow, however, permits are normally required from the Environment Agency. Heat is introduced to the dwelling and distributed either to a water heating system (ground to water heat pumps) or to an air distribution system (ground to air heat pumps).

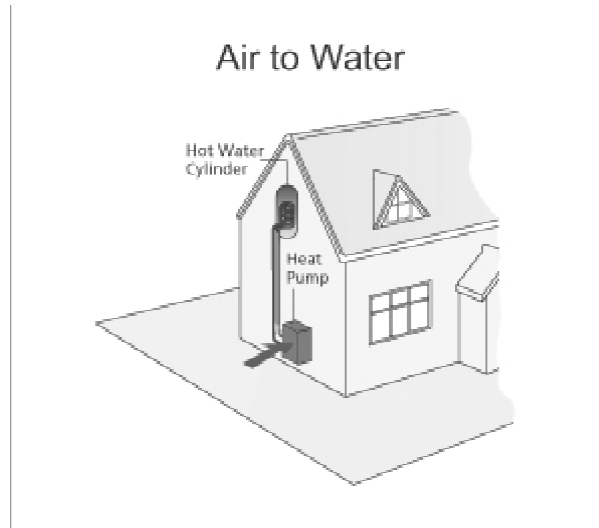


Fig. 7. Air to Water Heat Pump system [1].

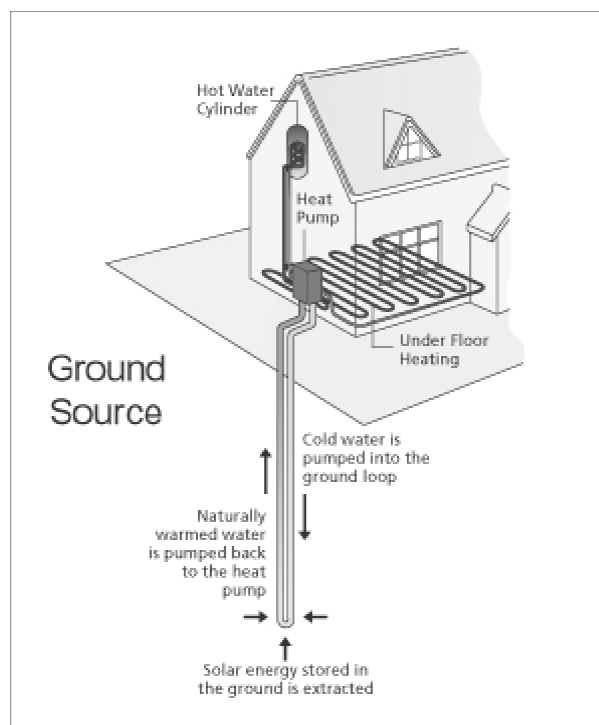


Fig. 8. Ground Source Heat Pump system [1].

Simultaneous Heating and Cooling

Some buildings require cooling in one part and heating in another. This type of system will have considerable energy efficiency because heat that would otherwise be wasted can be re-used. This type of system is also called Exhaust Air Heat Pump system.

There are two ways of achieving this:

1. Variable Refrigerant Flow (VRF)

This is a direct expansion refrigeration system that can divert hot gas from the condenser to parts of a building that require heat while cooling other parts at the same time. The installations are fully automatic and employ speed controlled compressors to match the system's output to the load demand of the building. With VRF systems, considerable savings on electrical power are available, in addition to favourable load demand flexibility.

2. Reversible Water to Air

This is a warm water loop arrangement. The building is equipped with a ring main water system with forward and return flow to each room.

Each room has a small self contained reversible water to air heat pump. If the room requires heat, the water to air heat pump operates in reverse and takes heat from the ring main water system and transfers this into the room. If cooling is required, the water to air heat pump takes heat from the air and stores it back into the ring main water system.

In the case where extra heating or cooling is required that exceeds the ring main water system buffer capacity, a cooling tower and a gas boiler is in place to remove and inject heat into the ring main water system.

1.2 Motivations for this project and Objectives

Heat pumps are gaining more attention in the renewable energy sector, and their take up will depend on their Coefficient of Performance (COP) – this is the total useful heat output by the heat pump divide by its electrical consumption. Their performance will depend on how they are installed and operated. Policies to stimulate the take up of heat pumps require the heat pump and installers to be certified. This calls for greater understanding of heat pump performances in the UK and cost effective methods for testing them. Although air source heat pumps shows a lower average performance than ground source heat pumps in the EST trial (more details in section 2.6), they are capable of reaching a COP of exceeding 2.9 in the UK, Sweden and Japan, the minimum requirement of the Renewable Heating Incentive. Also, the upfront and maintenance costs are lower for air source heat pumps than other types of heat pumps, with minimum construction efforts.

There are much performance data available for air source heat pumps, but these are obtained under different conditions and test methods, and so their values vary greatly. Many testing standards have different system boundaries and are based on EN14511, which has a limited number of testing conditions in steady state. This means that COP obtained will not fully reflect the operating performance of the heat pump. Currently the only way to measure the real life performance of heat pumps is through field trials. These are expensive and time consuming to set up and run. This calls for the development of a hybrid test

platform that is capable of reproducing field performances as well as enabling more structured experimental investigations to better understand the operating performances. Manufacturers' quoted COPs are typically tested in the laboratory under a limited number of outdoor, inlet/outlet conditions, following EN14511. Manufacturers also carry out field tests, but these installations are fine tuned to favour performance of the heat pump. They will give an idea of the highest possible performance in an installation, but will not reflect all other installations. It is unclear why the COPs obtained this way differ from COPs obtained from other field tests. This forms another motivation for developing the test platform.

Further, 10 years ago expectations for heat pump COP has been 3 as the norm and recently 4, this also applies to air source heat pumps [2]. However, results from the EST field trial clearly show that many heat pumps falls below this expectation. This could be due to a variety of installation and site specific factors including user behaviours. Further understanding can help identify and improve on these factors, which would improve the COP of heat pumps in operating conditions, as studies in Germany and Switzerland published Seasonal Performance Factors (SPFs) clustering around the 2.5 – 2.9 mark with the lowest at 2.2. The SPF is the COP measured and calculated for a period, usually for a month, a season and a year, in this project SPF could be for period as short as a week. Even though system COPs obtained by EST could potentially be higher as hot water system heat losses were included, whereas SPFs do not, the SPF figures are still considered higher than EST figures. These countries have higher performance figures because they have more experience and knowledge of heat pump technologies. Therefore there is room for further investigations to be carried out in the UK on heat pump operating performances, which can lead to improved operating COPs.

A CO₂ variable speed transcritical heat pump is not covered by EN14511 and was not tested in the EST field trial. A transcritical heat pump differs to other heat pumps in that the refrigerant operates at pressures and temperatures above the critical point, more details of this is given in section 3.6. Given the increasing production and take up of CO₂ refrigerant heat pumps in Japan, there is motivation to investigate such a heat pump using the new testing platform.

Based on these motivations and the literature review in the next section, the following project objectives were defined:

Objectives:

- Investigate the possible uses of the testing platform by putting it in context with other test methods.
- Design appropriate control strategies to meet heating demands.
- Investigate impact of heating demand on heat pump performance.
- Investigate the benefit of including a radiator model.

- Obtain and analyze operating System Coefficient of Performance (SCOP) of the CO₂ transcritical air source heat pump for a range of heating levels.
- Characterise the heat pump under test.

2. Literature Review

2.1 Chapter Introduction

This chapter presents literature surveys that help in defining the purpose of the test platform in context, and aid in the design of the control algorithms for the test platform. This begins with a comparison of the carbon savings between heat pumps and gas boilers in the UK based on the National Carbon Intensity. Next is a comparison of the current testing standards for air source heat pumps, this helps to identify improvements offered by the test platform. Then, the role of heat pump in meeting the renewable energy target in the UK is given in context. This leads to a description of the Renewable Heat Incentive, a major scheme introduced to meet the renewable energy target, which will include heat pumps and potentially air source heat pumps in the domestic market. The heat pumps will also need to be certified under the Microrenewable Certification Scheme, making the testing of air source heat pumps more prevalent.

In order to help the design of control algorithms that will preserve the operating performance of the heat pump under test, the rest of the chapter contains typical heat requirements in the UK, user experiences and details on field trials. The Energy Saving Trust field trial in the UK identified factors that affect the operating performance of heat pumps in installations and collected questionnaires on user experiences. Other field trials in Germany, Sweden and Japan are also presented to bring the UK field trial into context to give more information on field testing. Lastly, laboratory based and other testing methods are described.

2.2 The case for Heat Pumps

To make a comparison of whether heat pumps have higher energy saving potential than other forms of heating, the amount of carbon savings can be used. This can be measured by the amount of CO₂ produced per unit of energy consumption. Heating accounts for 46% of carbon emissions in the UK [3]. Domestic heat pumps are clearly more efficient in electricity use than direct electric heating, due to the fact that heat pumps produce more heating per unit of electrical energy than electric heaters and their COPs are greater than 1, whereas electric heaters have COPs of less than 1. However this only accounts for a minority in the UK, where a comparison should be made with gas and oil. To make the comparison, the National Carbon Intensity is used [4]. This is the amount of CO₂ emission for each kWh of electricity generated. This varies widely in the EU, from a low of 0.05kgCO₂/kWh in Sweden up to 0.86kgCO₂/kWh in Greece, with the EU-27 2006 five year rolling average being 0.39kgCO₂/kWh [5]. In the UK heat pumps have a higher hurdle to jump than in many other countries to make carbon savings compared with main stream alternatives [4]. This is because UK has higher than EU average carbon emissions from its electricity of 0.55 kgCO₂/kWh [6][7] (grid five year rolling average, 2008). The competitor heating fuel used by more than 80% of the population is natural gas – the least carbon intensive fossil fuel. Calculations show that a heat pump would have to achieve a system efficiency of 2.6 in order to result in reduced carbon emissions, when compared with that of a new efficient gas boiler [4]. These calculations are based on delivering 16,000 kWh of heating and hot water energy per year (similar to recommended ‘medium’ annual gas usage figure, [8]), using current carbon intensity figures for gas and electricity [5] and assuming a gas boiler with seasonal efficiency of 88%. Based on this a heat pump will need to have a system efficiency of 3 to save 13% more carbon emissions compared with a gas boiler. Using system efficiency figures from the EST trial the average UK ground source heat pump emits 14% more carbon emissions than an efficient gas boiler, and the average UK air source heat pump 38% more [4]. In spite of this most heat pumps will replace oil, LPG and electric heating systems, which have higher carbon emissions than gas boilers. Those who are not connected to the mains gas grid will certainly benefit from heat pumps, this group currently account for 7.3% of households in England, 13.6% in Scotland and 15% in Wales [9]. The number of new built properties in the UK that are not connected to the gas grid make up around 10% of new homes [4]. This analysis does not include reversible heat pumps, and almost half of the heat pumps sold in Europe are reversible.

Although currently heat pumps in the UK domestic market are less carbon efficient than gas boilers, the future may be very different. In order for the UK to meet its low carbon targets, there is universal agreement that reducing carbon emissions per kWh of electricity is crucial. The target for the UK under the EU directive is to generate 15% of its energy from renewable by 2020. The UK has ambition to increase from 1.5% to 12% of all heat generated from renewables by 2020 [3]. The renewable energy target can be achieved by increasing the percentage of renewables (such as wind and solar), nuclear energy and introducing

carbon capture fossil fuel plants. Table 1 shows that the expected future carbon intensity can be reduced by a factor of 10 within the next 20 years. If these figures are achieved in the UK, then carbon emissions from average efficiency heat pumps should be lower than those from gas-based systems before 2020 and very much lower by 2030 and beyond. If such low carbon electricity can be supplied in sufficient quantities, then heat pumps would be an obvious choice for space and hot water heating. This has not yet taken into account that future efficiency of heat pumps may increase also. Even with the advantages, heat pumps will need to have the market share and an industry in place for installation. They also need to be cost competitive with alternatives, and account for any changes to housing infrastructure and heat distribution systems that may be necessary [4].

Table 1. Projections of Carbon Intensity of Electricity, UK, 2020 – 2050 [4].

Date	Carbon intensity kgCO ₂ /kWh	Source
2008 (five year rolling average)	0.55	[5]
2020	0.30	[10], to be achieved if current government ambitions on renewable energy and other low carbon sources are met.
2030	0.052	[10], medium investment strategy (0.04 – 0.13 kgCO ₂ /kWh with high to low investment range).
2030 – 2050	Falls to around 0.01	Markal modelling on behalf of CCC, [10].

2.3 Air Source Heat Pump testing standards

Heat pump performance measurement is standardised in BS EN14511:2007. This supersedes BS EN255-2:1997 for space heating applications but BS EN255-3:1997 is still valid for heating sanitary hot water. For COP, only electricity of the heat pump compressor is included, the heat pump unit auxiliary and all external electrical consumptions such as pumps, auxiliary heaters are excluded. The standard has been adapted by the European Heat Pump Association for testing to achieve their quality label.

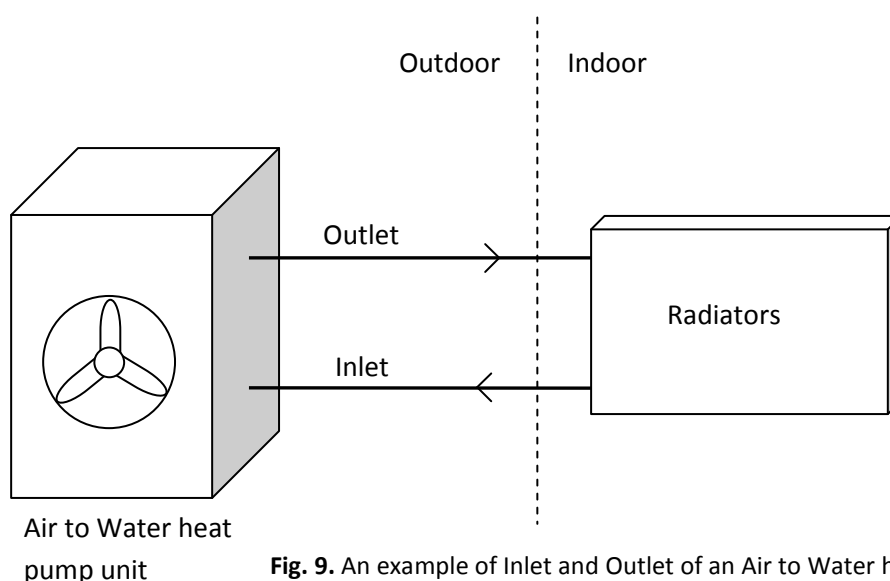


Fig. 9. An example of Inlet and Outlet of an Air to Water heat pump.

Testing under EN14511 is conducted at defined operating conditions, including outside air and outlet temperatures for air source heat pumps. Fig. 9 shows the inlet and outlet of an air to water heat pump. Table 2 lists the standard and additional test conditions for testing air source heat pumps in heating mode.

Table 2. EN14511 test conditions for air to water heat pump space heating.

Air temperature	Inlet temperature	Outlet temperature	Standard Conditions
7°C	30 °C	35°C	
7°C	40 °C	45°C	
-15°C	Adjusted	35°C	
-7°C	Adjusted	35°C	
2°C	Adjusted	35°C	
-15°C	Adjusted	45°C	
-7°C	Adjusted	45°C	
2°C	Adjusted	45°C	
-7°C	Adjusted	55°C	
7°C	Adjusted	55°C	

For additional test conditions the same flow rate is used as the standard conditions, but the inlet temperature to the heat pump for each air temperature will be adjusted according to the set outlet temperature, as shown in Table 2. For testing an exhaust air to water heat pump, the air temperature is 20°C, the inlet temperature is 30 °C and outlet temperature 35 °C.

The test has initial precondition and equilibrium periods before the data collection period to determine the heat pump performance. If the heat pump operates within tolerances and without defrost cycle, it is defined as a steady state operation and the data collection period lasts 35 minutes. The defrost cycle is necessary for an air source heat pump when the outside air approaches to 0°C, the outdoor unit will begin to freeze, reducing its efficiency and could cause damage to the unit, the heat pump will then run in a reverse mode to heat and melt the ice. If the heat pump performance varies outside tolerances or it undergoes defrost cycles, it is defined as a transient operation, in this case the test is extended to 3 hours and the average performance is taken into account.

EN14511 does not include the testing of CO₂ transcritical heat pumps, which gives motivation for testing such a heat pump in this project.

The testing procedure defined by EN255-3:1997 includes measurement of COP but the condition and method are different to those in EN14511:2007. For example, the hot water temperature is generally higher (at least 40) and the water inlet temperature is lower so the heat exchanger potentially operates with greater temperature range.

Given the variation of heat pump performance with ambient conditions, there is a need of a testing standard for seasonal performance measurements.

IEA Heat Pump Programme Annex 28 was set up to establish a methodology to give a consistent performance measurement for heat pumps operating under conditions that vary during the year and with optional additional elements such as auxiliary electric heaters. Their final report (IEA Heat Pump Programme Annex 28, 2006) and associated publications outline their proposed methodology which has been since taken forward to form the basis of BS EN15316-4-2:2008.

The test standard sets out a standard methodology for calculating the Seasonal Performance Factor (SPF) of heat pumps. The SPF is similar to COP but is an annual average figure and includes more system components. The system boundary is extended compared to EN14511 to include ground heat collector circulation pump or fan, back up heater, buffer tank circulation pump but does not include heat emitter circulation pumps.

There is provision within the standard for a simplified method for calculating SPF from COP data if national, tabulated adjustment factors are available, but in the general case, a more involved method involving temperature “bins” is required.

Hourly climate data, representative of the heat pump’s location is used to calculate the number of hours within temperature “bins” of ideally 1 Kelvin. That is the number of hours in the year when the temperature is between 1°C and 2°C, the number of hours between 2°C and 3°C, between 3°C and 4°C and so on. Space heating demand is assumed to follow a Time Temperature Difference (TTD) model. The TTD model assumes the rate of heat loss from a building or heating requirement is proportional to the difference between outdoor air temperature and a set point of 15.5°C by convention. Domestic Hot Water demand is taken as a constant and added to the heating demand. A COP of the heat pump is assigned to each “bin” based on the midpoint temperature of the bin and the operating temperature of the heat emitter system at that outdoor temperature. The COPs are obtained under EN14511 test conditions. If the heat demand within the “bin” is higher than the rated capacity of the heat pump in those conditions, a backup electric heater is assumed to be used, reducing the effective system COP. From the heat demand in each bin, the number of hours within each bin and the representative COP for that bin, electrical power consumption can be calculated and summed up to give a total for the year. This is given in equation (1).

$$S = \frac{\sum Q}{\sum W} = \frac{\sum_{T=-10}^{T_b} [k(T_b - T) \cdot t(T)]}{\sum_{T=-10}^{T_b} [k(T_b - T) \cdot \frac{t(T)}{C(T)}} \quad (1)$$

Where S is the Seasonal Performance Factor, Q is the total heat output, W is the total electrical consumption, T is the average temperature for each bin, T_b is the set point temperature for the building. k is the heat loss coefficient for the building, $t(T)$ is the total time in the year when the temperature is within the bin and $C(T)$ is the extrapolated COP at temperature T based on the outlet temperature and heat emitter temperature.

EN15316 is the closest to the test boundary of the test platform in this project, and the closest to that of a field test, as it includes most system components. Other heat pump testing standards exist and are compared in Table 3 [11].

Table 3. System boundaries for different heat pump test standards [11].

Component	EN14511	EN15316 4-2	VDI4650-1	prEN14825	Lot 1	Lot10
Compressor	✓	✓	✓	✓	✓	✓
Brine Fan/Pump	Head Losses	✓	✓	Head Losses	Head Losses	Head Losses
Back-Up Heaters	✗	✓	✓	✓	✓	✓
Buffer Tank Pump	✗	✓	✗	✗	✓	✗
SH DHW Buffer Fan/Pump	Head Losses	✓	Head Losses	Head Losses	Head Losses	Head Losses

Lot 1 and Lot 10 are under the European Directive 2009/125/EC. Head Losses are losses in flow energy due to friction, turbulence and bends in pipes, these can be estimated from tables instead of direct measurement.

prEN14825: The calculation methodology and measurement procedure of this standard are based on the standard EN14511. prEN14825 takes into account thermostat off mode, standby modes and crankcase heater. Unlike EN15316, different running conditions are set according to climate (cold, average, warm) and space heating emitters, these are tested at 6 test conditions.

European Directive 2009/125/EC Lot 1: Calculation of energy consumption is quite similar to prEN14825, except heat demand, which includes more items in addition to heat load, like buffer heat losses and distribution heat losses as mentioned in EN15316.

Lot 10: Similar to EN14825.

VDI 4650-1: Does not measure energy input of auxiliary devices at the heat sink side.

It is clear from the review of the testing standards for heat pumps that there is a need for investigation and development of a laboratory based test platform that attempts to measure the operating performance of the whole heat pump system, similar to that of a field test. This test platform should not be limited by steady state operation and fixed operating conditions as in the above test standards. Additionally, the heat pump's dynamic effects as a market ready product will be reflected in the operating COPs obtained. Yet the test platform under development carry benefit over a field test as more structured

experiments can be carried out by using different heat demands, DHW profiles and heating patterns.

2.4 Renewable Energy Targets for Heating and Heat Pumps

The EU Directive on renewable energy 2009/28/CE sets ambitious targets for all member states, such that the EU will reach 20% share of energy from renewable sources by 2020. The Directive includes both Air Source heat pumps and Ground Source heat pumps within its definition of renewable sources of energy on the condition that they meet minimum performance standards, defined as the final energy output significantly exceeds the primary energy input to drive the heat pumps. Annex VII of the directive determines the accounting method for energy from heat pumps. It stipulates that only heat pumps whose energy gain is at least 15% over the input primary energy shall be taken into account (calculated as the mean on the European scale), as based on measurement of useful heat delivered and the seasonal performance factor. Because the measurement procedures for useful heat and the seasonal performance factor have not been finalised (they are due to be produced no later than 1 January 2013) it is not clear precisely what COP this will equate to. Current estimates are that a COP of above 2.875 will be required [4].

Under the renewable energy Directive, the UK has a legally binding target of generating 15% of its energy from renewable by 2020. Heating accounts for 47% of total UK final energy consumption and 77% of energy use across all non-transport sectors. In terms of carbon emissions, heating accounts for 46%. The most recent data show that approximately 69% of heat is produced from gas. Oil and electricity account for 10% and 14% respectively, solid fuel 3% and renewables only 1.5% [3]. Clearly heating has a large share in meeting the renewable target. The UK government has ambition to move from 1.5% to 12% of all heat generated from a renewable source by 2020. The strategy set to achieve this is to introduce the Renewable Heat Incentive scheme, which offer incentives on a vastly increased scale when compared to the previous Low Carbon Building Programme. The original intention was that this would represent over £850m of investment, however this has been reduced by 20% following a government spending review.

2.5 Renewable Heat Incentive

To meet the challenging renewable energy targets, the UK government has introduced the Renewable Heat Incentive (RHI). The scheme focuses on renewable energies only, and not any low carbon non-renewables. The scheme is divided into two phases, phase 1 has been introduced in 2011 and focuses on non-domestic sectors, phase 2 will include domestic sectors and due to be introduced in October 2012. Before the introduction of phase 2 instead of tariffs, Renewable Heat Premium Payments is available to offer one off payments to owners of renewable heat installations. The reason being it is particularly difficult to predict the level of take up and the performance of different heat technologies in the domestic sectors [3].

On-going Obligations

Applicants of RHI will need to full-fill on-going obligations. These are self maintenance requirement and information and inspection requirements. Due to the wide range of technologies it is not practical to specify a particular level and frequency of maintenance and so the equipment is to be maintained in line with any manufacturer's instruction where available. Participants will be required to keep any evidence of maintenance work carried out. To ensure Ofgem is able to monitor compliance with the conditions of RHI, applicants will have to agree up front that they will provide any relevant information as requested by Ofgem and allow an inspection of the installation to ensure the eligibility criteria are met. This may be upfront as part of the accreditation process, on a regular basis, or an ad hoc spot check.

Microgeneration Certification Scheme (MCS)

All biomass, ground and water source heat pumps and solar thermal plants of 45kW capacity or less will need to certified under the Microgeneration Certification Scheme or equivalent schemes, such as Solar Keymark for solar thermal installations. This means that both the technology and the company or person installing it will need to be certified. When applying for RHI the applicant will need to supply MCS or equivalent certification.

This certification system is considered necessary due to the emerging nature of renewable heat market in the UK, to safeguard against poor quality renewable heat technologies and inefficient installations. This will in turn benefit the applicant, the environment and maximise value to the society.

Larger installations of greater than 45kW capacity are believed to be more likely to obtain the necessary expertise to ensure high quality installations and value for money, so they do not need to be certified.

For the above reasons for establishing the MCS, testing the operating performance of heat pumps will become more and more relevant, and forms part of the motivation for this project.

Replacing Existing Renewables

For the replacement of existing renewable heating system RHI will be eligible for support, given that the existing installation is in genuine need of replacement.

Supported Technologies and Fuels

The following technologies and fuels are supported in phase 1 of RHI.

- Biomass Boilers
- Heat Pumps (Ground, Water Source)

- Deep Geothermal
- Solar Thermal
- Heating from Biogas Combustion
- Biomethane Injection to the Grid
- Renewable District or Community Heating
- Renewable Combined Heat and Power

Heat pumps are required to have a COP of at least 2.9 to be eligible for RHI. Other heating technologies not included in phase 1 may be included in Phase 2. Notably air source heat pumps are not included in phase 1 since more work is needed to better understand the costs associated with the technology, and the performance of those heat pumps that have a cooling mode.

Financial Incentive

In phase one that covers the non-domestic sectors, payments for participants in the RHI will be calculated by multiplying the appropriate tariff by the amount of eligible heat. Payments will be made over a 20 year period. The payment frequency is every quarterly period following the submission of the required periodic information.

The tariff varies depending on the type and size of the technology. The tariffs were calculated based on the following cost principles:

- Compensate for the additional cost of renewable technology over fossil fuel heating.
- Provide an incentive to overcome non-financial barriers.
- Provide a return on the additional capital invested.

As an example ground source or water source heat pumps with less than 100kW capacity is eligible to receive 4.3 pence/kWh of tariff, and those with capacity more than 100kW will receive 3 pence/kWh.

Tariffs for the domestic sector may have similarities to this.

Renewable Heat Premium Payment

Before the introduction of the second phase and tariffs for the domestic sector, domestic heat pumps are supported by the temporary Renewable Heat Premium Payment scheme. This makes one-off payments to help participants to buy renewable heating technologies. Table 4 shows the amounts for different heating technologies.

For Solar Thermal products, any householder in England, Scotland, and Wales can apply. For ground to water, air to water, or water to water heat pumps, and for biomass boilers, those who are off the gas grid can apply (in other words those who rely on oil, liquid gas, solid fuel or electricity for their heating). Applicants must also satisfy basic energy efficiency requirement for their home, such as sufficient loft and wall insulation [12].

Table 4. Renewable Heat Premium Payment amounts [12].

All houses	Houses not heated by gas from the grid
£300 – solar thermal – voucher valid for 3 months	£950 – biomass boiler – voucher valid for 6 months
	£850 – air source heat pump – voucher valid for 5 months
	£1250 – ground source or water source heat pump – voucher valid for 6 months

2.6 UK Heat Demand and Domestic Hot Water usage

In a micro-CHP (Combined Heat and Power) test trial by the Carbon Trust around 2007, heat demands for 8 domestic house clusters were gathered [13], and is shown in Fig. 10. Each

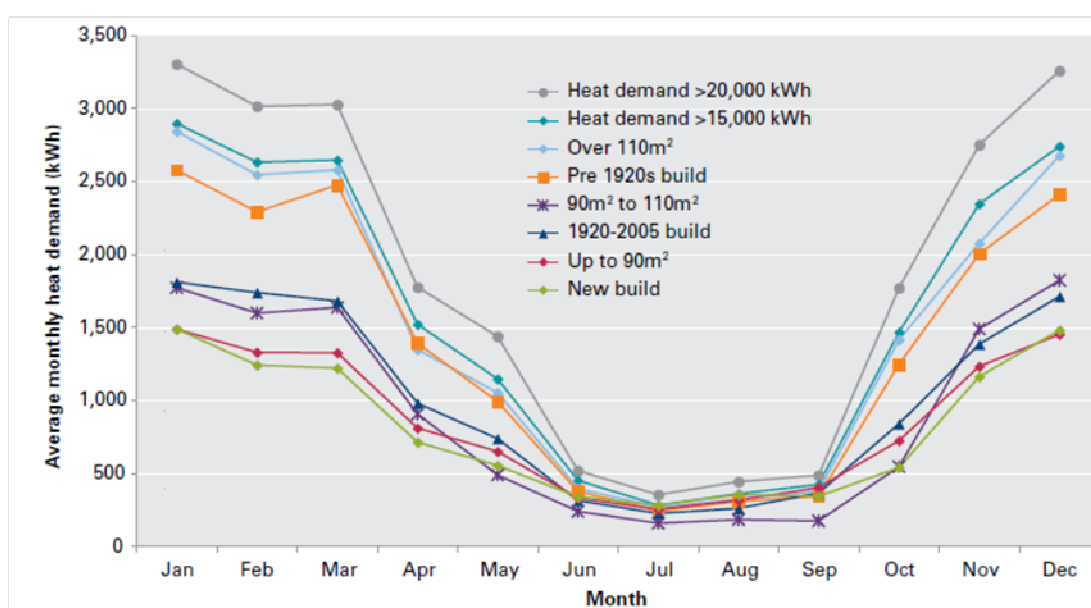


Fig. 10. Average monthly heat demands for defined cluster scenarios [13].

data point is an average for a number of sites belonging to that cluster, the smallest cluster has 15 sites and the largest cluster has 50 sites. As shown, 3 of the clusters relate to the age of the housing stock, another 3 relate to the floor area and the remaining 2 divide the houses between 2 heat demand levels of greater than 15,000 kWh and 20,000 kWh respectively. The heat demand is the sum of heating and domestic hot water usage. The clusters share a similar characteristic over the seasons, all with a significant reduction in demand in summer. Differences are seen over the winter months, the level of heat demand increase with age of housing and the size of the property. Note that the clusters are specific sites for the field trial and do not necessarily represent the wider UK housing stock.

For heat demand by location Table 5 [14] shows the Degree Days for 3 regions in the UK, London, Newcastle and Scotland. Scotland has the highest total yearly heat requirement, then Newcastle, then London with the least annual heat requirement.

Table 5. Degree Days for 3 locations in the UK [14].

	LONDON	NEWCASTLE	SCOTLAND
January	360	374	362
February	292	307	321
March	232	279	304
April	125	198	218
May	76	134	174
June	35	83	110
July	15	42	48
August	13	32	42
September	30	77	88
October	87	143	169
November	190	236	262
December	372	393	423
TOTAL	1827	2298	2521

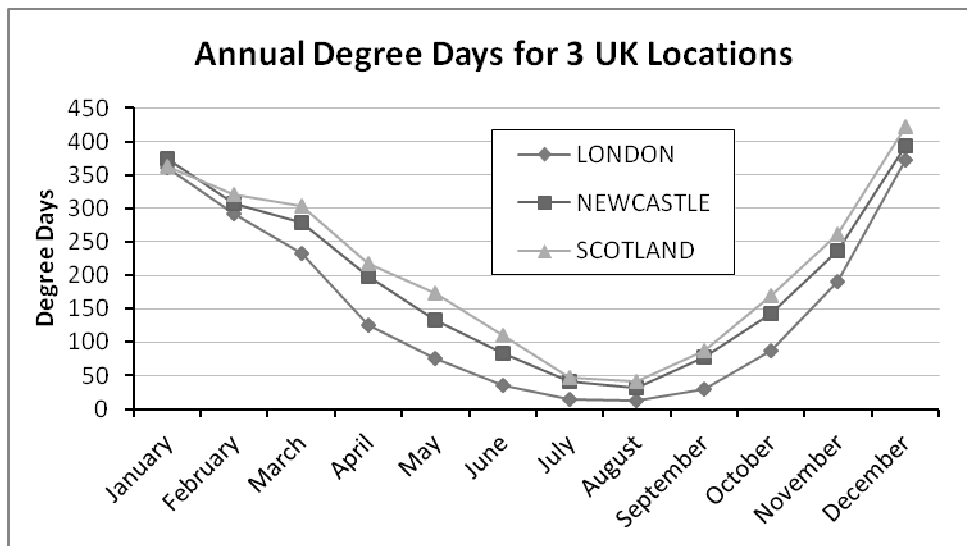


Fig. 11. Annual Degree Days for 3 locations in the UK.

The degree days are similar to the “bins” introduced in section 1.4 except they use daily average temperatures instead of hourly temperatures. Therefore degree days are representative of heat demand and can be converted to heat demand when multiplied by the heat loss coefficient of the house. The graphical presentation of the same data is shown in Fig. 11. As can be seen, contrary to the heat demand by cluster, the characteristics for the 3 regions show a bigger difference between heat demands over the entire year, with smallest differences for the most of the winter months. This would be primarily due to the weather.

In 2008 EST monitored domestic hot water consumptions in dwellings [15]. The sample consisted of 124 dwellings, 17 of these were unusable leaving 107 samples for analysis. The sample was divided into 68 regular boilers and 39 combi boilers. Another total of 23 dwellings were equipped with additional sensors for determining the destination of each hot water use, such as kitchen sink, shower, bath, and bathroom basin. 21 samples were used out of the 23, and divided between 13 regular boilers and 8 combi boilers. The main difference between a regular and a combi boiler is that the combi boiler heats up the mains cold water supply as hot water is needed and it does not need a hot water storage tank. Fig. 12 shows the hot water usage volumes for each of the destinations for a sample dwelling. Fig. 13 shows the proportion of heat energy used for each of the destinations for the same dwelling.

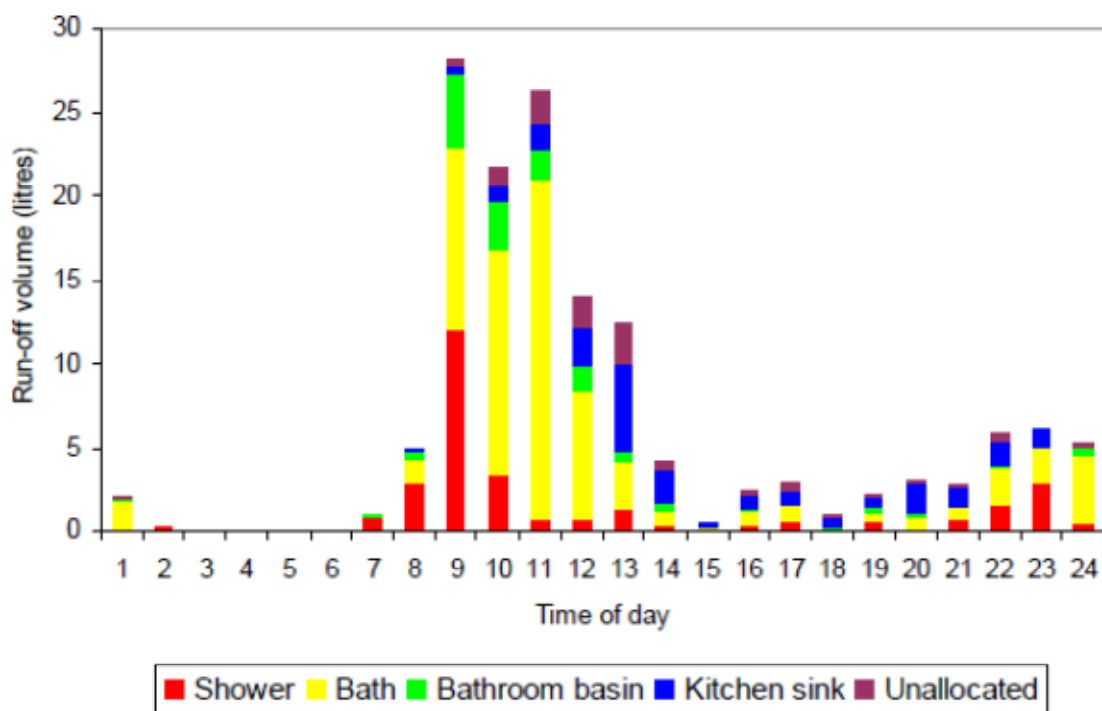


Fig. 12. Hot water usage volumes for each of the destinations for a sample dwelling over a 24hrs period [15].

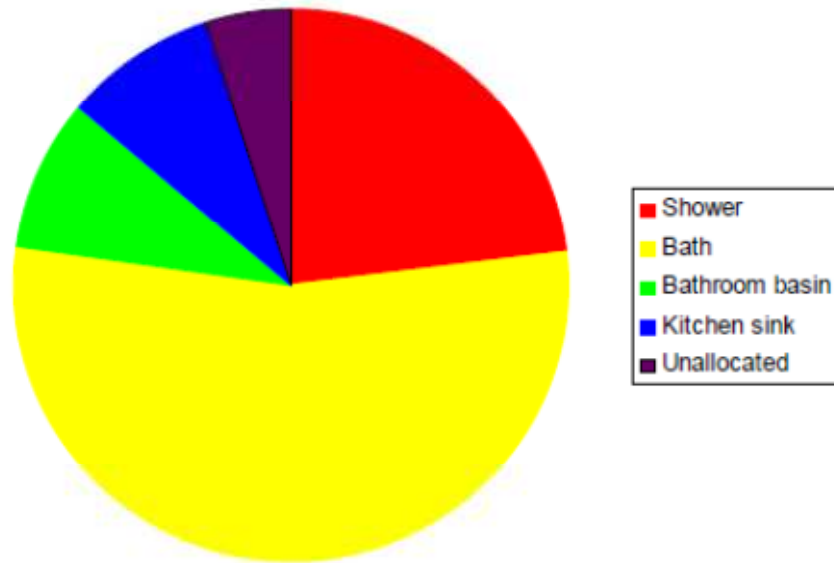


Fig. 13. Proportion of heat energy used amongst the hot water usage destinations [15].

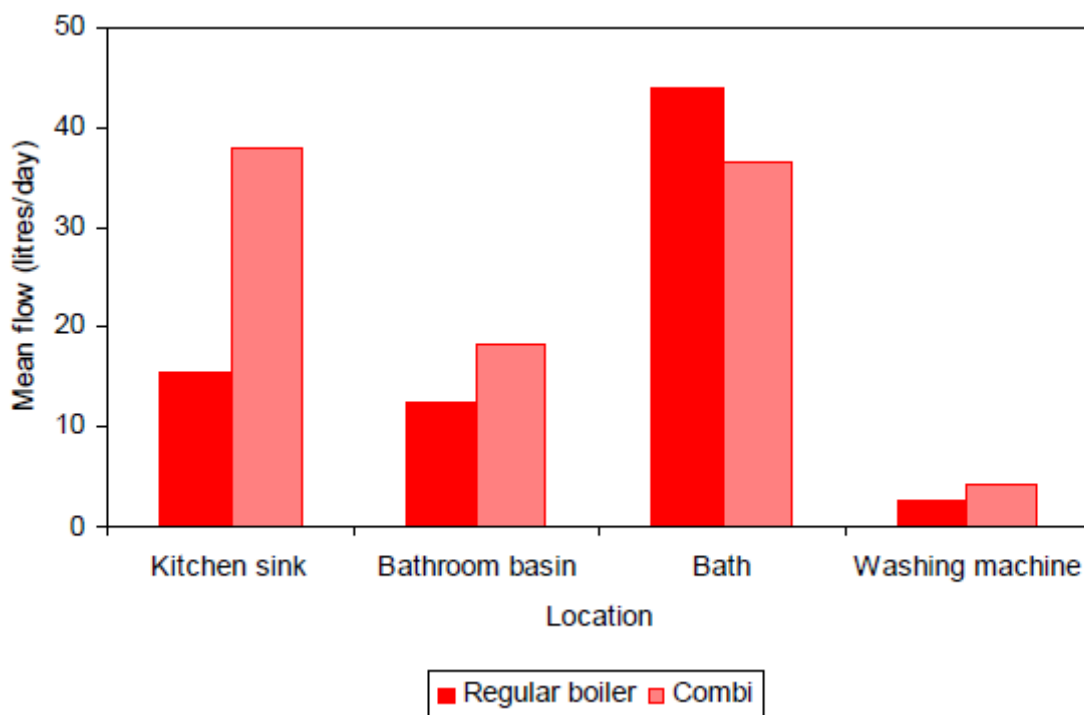


Fig. 14. Mean hot water usage volumes for Regular and Combi boilers at different destinations [15].

The mean hot water usage volumes for regular and combi boilers at different destinations is shown in Fig. 14. The large difference at the kitchen sink is explained by the need of hotter water at the kitchen sink by the household, and water is wasted whilst a combi boiler responds to the request. At other destinations lower hot water temperature was accepted.

2.7 The Energy Saving Trust Field Trial and user behaviour in the UK

In 2008 the Energy Saving Trust (EST) carried out the first large scale heat pump field trial in the UK to determine how heat pumps perform in real-life conditions [16]. The year-long field trial monitored performance and occupancy behaviour at 83 sites across the UK. The findings provide valuable information about factors that affect the COPs obtained. From the field trial COPs for air source heat pumps ranged from 1.2 – 3.3, system COPs ranged 1.2 – 3.2, with mid-range system COPs near 2.2. It can be seen that the variation in COPs is quite large, and EST has identified factors associated with these variations, such as installation, radiator sizing, heating control and user behaviour. However it is unclear how domestic hot water affects COP, and the need to further investigate why COP varies greatly on seemingly identical installations. The new testing platform being developed in this project aims to help answer these questions. Also, none of the heat pumps in the EST field trial was a CO₂ transcritical heat pump [2], hence the inverter controlled CO₂ transcritical heat pump being tested in this project can bring about knowledge about the operating characteristics of such heat pump.

In the EST field trial, user experiences and behaviours were studied by obtaining feedbacks from participants. The findings are divided between private properties and social housings. The following lists the results [17].

Overall, the results show that heat pumps are welcomed by householders, the kind of problems experienced by users, and how operating efficiency may be improved by greater user knowledge of heat pump systems including favourable heating patterns.

How satisfied have you been with your heat pump?

- Heat pump system meets my household's requirements for room heating: 73%
- The heat pump system has made my home warm and comfortable: 83%
- Pleasure from using low carbon energy source: 80%

How does your heat pump system compare with your previous heating system?

- Much Better/ Better: 75%
- Neither: 10%
- Worse/much worse: 15%

Users' heat pump problems

- Uncertain how best to operate the system and its controls: 44%
- Difficulties understanding instructions on operating and using the system: 30%
- Unable to heat rooms to required temperature: 23%

- Slow warm up of heating system: 21%
- Intrusive noise: 19%

For Private and Social properties:

How satisfied have you been with your heat pump?

- The heat pump system has made my home warm and comfortable:
- Private 91% - Social 71%

How does your heat pump system compare with your previous heating system?

- Worse/much worse: - Private 7% - Social 27%

Users' heat pump problems

- Intrusive noise: - Private 9% - Social 33%

Higher system efficiencies were associated with:

- Greater user knowledge and understanding of heat pump systems

Users with a lot of/fair knowledge: - Private 82% - Social 40%

- Continuous (rather than intermittent or timed) heating patterns

Users leave heating on at night: - Private 82% - Social 55%

From the study it can be seen that heat pumps can satisfy UK users, and knowledge and understanding of the heat pump systems and how they are operated affects the system efficiency.

2.8 Field trials in Germany, Sweden and Japan

Germany

A field trial carried out in Germany from 2007 to 2009 installed 77 fixed speed retro-fitted heat pumps (both air sourced and ground sourced) all over the country [18]. The mean SPF for air source heat pumps was 2.33. The field trial identified factors affecting performance as the heat sink type (radiators or under-floor heating), the heating supply temperature, and the existence of buffer storage. All air source heat pumps tested had buffer storage, only some of the ground source heat pumps did not. The results show that heat pumps with buffer storage tend to perform better, but the increase in storage volume shows a trend of decreasing performance. In this project factors affecting COP will be investigated, however they will not be limited to those identified in the field trial, and the effect of each factor may

not be the same bearing in mind that an inverter driven type heat pump is tested in this project.

Sweden

This field trial study from 2008 to 2010 included heat pumps in the Swedish market. 5 heat pumps were tested. They included a water to water heat pump, air source heat pump, and 3 ground source heat pumps with different configurations. All heat pump systems were installed in single family homes and were used for room heating and domestic hot water. The test sites were located in southern Sweden (Stockholm and south). 4 sites were located in climate zone 3 according to National Board of Housing BBR18, with one in climate zone 4 [19]. Each climate zone has particular monthly temperature ranges and solar irradiances, and would therefore affect the performance of a solar thermal or heat pump installed in that zone.

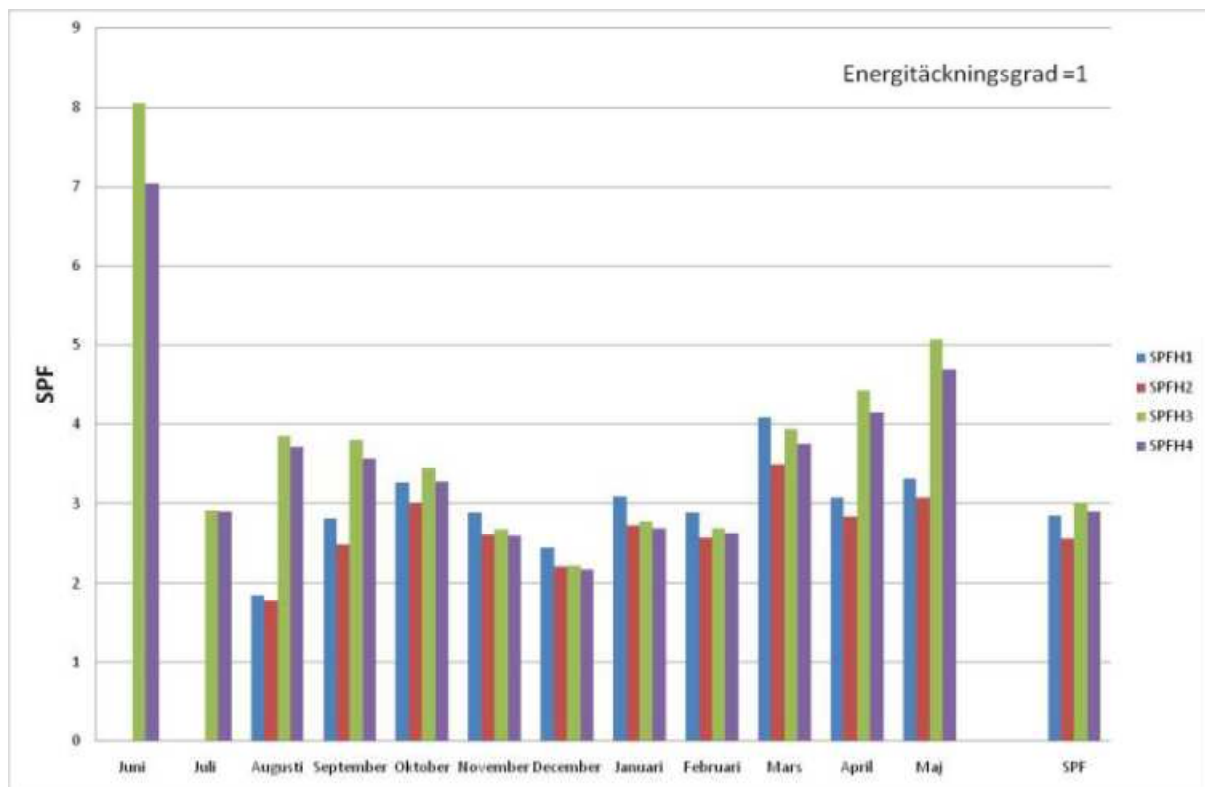


Fig. 15. Monthly SPFs and annual SPF obtained for the air source heat pump [19].

The average outdoor temperature for the sites are about 7.5°C, with lowest temperatures of around -10°C. The system SPF for a whole year ranged from 2.5 for a ground source heat pump to 4 for a ground source heat pump with exhaust air heat recovery. The air source heat pump had an annual system SPF of 2.9. The test cases for the air source heat pump and the ground source heat pump with exhaust air heat recovery are described below.

The house for the air source heat pump was built in 1991, with 2 floors of 140 m² each. The house has underfloor heating on both floors. The household consists of 2 adults and 2 teenage children. The heating system consists of an air to water heat pump of 14 kW capacity and a solar thermal collector of 10 m², which are both coupled to a storage tank of 500 litres. The storage tank has a lower and an upper portion of 250 litres each, which is thermally insulated against each other to reduce the thermal conductivity. The upper portion is for domestic hot water and the lower portion for heating. Circulation pumps in the system are speed controlled and turn off when not needed. The heat pump has an auxiliary heater in the form of an electric water heater but it has been turned off for the entire measurement period. The system is new and was installed in May 2010. The monthly SPF for the test year is shown in Fig. 15, along with the annual SPF.

On the graph SPFH1 refers to system test boundary and includes only the compressor. SPFH2 includes the compressor and fan of the heat pump unit. SPFH3 includes the heat pump unit, solar thermal and auxiliary for the buffer tank. SPFH4 includes the whole system, in addition to SPFH3 it includes the auxiliary circulation pumps of the radiators.

In Fig. 15 the SPFs for June is very high, this is contributed by the solar thermal heater. It alone covers the entire heat demand in June and the heat pump is off, hence SPFH1 and SPFH2 do not exist for this month. The SPFs for July is lower because although the solar thermal produced a lot of heat for this month, the heat demand for this month is much lower than June, and so the over capacity of the solar thermal resulted in low SPFs. For August SPFH1 and SPFH2 are low because the heat pump produces less heat for that month compared to other months, and the compressor of the heat pump needs to run at a minimum despite the low heat produced. The SPFs for December are quite low probably due to the turn on of the electric heaters since the heat demand for that month is the highest.

The ground source heat pump is placed in a one and half storey house, built in 2009, with an area of 108 m² of ground floor and 77 m² on the upper floor. The ground floor has underfloor heating, while the upper level has radiators. The household consists of 2 adults and 2 children. The ground source heat pump has a capacity of 6 kW, which is controlled by both outdoor and indoor temperature. It is directly connected to the underfloor heating and radiators while for domestic hot water a 180 litre buffer tank is separately heated by the heat pump. The temperature of the coolant into the ground heat exchanger is raised by heat exchange with outgoing building exhaust air. All circulation pumps are controlled by the heat pump (on / off controlled). Underfloor heating circulation pump is speed controlled. The heat pump has auxiliary heater in the form of an electric water heater. The SPFs for this heat pump is shown in Fig. 16.

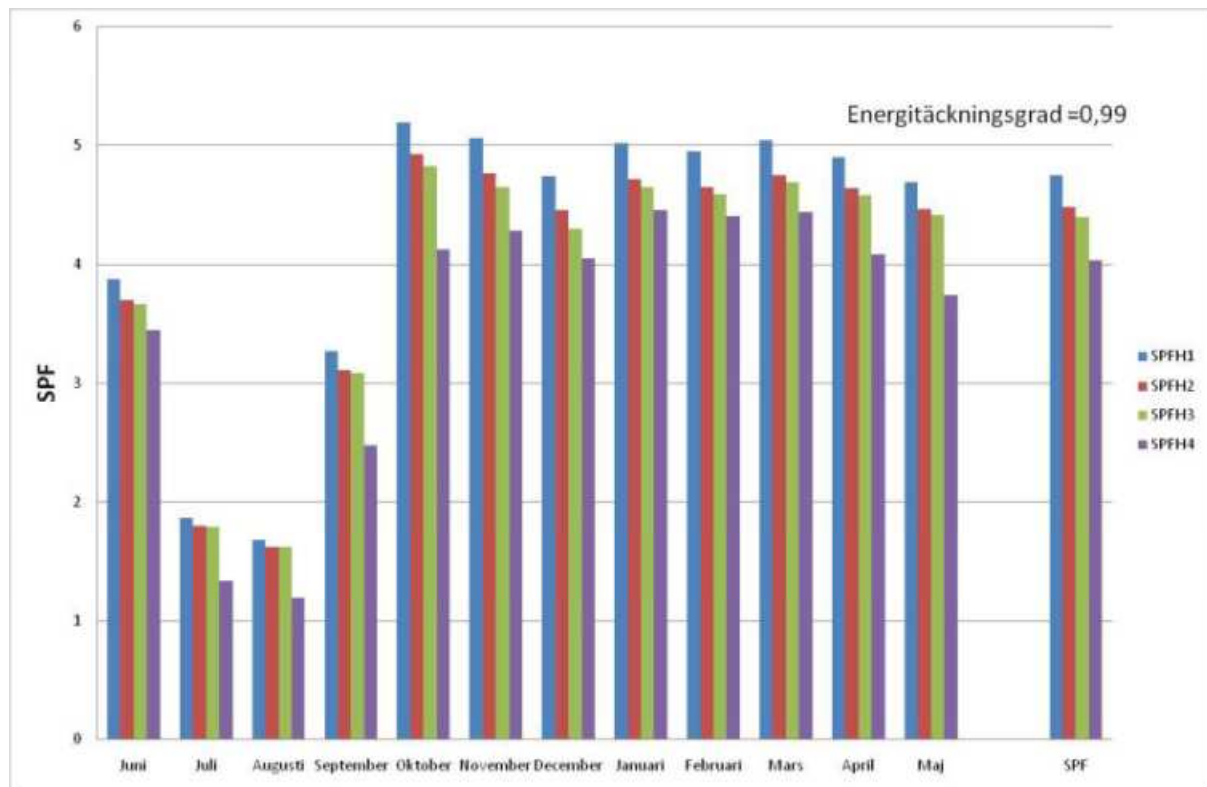


Fig. 16. Monthly and annual SPFs for the ground source heat pump [19].

In Fig. 16 the SPFs are lower from June to September, because these months have much lower heat demands compared to the other months. The heat pump in this case has electrical consumption that decreases slower than the decrease in heat load, and this resulted in lower SPFs at lower heat loads.

Japan

In 2006, 36 “Eco Cute” models of air source heat pump water heaters (from mixed manufacturers) installed in customers’ homes were monitored. The annual COP was 3.16 when the hot water temperature was at 40°C [20]. “Eco Cute” is a classification in Japan of air source heat pumps that uses natural refrigerant, namely CO₂.

Also in 2006 a 4.5kW capacity “Eco Cute” model of air source heat pump for domestic hot water heating only [rated COP 4.8] was modelled numerically, and compared with a field test of the unit in the Kinki district. From the field test the annual system efficiency when producing water at between 70°C to 85°C was 3.17 [21]. Fig. 17 shows the monthly system efficiency for that year. The system efficiency is identical to the SPF if the SPF is tested for the whole system including auxiliaries for the heating system.

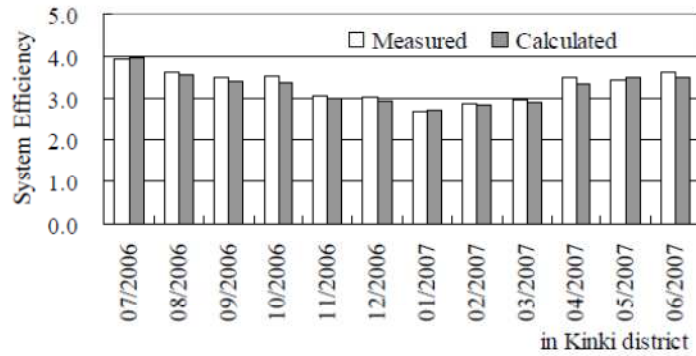


Fig. 17. Monthly system efficiencies of the field trial unit and modelled efficiencies [21].

For ground source heat pumps, two field trials will be described here. The first was carried out at a low energy experimental house built by Hokkaido University in 1997. The house has two floors with a semi-basement. The heating method was underfloor heating with radiators under windows. The ground source heat pump has 1.1kW electrical rating with 930 Litre buffer storage tank [22]. The result for this trial is shown in Fig. 18.

Operation time	12.5 [h/d]
Outdoor air temperature	1.5 [°C]
Room temperature	18.6 [°C]
Relative humidity	0.21 [% (RH)]
Brine Temp.	40.8 [°C]
Heat extraction rate	40.8 [W/m]
C.O.P.	4.0
S.C.O.P.	3.1

Fig. 18. COP and System COP (SCOP) for the Hokkaido University field trial [22].

In the second ground source heat pump field trial, 2 ground source heat pumps were field tested in a low energy house in the Sapporo city of Hokkaido [22]. The low energy house has two floors with a total living floor area of 200 m². The first ground source heat pump has a 10kW capacity and is responsible for floor heating, heat is stored at night time into thermal concrete storage. The second ground source heat pump has 4.5kW capacity and is assisted by an evacuated solar collector. The house began occupation from November 2007, and was monitored from January 2008. The space heating heat pump was monitored for a day (14 hrs heating period) on the 20th January 2008, for the outdoor temperature the COP were 4.3, and system COP 4.0. The hot water production heat pump was monitored on 20th February 2008 with water heated from 9°C to 65°C, the COP obtained was 2.8 and system COP 2.5. For the interest of the test platform under consideration in this project, the heating output and various operating temperatures are included in Fig. 19.

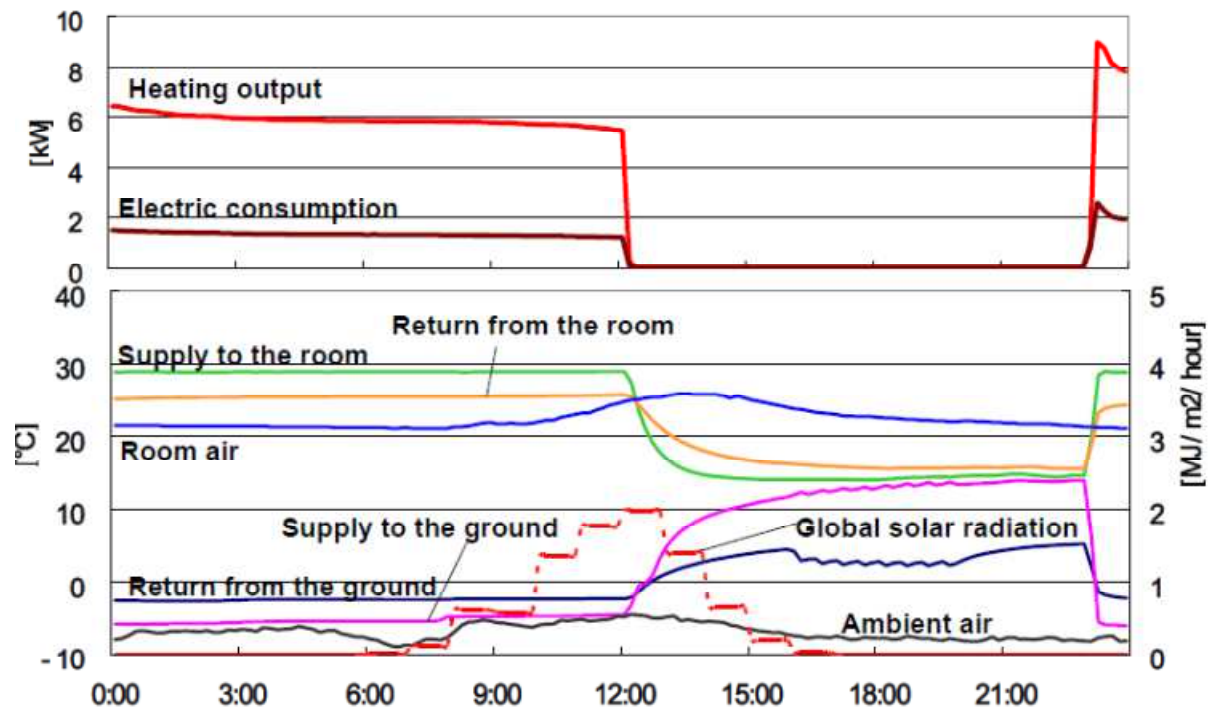


Fig. 19. Heating output and various operating temperatures for the first GSHP [22].

2.9 More on Test Methods

For a test platform to be effective, it should be able to make accurate and long term performance predictions under arbitrary conditions from tests that are short, simple and cheap to perform [23]. The expanding market, supportive policies and financial incentives for air source heat pumps means there is a prominent need for such effective test platforms. ISO 9459-part 5, is a testing standard for whole system “Black Box” type testing for solar and solar pre-heat hot water heaters. The Black Box approach offers simplicity and minimizes experimental efforts by avoiding internal measurements of the system under test. For this project this means no measurements are needed for inside the heat pump or its buffer tank. Although this established test standard is for solar water heaters, it can be transferred to test air source heat pumps. Furthermore if the test method does not take into account system state dependence of the past, and thus the dynamic behaviour of the system, the testing time would be much longer [23]. Therefore this should be investigated in this project.

The calculation method for predicting heat pump performances detailed in [24] uses input data from performance tests to predict COP values based on weather data and heat demands. However the performance tests follows EN 14511 [25], which tests the heat pumps at a number of pre-set inlet, outlet temperatures and weather conditions, hence this would not reflect the performance of heat pumps in operation, and so the calculated COPs using this method may have a limited scope. It is important in this project to learn that in [24], COPs would differ in full load and part-load operations. For fixed speed compressor

heat pumps COPs tend to be lower for part-load operation due to on-off cycling losses of the compressor. Variable capacity and inverter driven heat pumps have improved COPs at part-load. In adequate designed systems on-off cycling losses are small and are neglected in the calculation.

The test methodology for calculating the Seasonal Performance Factor (SPF) is described in [11]. Since data are directly used from testing, in this case the SPF is identical to the calculation for COP except it is for a season. This includes whole system test of including every system component such as circulation pumps, buffer tank and auxiliary heating. However the testing procedure again uses EN14511, which tests under a limited number of operating conditions. The operating modes of the heat pump system under test are distinguished in [11] as space heating, domestic hot water, combined space heating and domestic hot water, and defrosting mode. In some of these system tests in [11], auxiliary electric heating is not included. In this project auxiliary heaters are turned off for some of the tests and on for other tests to investigate the impact it has on performance.

Other testing methods exist that may not closely adhere to the above testing standards. These may be for research purposes, heat pump prototypes, design of heat pumps, optimization and improvements. A few examples now follow.

Two air-source heat pump water heaters with external condenser coil and wrap-around condenser coil are tested in [26] using the “Black Box” approach that only considers inputs and outputs. The test is carried out by monitoring the tank temperature rise, the flow rate in the condenser and power consumed by the compressor for 6 ambient temperature and humidity combinations. This is somewhat different to the whole system black box approach for continuous operation. It is interesting to see from the results of this test that humidity has just as much impact on the COP as ambient temperature.

In Singapore, a solar assisted heat pump dryer and water heater has been designed and built [27]. The system was both tested and simulated. The tested system was located on the rooftop of a four-storey building at the National University of Singapore. The dryer inlet condition was controlled and different dryer inlet conditions were set for each run of the experiment. The test was performed outdoor under the local meteorological conditions. After the dryer has reached steady state condition, the experiment was started with the drying material placed inside the drying chamber. The various instruments are logged using data loggers. Each experiment ran a minimum of 4 hours. Comparing results from the experiments and from the simulation, COPs shows a significant difference of around 2. Because the system built is rather unique, the test method is adapted to suit its application and investigative requirements.

An example of an experimental research based performance test is found in [28]. The test is used to determine the optimum refrigerant quantity and optimum condenser pipe length that would achieve the maximum COP. The heat pump unit is placed in an atmospheric

chamber, and the condenser enclosed thermal tank is repeatedly heated from 15°C to 55°C to obtain COP values for different refrigerant filling amounts and condenser pipe lengths. In this case the system is perhaps not treated as a black box as heat pump components were monitored including thermal storage temperatures. Since the system is tested for 3 ambient temperatures and is not the complete system, results could be different for a finalised product test.

In another test [29], a solar-boosted air source heat pump water heater with wrap-around condenser similar to that in [26] was investigated. This test was carried out to determine how 3 typical loading conditions affect the system performance. To achieve this, the system was constructed for this experiment. There were temperature sensors soldered to the condenser to monitor refrigerant temperature and sensors monitoring tank temperature variations. The test is carried out under outdoor weather conditions, each test run lasts 24 hours with ambient temperature, solar radiation, compressor power and heat transfer continuously monitored. The 3 typical loading conditions are: a tank full of cold water; a tank half of hot water and half of cold water; a tank with small amounts of hot water drawn off at intervals. It can be seen that clearly this test method is very experimental with the heat pump built to specification and everything within the heat pump monitored, but there is an element of operation testing for each test run lasts 24 hours under natural weather condition.

Lastly, there is the purely simulated test method as in [30]. The purpose of this test was to develop a new type multi-source heat pump water heater, using solar as the main source of energy and air as the supplementary energy. For the simulation model to be built a mathematical model was first developed, the heat pump and solar system was assumed to be steady state and the storage tank was a dynamic model. The simulation produced performance data from several hours in duration to monthly averages for a year using local weather data. Although the simulation method appears to have the benefit of producing a large amount of data, the model is based on assumptions which may impact on accuracy as was seen in [27].

From the above review on testing methodologies it is clear the important role performance testing plays in various applications, and the need to investigate a simpler, more cost effective way of testing that will reflect the real world performance of the heat pump under test.

2.10 Chapter Conclusion

The UK has a higher hurdle to jump than in many other countries in the EU in terms of making carbon savings from heat pumps, since it has higher than average carbon emissions from its electricity. Calculations show that heat pump would have to achieve a system efficiency of 2.6 in order to result in reduced carbon emissions when compared with a new gas boiler [4]. In comparison to the current testing standards for air source heat pumps, the

test platform in this project focuses on whole system testing with continuous operating conditions, rather than a fixed set of operating conditions. This offers the obvious benefit of producing test results that will reflect the real world performance of the heat pump.

To reach the UK renewable energy target of 15% of energies from renewables by 2020, ambition is set by the UK government to increase the proportion of heat generated from a renewable source from the current 1.5% to 12%. For heat pumps to play a part in this they would need to have a COP of above 2.875 based on the EU Directive on renewable energy [4]. This figure is not finalised as it depends on how the heat pump is tested for its COP. The Renewable Heat Incentive is the main scheme in the UK to encourage the adoption of renewable forms of heat generation by offering long term financial support for those who qualify. It only qualifies for heat pumps with a COP of above 2.9. Currently it only supports the non-domestic sector and does not include air source heat pumps, however air source heat pumps are likely to be included in the second phase of the scheme along with the introduction of the domestic sector incentives. Before the introduction of the second phase, there is in place the Renewable Heat Premium Payment scheme. This makes one off up front payments to those in the domestic section who install a renewable heat technology, which includes both ground source and air source heat pumps. This project offers a test method for evaluating the COP for an air source heat pump with the advantage of obtaining COP that reflect real world performance of the heat pump.

The field trials described gives an idea of the performance (COP/SPF) of heat pumps operating in real life under different conditions, with different emitter types and housing constructions. The information given from these field trials aids the design and validation of the test platform. For example, the EST field trial produced system COPs for air source heat pumps that ranged from 1.2-3.2, with mid range near 2.2. The factors behind this large variation in performance were identified as due to installation, radiator sizing, heating control and user behaviour. Due to the limitation in experimentation in field trials, the test platform in this project can investigate such factors further. Also none of the heat pumps under test was a CO₂ transcritical heat pump.

The field trial in Sweden included a 14kW capacity air source heat pump with a solar thermal collector of 10m². They both provide hot water and heating to a house built in 1991 with 2 floors of 140m² each. The heating is provided by underfloor heating in both floors. The average outdoor temperature is about 7.5°C, with the lowest temperature around -10°C. The monthly SPFs are recorded for a year for different system boundaries up to the whole system. The result (Fig. 15) helped to identify the influence of the solar thermal on the monthly SPFs. This for example gives information on how to explain future results from this project as it also has a solar collector.

In the second ground source heat pump field trial carried out by Hokkaido University in Japan, two ground source heat pumps were field tested in a low energy house in the Sapporo city of Hokkaido. The low energy house has two floors with a total floor area of 200m².

Although the heat pumps tested are ground source rather than air source, the data collected showed real-time heating output and electrical consumption of the heat pump (Fig. 19), which are useful for validating the heating demand and investigating heat pump operation in this project.

3. Theory

3.1 Chapter Introduction

This chapter introduces theories that are relevant to the investigations relating to the air source heat pump testing platform.

3.2 SCOP

For this test platform the operating System Coefficient of Performance (SCOP) is taken as the total heating output including domestic hot water (DHW) divided by electrical consumption of the heat pump system, including all auxiliary for the buffer tank and the heat sink. This is given in equation (2).

$$SCOP = \frac{\text{Radiator Heating} + \text{DHW power}}{\text{System Electrical power}} \quad (2)$$

The system electrical power includes all the auxiliary power such as circulation pump and buffer tank, but it would not include the solar preheat electrical consumption if this is not included in the test. The DHW power can be calculated in two ways, including and excluding solar preheat.

The heat power for radiator heating and DHW is calculated based on the energy required to raise a unit volume of water by 1K. This is given in equation (3).

$$P = \dot{m} \cdot C \cdot \Delta T \quad (3)$$

\dot{m} is the mass flow rate in kg of water per second, C is the specific heat capacity of water, which is around 4186 J/(gK), and ΔT is the temperature raised per volume of water.

The total heat power is then summed over 1 second time steps for high accuracy to arrive at kWh values. The electrical power is summed up by an Elster A100C kWh meter. Equation (3) then becomes,

$$SCOP = \frac{\text{Total Heat Output kWh}}{\text{System Electrical kWh}} \quad (4)$$

Equation (4) is used to work out COPs for different durations. An Integra 1630 meter is used for monitoring the electrical power waveform of the heat pump.

3.3 Seasonal Performance Factor

The Seasonal Performance Factor (SPF) in this case is simply the total heat output over a month divide by the total system electrical consumption over the same period, as defined in the previous section. The quarterly or yearly SPF can be calculated similarly.

$$SPF = \frac{\text{Total Heat Output kWh (A Month)}}{\text{System Electrical kWh (A Month)}} \quad (5)$$

The SPF can be calculated by equation (5).

3.4 Carnot Efficiency

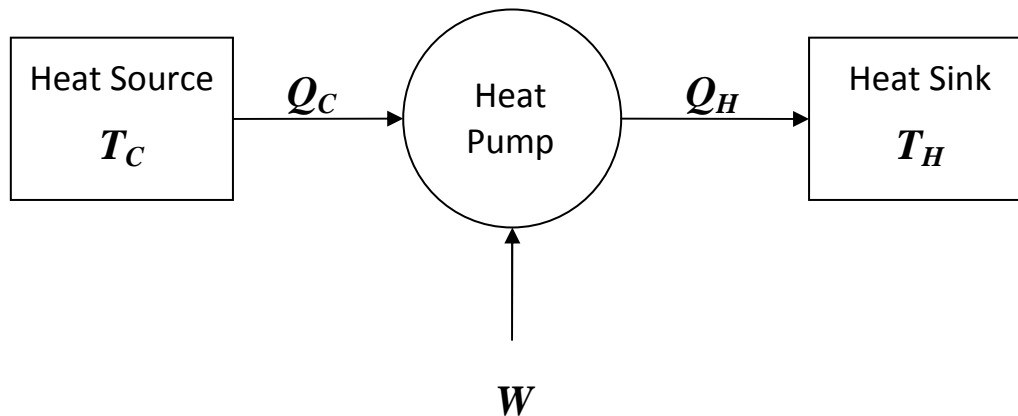


Fig. 20. Carnot model for a heat pump.

Referring to Fig. 20, the coefficient of performance of a heat pump is:

$$COP = \frac{Q_H}{W} \quad (6)$$

where Q_H is the quantity of heat discharged to the hot reservoir (i.e. the house) and W is the work done by the heat pump which may be written as:

$$W = Q_H - Q_C \quad (7)$$

For a Carnot cycle:

$$\frac{Q_C}{Q_H} = \frac{T_C}{T_H} \quad (8)$$

where T_C and T_H (in Kelvin) are the temperature of the cold and hot reservoir respectively. Therefore, the COP may be written as:

$$COP = \frac{T_H}{T_H - T_C} \quad (9)$$

As an example, for the CO₂ transcritical heat pump in the current test platform, the maximum theoretical efficiency operating between reservoirs of 13 °C outdoor and 55 °C buffer tank is 7.8. In practice the COP is between 1.9 – 2.6 due to losses.

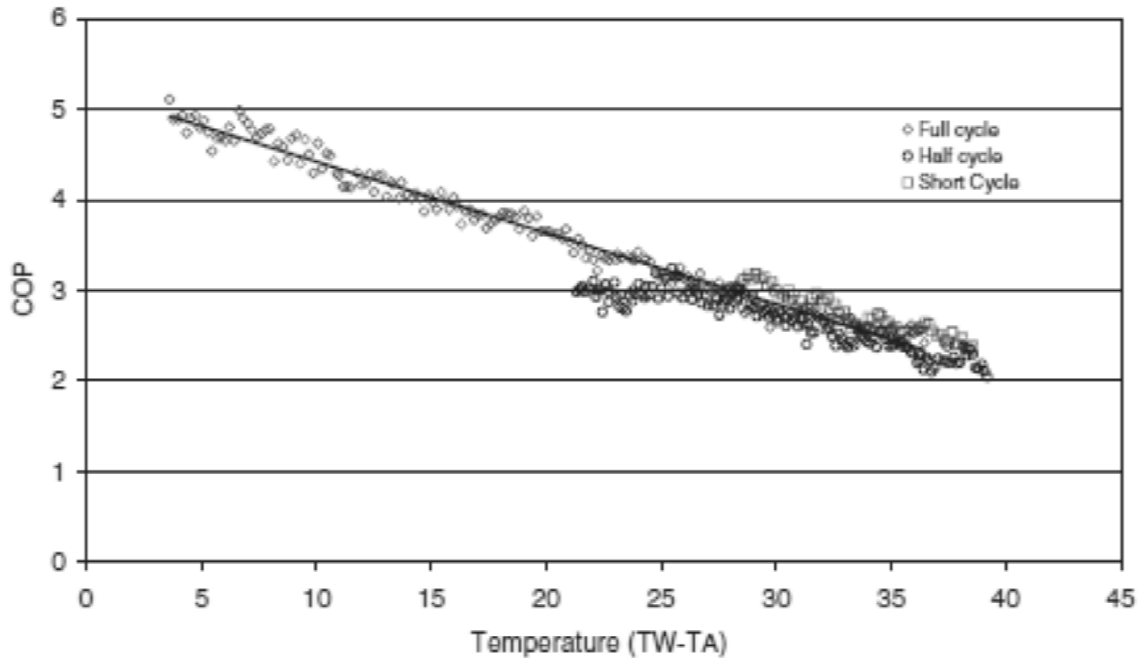


Fig. 21. COP variation with heat sink and outdoor temperature [29].

To get an idea of how COP varies with different heat source (outdoor air) and heat sink temperatures, Fig. 21 shows a graph for this from experimental data [29]. On the x-axis TW is the heat sink or hot water temperature, TA is the ambient or outdoor air temperature, their difference was plotted against COP. It can be seen from the figure that the larger the difference between hot water and outdoor temperature the lower the COP becomes.

3.5 Basic and Generalised Heat Pump Operation

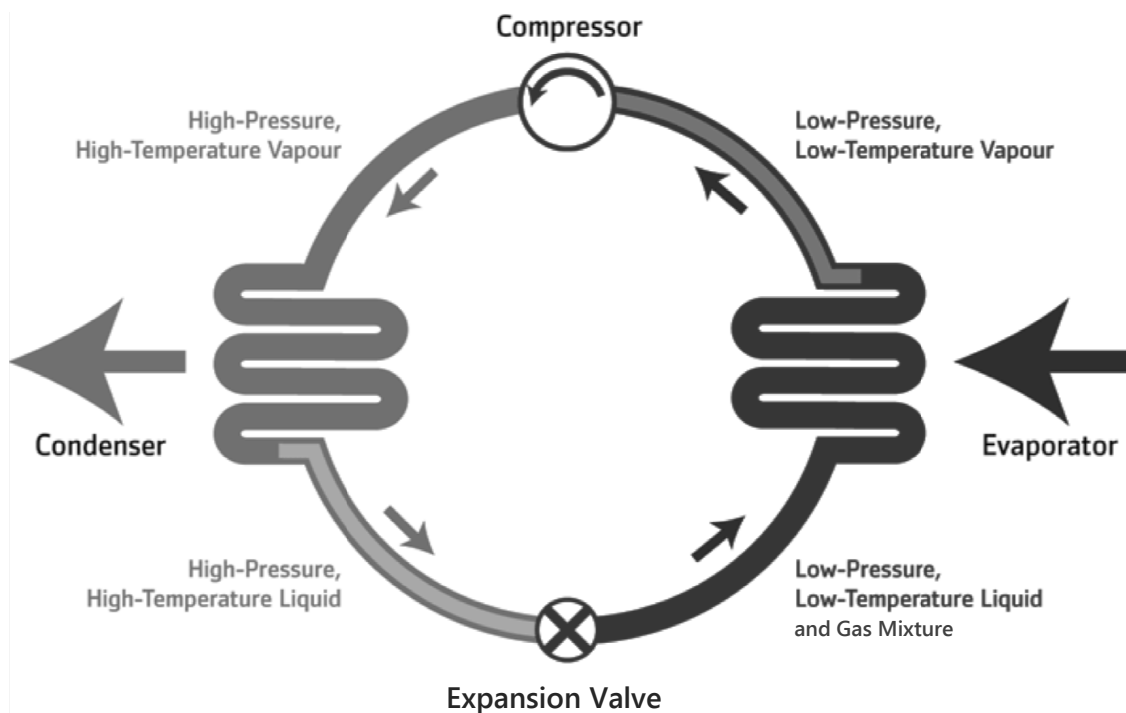


Fig. 22. Vapour Compression Cycle for a heat pump.

Fig. 22 shows the basic vapour compression cycle for a heat pump. From right side of the diagram, the refrigerant takes heat from its ambience as a low-pressure, low-temperature liquid, sometimes at this point there is a mixture of liquid and vapour. The liquid having taken on more energy becomes warmer and undergoes phase change to become a vapour. The vapour is then compressed by the compressor to produce a high-pressure high-temperature superheated vapour. The condenser then rejects heat from the vapour and condenses it back to liquid. The liquid is then reduced in pressure by the expansion valve and the cycle begins all over again. In the case when the liquid becomes a mixture of liquid and vapour after the expansion valve, the vapour portion becomes superheated as it takes on more heat from the ambience.

Throughout the cycle electrical energy is needed by compressor to keep the whole process going, and the ratio of heat energy output to the electrical consumption of the compressor is the basic coefficient of performance (COP).

3.6 Radiator Sizing in the UK

The role of radiators in room heating is considered. The radiators essentially interfaces between the heat pump buffer tank and the rooms to be heated, therefore they have a part to play in determining how much heat is released into the house. Imagine a fairly large room

with a single radiator unit, this radiator will be able to bring the room to a certain temperature. Now imagine the same room with two such radiator units; starting at the same starting temperature the room is now heated up faster and reaches a higher final temperature. This thought experiment demonstrates that the size of the radiator, or more precisely the surface area of the radiator will determine both the rate and amount of power released into the house, which is equal to the power taken away from the heat pump buffer tank. The UK uses the BS EN442 standard to test radiators to determine their rated power outputs. Installers or householders can then select radiators based on heating requirement of the house, and forward and return water temperatures of the radiator.

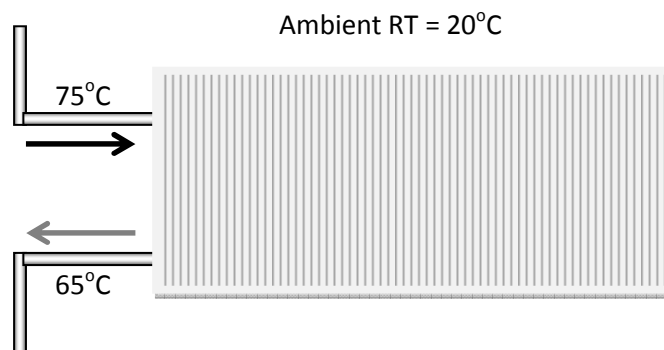


Fig. 23. Radiator flow temperatures and ambient room temperature.

As shown in Fig. 23, BS EN442 requires that all radiators manufactured in Europe undergo tests with a forward flow temperature of 75°C and return temperature of 65°C and a room temperature of 20°C, with the inlet outlet connected Top Bottom Same End (TBSE). The mean water temperature (MWT) inside the radiator is the average between the forward and return temperatures, which in this case is 70°C. Theoretically, the power given off by the radiator into the room is proportional to the difference between the MWT and room temperature (ΔT), the flow rate, and the size and surface area of the radiator.

Mathematically this can be expressed as:

$$P = \alpha \dot{m}C\Delta T \quad (10)$$

Where P is the power given off by the radiator, \dot{m} is the mass flow rate of water through the radiator, C is the specific heat capacity of the water, and α is a constant based on the heat emitter properties. Notice that this is basically the same equation as equation (3), used for calculating heating for the test platform as introduced earlier.

In terms of heat pumps a method used today in the UK for rating the suitability of existing radiator size with respect to heat pump performance is given in [31]. First the heat loss of the room is determined based on insulation measures and building material. Next the radiator output based on manufactures' tables obtained under EN442 is determined at mean water to air temperature of 50°C. Finally the Oversize Factor is determined by dividing

the room heat loss by the radiator heating output. The performance rating with respect to heat pump for the radiator is then found from Fig. 24.

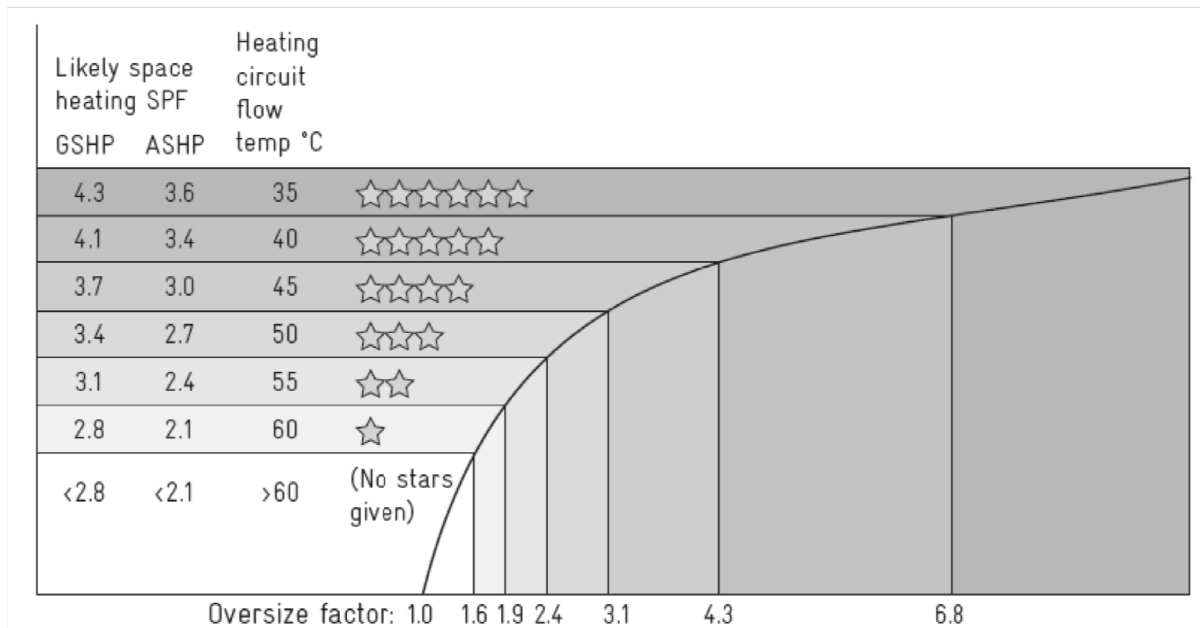


Fig. 24. Rating performance of heating system using the Oversize Factor [31].

The increase of performance with the Oversize Factor means that the water temperature will be lower for an existing oversized radiator, and hence the heat pump will be able to operate with higher efficiency.

3.7 The CO₂ Transcritical Cycle

In the transcritical cycle, the refrigerant goes above the critical pressure on the condenser side, and return to sub-critical pressure at the evaporator side. Fig 25 shows the phase diagram for CO₂ (R744). The triple point is the temperature and pressure at which the three phases of the refrigerant coexists in thermodynamic equilibrium. At temperature below the triple point, liquid form of the substance cannot exist. The critical point is the temperature and pressure above which no phase boundaries exist, the liquid and vapour phases merge into one phase. At temperature and pressure above the critical point, the substance goes into the fluid region where the substance conform to arbitrary definition of what is considered liquid and what is considered vapour. The dashed line around the fluid region indicates that there is no phase change upon entering the region. The condition in the fluid region is referred to as a supercritical condition or very often as the gas condition. For most refrigerants they are used within the triple point and critical point. For CO₂ however it traverses beyond the critical point [32].

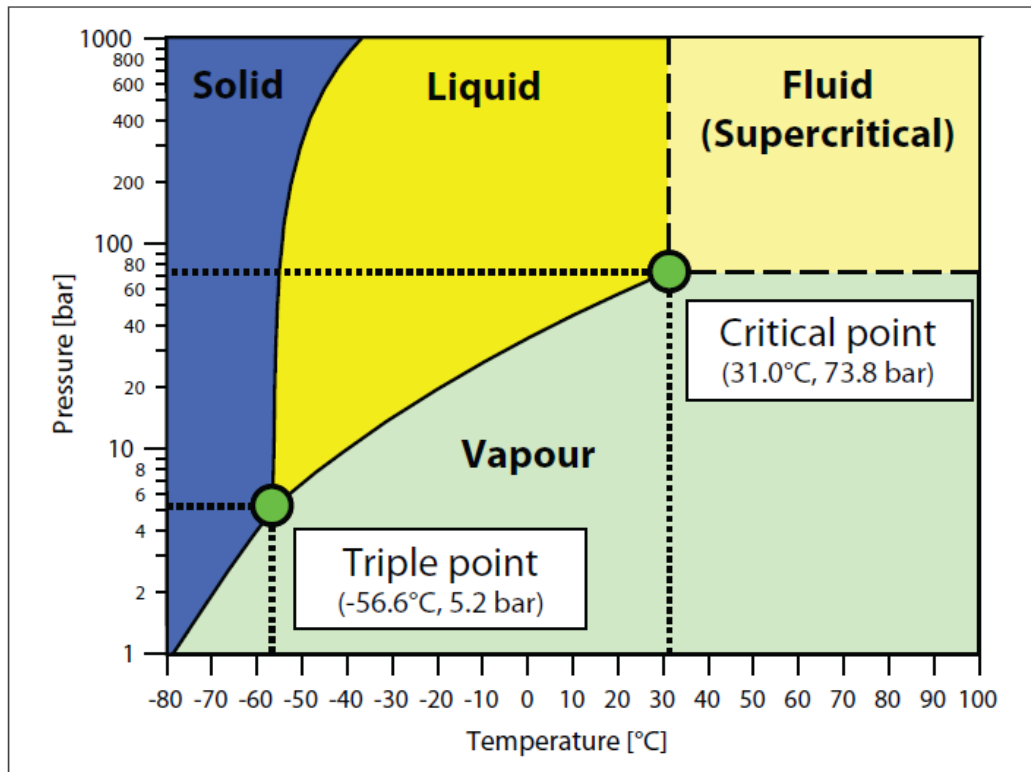


Fig. 25. Phase Diagram for CO₂ [32].

Because CO₂ becomes in the gas condition at the condenser side the condenser is instead called a gas cooler. Fig. 26 shows the compressor cycle for a transcritical heat pump.

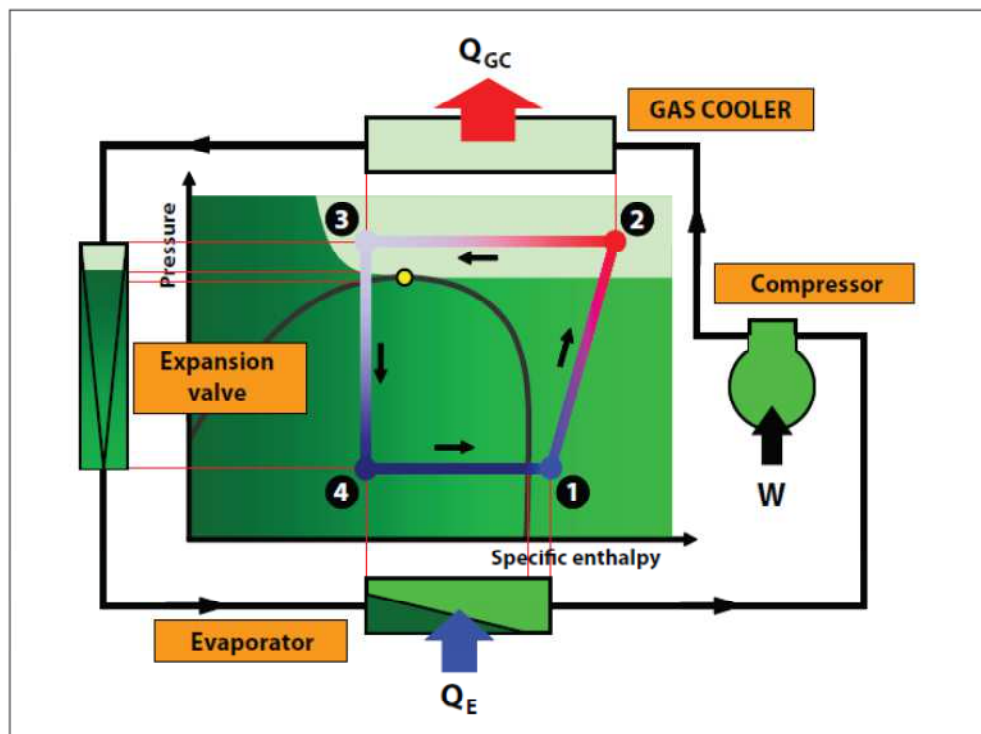


Fig. 26. Transcritical Heat Pump with respect to pressure-enthalpy diagram [32].

Q_{GC} is heat rejected at the gas cooler, and Q_E is heat absorbed by the evaporator. The yellow dot at the maximum pressure on the pressure-enthalpy diagram is the critical pressure. At points 1 to 2 the refrigerant is compressed beyond the critical point and into the fluid region. The pressure required is high compared to other refrigerants and subcritical heat pumps but the temperature required is low compared to other refrigerants. One of the challenges of constructing a CO₂ heat pump is to cope with this high operating pressure. The critical pressure of CO₂ is 72.8 atm or 73.76 bar, the heat pump operates at a pressure above this. At points 3 to 4, the refrigerant is expanded by the expansion valve and re-enters into the subcritical vapour / liquid region.

3.8 Fixed Speed vs Variable Speed Heat Pumps

The basic difference between variable speed and conventional refrigeration systems is in the control of the system capacity at part-load conditions. In a variable speed refrigeration system the capacity of the refrigeration system is matched to the load by regulating the speed of the compressor motor. Variable speed systems can be realised in a number of ways, which can be divided into two groups. The first group is which the load is indirectly coupled to the motor, a speed control mechanism connects the load and the fixed speed motor. The second group are those with the load directly coupled to the variable speed motor [33]. Heat pumps can be divided into similar groups.

In one study an analysis was carried out on energy conservation of variable-capacity compressors in domestic and small, commercial, air-conditioning systems [34]. The authors reported the effects of using variable capacity control and identified essential modifications to achieve maximum efficiency gains. Although no specific technique for displacement control was recommended, it was emphasised that energy could be saved on seasonal basis because the system would operate at lower capacities due to reduced frictional losses in the compressor. Energy savings were also anticipated due to reduced pressure ratio imposed on the compressor by the lower temperature difference at lower loads in both condenser and evaporator. It was concluded that variable capacity control could provide energy savings of 28–35% on a seasonal basis.

Another experimental investigation on a 3kW heat pump with a rotary compressor was reported in [35]. The practical limits on compressor speed variation were found to be between 25 and 75Hz. The results indicated improvements in Energy Efficient Ratio (EER = COP × 3.412) with the inverter driven compressor, compared to a fixed-capacity system. The reason stated for the improvements was higher efficiency at part load, which reduces the power consumption and cycling losses. The improvement on energy saving over the single capacity system was between 20–26%. The cycling losses were estimated to be between 5–7%.

In one other study the investigations concentrated on capacity control of domestic sized heat pump systems. The investigations showed that a variable speed control could achieve a 15% improvement in energy conversion efficiency, compared to a conventional system [36].

4. Test Platform

The testing platform for evaluating and investigating operating COPs, in this case of a inverter driven CO₂ transcritical heat pump is shown in Fig. 27.

The valves and meters' inputs/outputs are acquired as well as controlled by the Labview software. The test platform is situated at Blyth, UK, which uses the natural weather at that location to perform tests.

4.1 System Components

The main system components of the test platform are the heat pump unit, heat pump buffer tank, solar thermal, solar thermal buffer and cooling tank.

The heat pump unit is a Sanyo CO₂ ECO model situated outdoor and installed according to a real installation. The heat pump buffer tank is 220 litres that provides both DHW and heating. The domestic hot water is isolated from the tank by running a coil through the tank, the inlet of the coil is connected to the solar thermal buffer tank. Hence if the solar buffer tank is hot, the coil will take less energy from heat pump's buffer tank. The heat pump buffer tank has three internal baffles to enhance stratification, so that the lowest portion supplying to the heat pump has a lower water temperature that favours the heat pump's performance. The circulation pump for circulating water between the heat pump and its buffer is built into the buffer tank. The weather compensated control is included in the buffer tank by controlling a four-way mixing valve that senses the outgoing water temperature into the radiators. The water temperature is controlled with respect to the outdoor temperature.

The solar thermal is electronically controlled and can be switched on and off depending on the test system boundary. The solar thermal buffer tank is 130 litres, with temperature sensors along its height. Normally it has an average water temperature of between 45 to 55 °C.

The 500 litre cooling tank is responsible for taking heat away from the heat pump buffer tank. It consists of two finned coil heat exchangers placed at top and bottom of the tank. Each finned coil is further divided into 3 coils in parallel with each about 17mm in diameter. The total length of the finned coil is determined experimentally to be about 7m. The experiment involved perturbing the inflow temperature into the coil and timing how long it takes for the temperature change to be observed at the outlet of the coil. The coil length can then be calculated knowing the flow rate and total cross sectional area of the coil. The separation between the top and bottom coils is about 0.5 meters, with the total tank height of 2m. The top coil is connected to an outdoor chiller operating in on/off mode with a small buffer. The bottom coil is connected to the heating circuit that controls the amount of heating into the cooling tank.

4.2 Sensors

The main sensors of the test platform are PT1000, PT100 RTD Class A temperature sensors and paddle wheel flow meters. PT1000 temperature sensors are placed on the heating circuit and domestic hot water circuit. PT100 sensors are placed along the height of the cooling tank, and along the height of the solar preheat buffer tank. Flow sensors are placed on the heating circuit and domestic hot water circuit. Temperature sensors and flow sensors on the heating circuit and domestic hot water circuit are used to determine the useful heat power output and monitor flow temperatures. Temperature sensors along the height of the tanks are used to monitor and understand both the physical and dynamic behaviour of the tanks. These are logged by Labview for various parts of the test.

A note on sensor selection

There are mainly two types of temperature sensors: thermocouples and resistive temperature devices. Resistive devices can be further divided into RTD and thermistors. Thermocouples consist of two stripes of wires made of different metals joined together at one end. Change in temperature at the junction induces a change in Electromotive Force (emf) at the other ends. Resistive temperature devices rely on the fact that as temperature changes the resistance of the material changes accordingly. RTDs have resistance rising more or less linearly with temperature, whereas thermistors have resistance drop non-linearly with temperature rise [37].

RTDs are more stable than thermocouples, but their temperature range is not as broad: RTD operate from about -250 to 850°C whereas thermocouples range from about -270 to 2300°C. Thermistors have a narrower temperature range of -40 to 150°C.

Thermistors and RTDs share an important limitation compared to thermocouples. They function by passing a current through the sensor, whereas thermocouples are zero current devices. This means that thermistors or RTDs will heat up resistively if placed in a stationary medium, and can affect temperature readings.

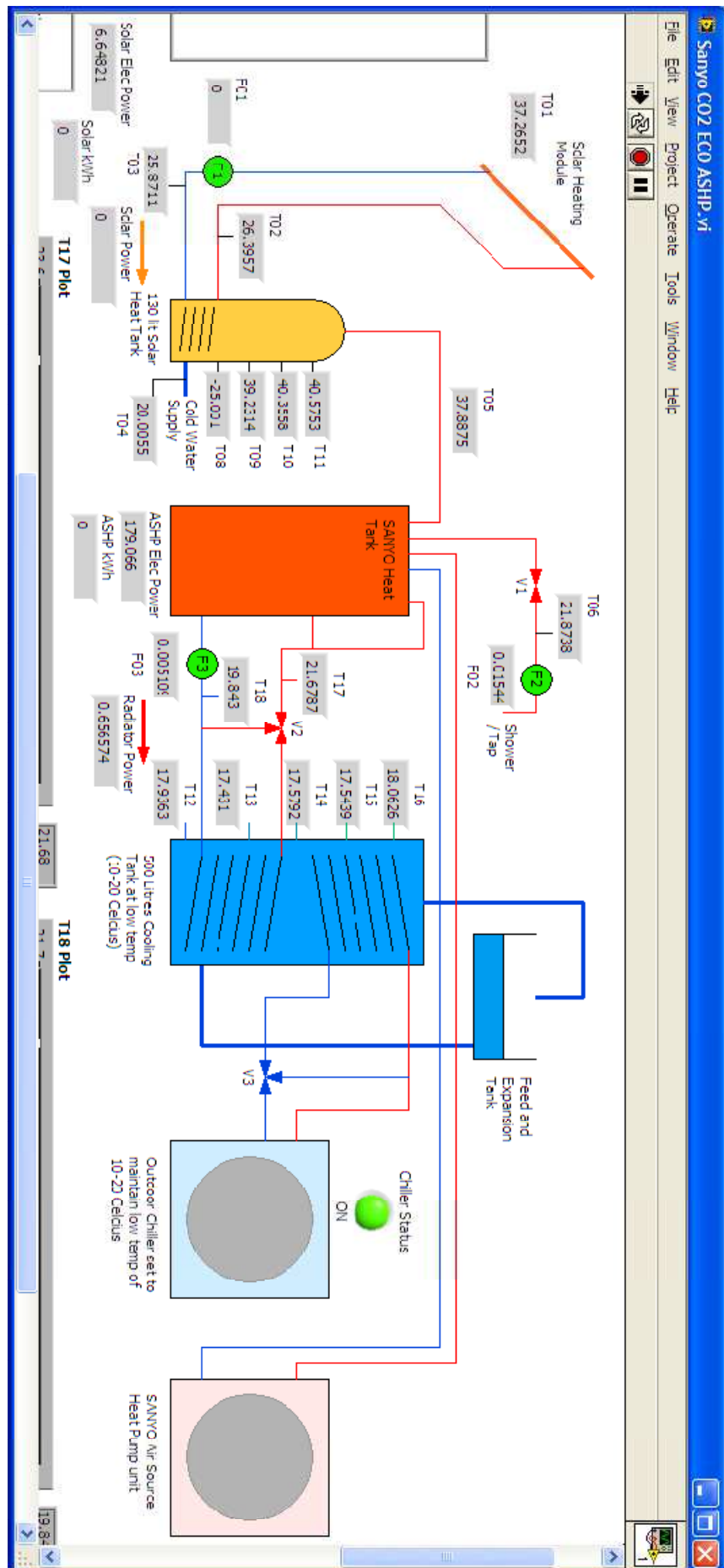


Fig. 27. Test platform setup as shown on the Labview user interface.

The flow sensors used in the test platform are paddle wheel type with Hall sensing. This type of flow meters is for accurate liquid measurements and consists of a multi-bladed rotor, perpendicular to the flow. As liquid passes through the blades the rotor turns. The rotational speed is directly proportional to flow rate, and can be sensed by magnetic pickup, photoelectric cell, or gears.

A major concern for this type of flow meter is bearing wear. A “bearingless” design has been developed to avoid this problem. Liquid entering the meter travels through spiralling vanes of a stator that causes rotation of the liquid stream. The stream acts on a sphere causing it to rotate in free space. The speed of rotation is proportional to flow rate and is detected electronically [37].

4.3 Data Acquisition and Control

The test platform uses NI Labview and NI CompactRIO.

Labview is a system design software that provide the software tools needed to create and deploy measurement and control systems through hardware integration. It employs a graphical programming interface that gives the user an intuitive way of programming.

For hardware interface NI CompactRIO is used. It is a reconfigurable embedded control and acquisition system. The CompactRIO system’s rugged hardware architecture includes I/O modules, a reconfigurable Field Programmable Gate Array (FPGA) chassis, and an embedded controller. The CompactRIO is programmed by Labview for a variety of embedded control and monitoring applications.

In the test platform, the CompactRIO has several analogue current input modules for the flow and temperature sensors; a digital input module for on/off indicators, solar thermal flow meter, and kWh meters; a digital input module for controlling the circulation pump on/off; and an analogue voltage output module for controlling valves and pump.

A Labview program was created to monitor and log all the sensors, and to calculate the COPs with different system boundaries. Labview was also used to design control algorithms for DHW automatic draw-offs and controlling heating outputs.

4.4 Heating Circuit 1

The first heating circuit under investigation for controlling heating output is shown in Fig. 28.

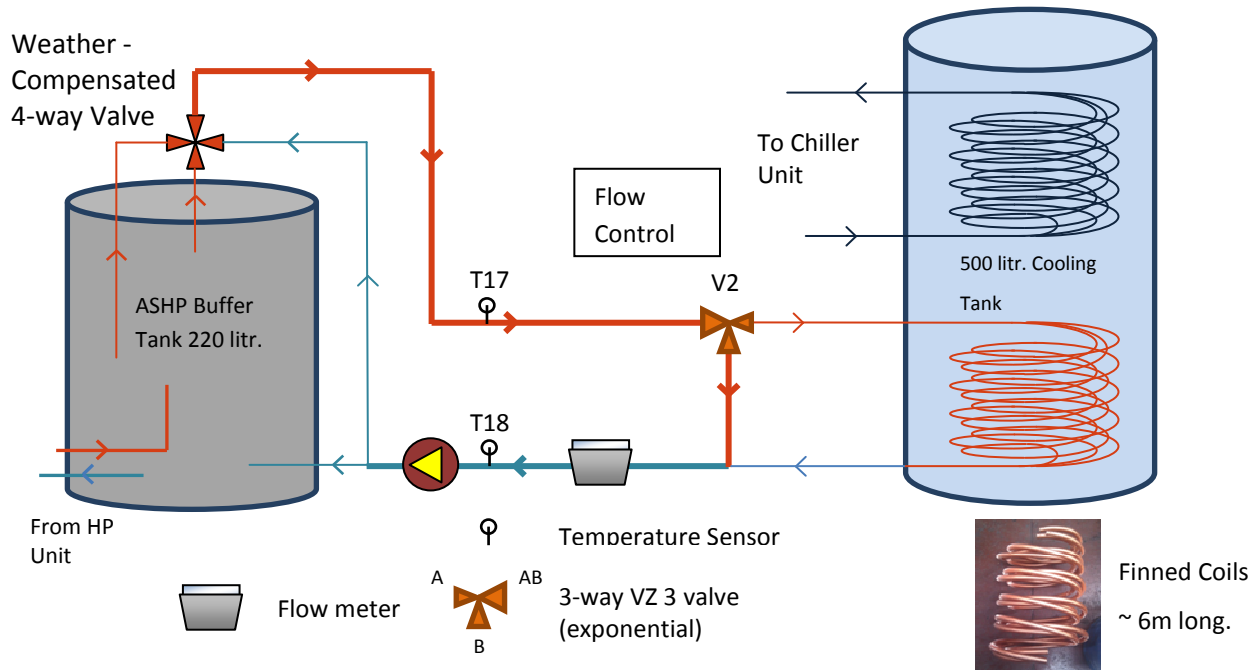


Fig. 28. Heating Circuit 1.

This heating circuit is to be called heating circuit 1, as this is modified later in the project and will be introduced in the following sections.

The heating circuit utilises a Grundfos UPS domestic circulation pump. For ease of explanation the heating circuit is divided into the Buffer Tank Side and Cooling Tank Side. The Buffer Tank Side in this case includes the circulation pump and the flow loop that goes in and out of the heat pump buffer tank. The Cooling Tank Side includes the flow loop going in and out of the finned coil heat exchanger within the cooling tank.

Referring to Fig. 27, using equation (2) from section 3.1 the radiator heating output is calculated by taking ΔT as $T17-T18$, where $T17$ is the forward flow temperature of the heating circuit and $T18$ is the return.

To control heating, heating circuit 1 diverts some of the flow from the heat pump buffer tank into the finned coil (Fig. 28), the heat is then absorbed by the cooling tank. The top coil of the cooling tank is connected to the chiller to maintain the tank temperature. The chiller works in on/off operation. Because controlled valve V2 has a 50:50 diversion on fully open

the flow into the cooling tank is quite low (perhaps around 3 – 7 litres/minute), this results in long flow delay between forward and return flows due to the length and large overall cross sectional area of the finned coil. However this is not taken into account in the design of this heating circuit.

4.5 Radiator Model

A radiator model is incorporated into the control for the heating circuit in order to meet the operating requirement of the heat pump system. The heat pump buffer tank has a weather compensated control that controls the water temperature into the radiator depending on outdoor temperature. In order for the test platform to cope with this and control the heating in a natural way, the forward and return flow temperatures from the buffer tank ($T17$ and $T18$ in Fig. 27) are used to calculate the instantaneous heating demand based on a radiator model. The radiator model adopted was taken from [38]. This radiator model was chosen because it is general and basic, and yet it has an exponential term which more accurately describes convective radiators. The general and basic nature of the model means that it applies to many radiator types and simple to implement, the exponential nature of the model would test the robustness of the control algorithm.

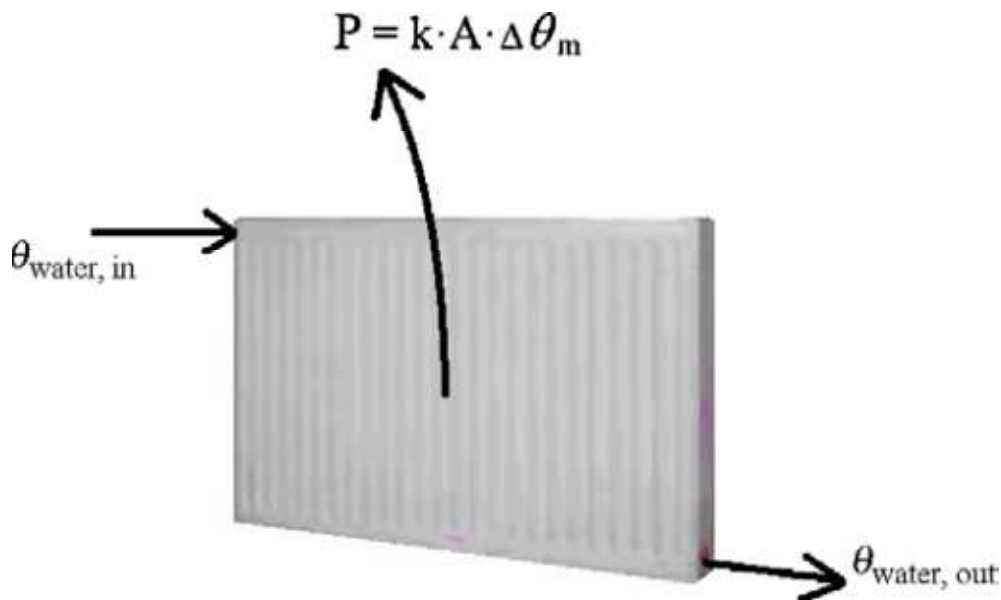


Fig. 29. Diagram of radiator model.

$$\Delta\theta_m = \frac{\theta_{\text{water, in}} - \theta_{\text{water, out}}}{\ln(\theta_{\text{water, in}} - \theta_{\text{air}} / \theta_{\text{water, out}} - \theta_{\text{air}})} \quad (11)$$

Fig. 29 illustrates the radiator model. P is the heating power output warming the surrounding air, $\theta_{water,in}$ is the temperature of water entering the radiator and $\theta_{water,out}$ is the temperature of water leaving the radiator; k is the total heat transfer coefficient, A is the total surface area of the radiator, and $\Delta\theta_m$ is the mean temperature difference between radiator surface and ambient air. $\Delta\theta_m$ is calculated by equation (11). There are other ways to calculate $\Delta\theta_m$ in other radiator models, but this model has an exponential term (equation 11), which introduces non linearity that more accurately describes convective radiators and helps to test the robustness of the control algorithm. To implement this radiator model in Labview the multiplier kA in the heating output equation is estimated by using a known heating demand for the test platform based on the outdoor temperature on that day and then taking $T17$ and $T18$ as the $\theta_{water,in}$ and $\theta_{water,out}$. This is legitimate in this case as the heating circuit design follows that of a standard installation practice. θ_{air} is taken as 20°C for the estimation and this value is also used in the control algorithm.

The purpose of the radiator model is two fold. First, it is used as a heating demand generator to test the robustness of the control algorithm in Labview and also it can be used standalone to test the performance of the air source heat pump. Second, it can be used together with Simulink to generate realistic heating demands for various house models in different outdoor temperatures. Simulink is a software tool (linked to Matlab) for modelling, simulating and analyzing multi-domain dynamic systems. A Simulink model was built to generate direct heating demand every 15 minutes for the heating circuit to control, and does not fully incorporate a real time radiator model. This has the disadvantage of introducing unnatural behaviour to the heat pump as the heat pump heating circuit is not included in the Simulink model. In reality the heat pump buffer tank weather compensated control will not produce exactly the heating demand generated by the Simulink model. However incorporating radiator model will bring a step closer of obtaining the operating performance of the heat pump, because in this way the heat pump heating circuit is included in the calculation of the heating demand. There is also the option of using the radiator model alone to generate heating demand, as it will remove the 'demand generated every 15 minute' limitation imposed by Simulink to give continuous real time heating demand. The following section gives an account of the current Simulink model [39].

4.6 Simulink Model

The thermal model used within this Simulink model [39] was based on a typical north east semi detached home. This model was build using Matlab® 7.1, Simulink® 6.3 (including Instrument Control Box 2.3 and Real Time Workshop 6.3). Simulink® is a visual programming language extension of Matlab®, which allows for complex systems to be built up from various mathematical and electrical block libraries. There are a large range of possible libraries, and the opportunity to create new libraries using Matlab, C or FORTRAN. The model took and returned data from the Labview controlled heat pump test across Narec's

network via tcp/ip, and also receives data from Narec's weather station. The basics of the model are shown below in Fig. 30.

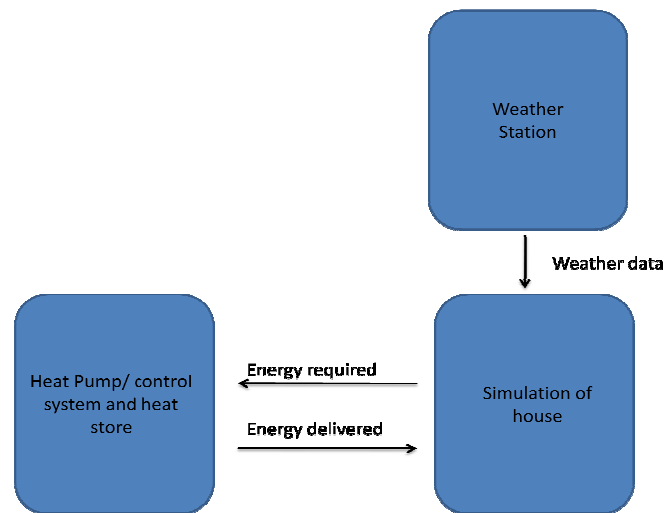


Fig. 30. Interaction between model, weather station and heat pump [39].

The model is based around calculations on fabric loss and air change rate losses. The building also clearly gains energy from the outside when the weather is warm. For the thermal calculations, because such systems are dependent on the state of the system in the previous time step, Simulink® was the ideal choice of software package, as it is well designed to feed in data from previous iterations. The model takes data from both the Narec weather station and the heat pump test control system. It interacts with the hardware by requesting a certain amount of energy, and then receiving an answer from the heat pump control system as to how much energy it can really receive.

The model takes a multizone approach, calculating not only the loss of energy to the outside, but also tracking the flow of energy from one room to another within the building. This is, as with the energy loss, calculated in terms of fabric and air change.

Although the model does have the capability to include solar gain, for the purpose of this test that section has not been used, as the modelling part is not yet complete. Fig. 31. shows the virtual model in more detail.

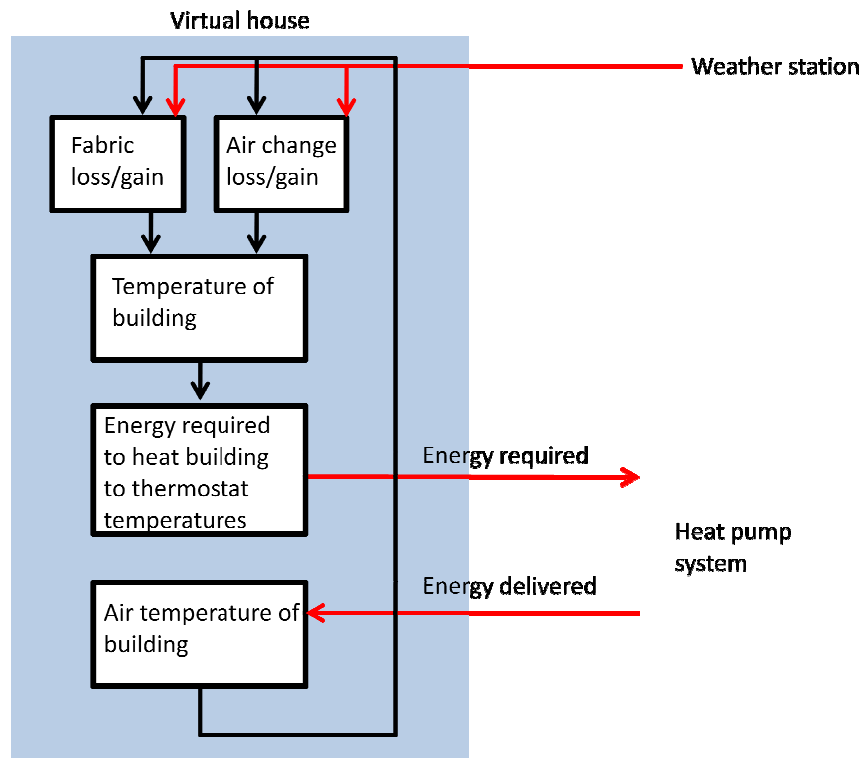


Fig. 31. Simulink thermal model [39].

Air Change losses:

The air change losses are simply the energy lost from air escaping a building. First, take the general formula for heat transfer:

$$Q = mc\Delta T$$

Q = heat energy [J]

m = mass [kg]

c = specific heat capacity [$\text{Jkg}^{-1}\text{K}^{-1}$]

ΔT = Temperature difference [K]

Substitute in $m = V\rho$

$$Q = V\rho c\Delta T \quad (12)$$

This gives the total energy required to heat a volume of air. In order to calculate the instantaneous power required in a building with N air changes per hour of volume V , put in a factor of $N/3600$.

$$P = \frac{NV\rho c\Delta T}{3600} \quad (13)$$

For air at sea level, the following values apply;

$$c = 1012 \text{ Jkg}^{-1}\text{K}^{-1}$$

$$\rho = 1.2 \text{ kg m}^{-3}$$

$$P = \frac{1012 \times 1.2 \times NV\Delta T}{3600}$$

This clearly simplified to;

$$P = 0.33NV\Delta T \quad (14)$$

P = heat power [W]

m = mass [kg]

c = specific heat capacity [$\text{Jkg}^{-1}\text{K}^{-1}$]

ΔT = Temperature difference [K]

0.33 = constant [$\text{J m}^{-3}\text{K}^{-1}$]

An alternative approach to the Simulink model outlined above is shown in Fig. 32. This attempts to incorporate the radiator model into the test program.

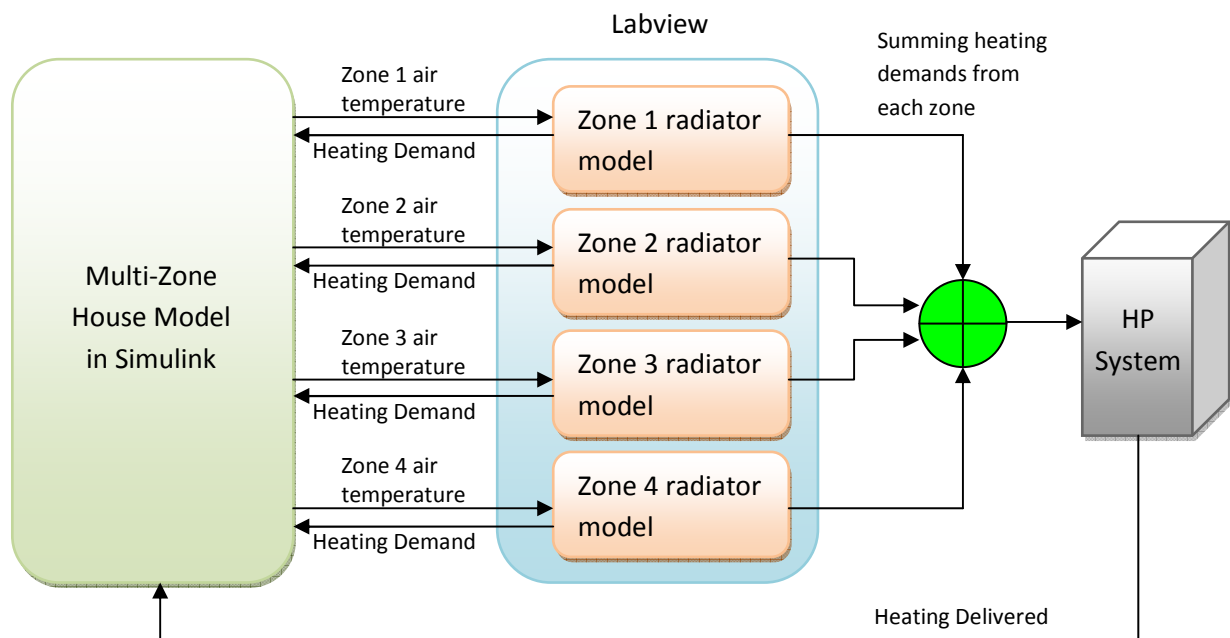


Fig. 32. Incorporating the radiator model with Simulink.

In this software structure, the radiator model is included in Labview and is divided into zones. Each zone generates a heating demand based on the zone air temperature from Simulink and the forward and return flow temperatures of the heating circuit i.e. T_{17} and T_{18} . The individual zone heating demands are fed back to Simulink for allocating heating delivered by the heat pump system to each zone so that it can work the zone air temperatures for the next step. The zone heating demands are summed up and forwarded to the heating control algorithm, then the actual heating delivered is fed back to Simulink for allocation into each zone. The whole process is then repeated for the operating test.

4.7 Test method and procedures

In this project the test platform treats the heat pump system including its buffer tank as a “Black Box”. No sensors are placed within the heat pump or the buffer tank and the heat pump system is tested as a commercially available product. Hence the heat pump will be in its operating condition. The heat pump is an external condenser type (i.e. the condenser is situated outdoor) and is tested outdoor under local weather conditions.

The test platform is capable of carrying out tests for space heating, domestic hot water, combined domestic hot water and space heating. Domestic hot water test uses a daily tapping pattern of various flows for shower, basin, kitchen sink or bath. For tests involving domestic hot water, the effect of solar preheat would be investigated by first excluding the preheat function and then repeating the test by including it. To characterise the heat pump system the tests would involve using fixed levels of heating demands, eventually the testing would move onto using heating demands generated by Simulink or radiator model. COPs, daily COPs and SPF for weekly and monthly durations will be gathered for each of the tests along with weather data, heat outputs and heat pump instantaneous power consumption. So far only daily COPs based on arbitrary heating levels are gathered. Results will be analyzed quantitatively by comparing them against each other for similar weather conditions and against tests elsewhere to identify the factors impacting performance as well as to characterise the heat pump system performance. This includes the identification of dynamic state dependencies and investigation into the possibility of shortening test duration. In later tests domestic hot water draw off pattern will be varied to see the affect of different loading pattern has on the heat pump system.

5. Initial Experimental Results

5.1 Chapter Introduction

This section presents results from using heating circuit 1 and provides an analysis of the results. It begins by commenting on the difficulties and advantages of this heating circuit. This is accompanied by an explanation of the 3-band variable step control scheme designed to overcome the control difficulties. Noises present in the heating control variable is approached and explained via theoretical analysis and published experimental work on in-pipe turbulence. To further understand the heating process of the test platform, the cooling tank was investigated by logging vertical tank temperature variations for different heating levels. The temperature waveforms are analyzed by comparing them with published experimental results on natural laminar and turbulent convections along with their theories.

5.2 Heating Circuit 1 control

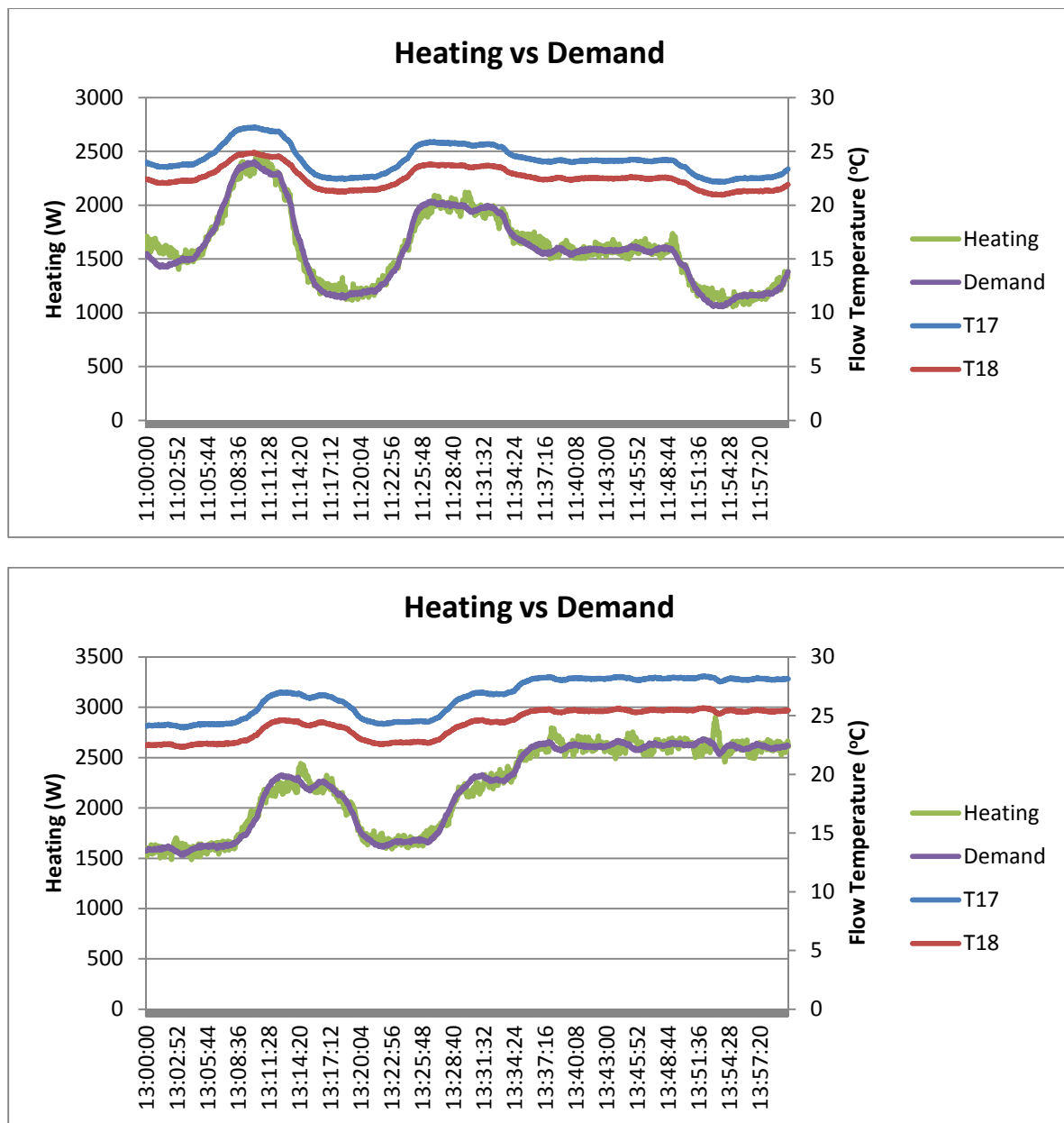


Fig. 33. Showing 2 periods of controlling heating against demand.

Fig. 33 shows 2 one hour periods of controlling heating against the radiator model introduced in the previous section. As seen the control algorithm is able to follow closely the demand. A number of control issues were overcome to arrive at this and these are discussed below.

The advantage as well as the weakness of this heating circuit is the high flow rate around the buffer tank side circulating loop. This is the loop going in and out of the buffer tank and includes the circulation pump. The advantage of this configuration is that any return flow

from the cooling tank finned coil rejoins with the bypassed flow and this would reduce temperature fluctuations in the returned flow. The weakness of the high flow rate on the buffer tank side is that any change in the control valve V2 (see figure 28) will cause accumulative overshoot and undershoot of the bypass loop temperature, and this in turn will affect the buffer tank weather compensation 4-way mixing valve resulting in further heating fluctuations. The same happens if the control valve is stationary and the inflow temperature from the buffer tank changes, overshoot and undershoot in $T17$ and $T18$ will occur.

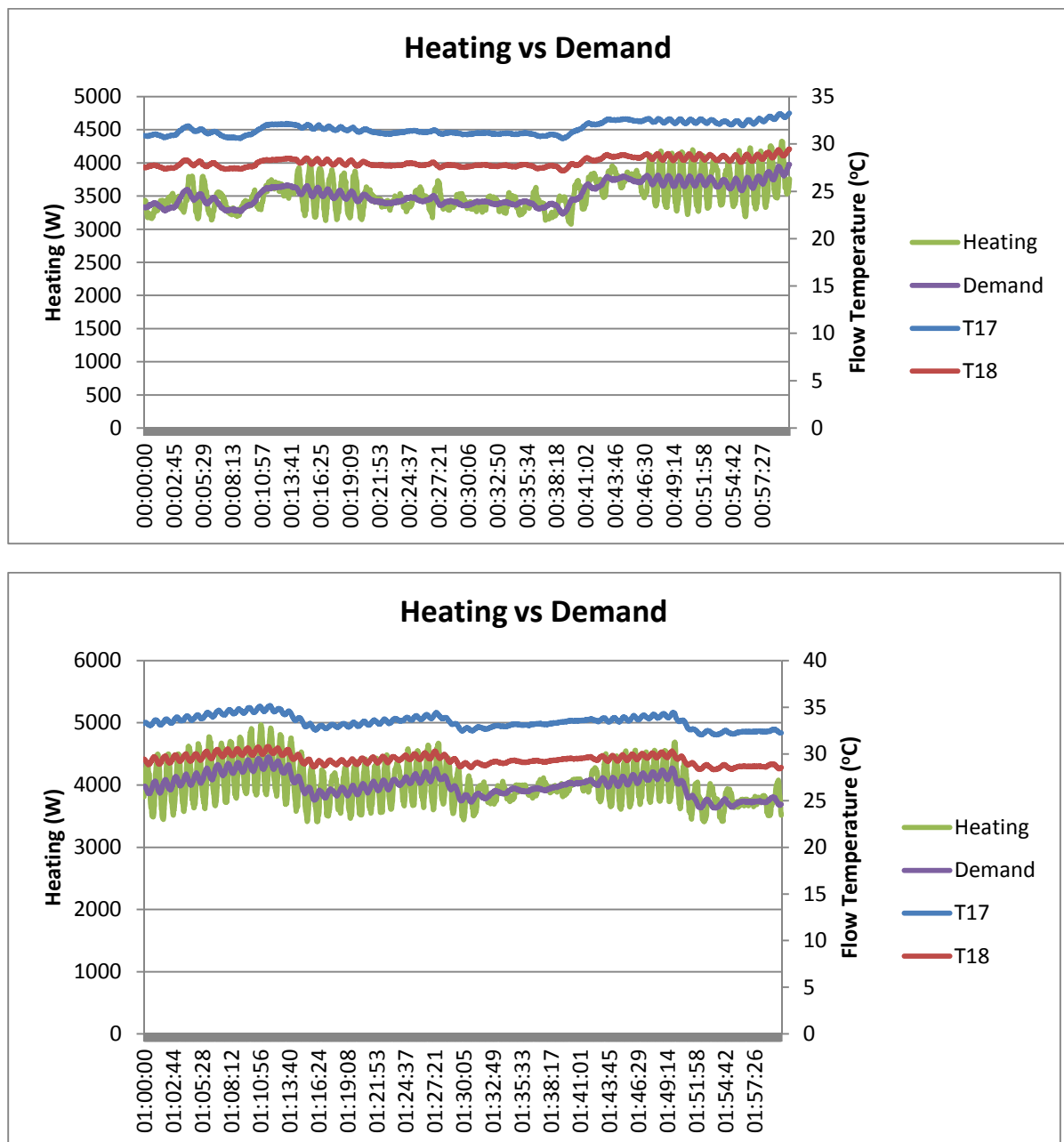


Fig. 34. Control resonances for 2 one hour periods.

There is a control issue with regard to accommodating the unknown weather compensated control of the buffer tank. Part of the reason for including the radiator model was to investigate how to accommodate this, since if the heating demand is generated based on $T17$ and $T18$, this will fall within the range of possible heating levels of the weather compensated control at that point in time. The additional advantage as mentioned in the previous section is that if done correctly this will maintain the natural behaviour of the weather compensated control. In terms of control, resonances will occur at different frequencies if $V2$ is varied at a particular frequency, and this is shown in Fig. 34.

The resonance is caused by the control valve $V2$ resonating with the weather compensated 4-way valve because if the weather compensation employs a PID controller it will have certain PID settings tuned for this application. The overshoot effect on $T17$ and $T18$ mentioned earlier also contributes to the resonances. If $V2$ is adjusted too frequently, the weather compensated control will not be able to keep up with the changes in $T17$ and resonances will occur. It was found that the frequency of $V2$ adjustment whilst maintaining control stability is lower than that required to keep up with changes in demand. To overcome this a 3 band control scheme was designed and implemented. Each band is activated based on the level of control error, the outer band gives $V2$ the largest step change per second, while the inner band gives the smallest step change. Fig. 35 illustrates how this works. The implementation of the 3 band control scheme resulted in the elimination of the resonances while still able to keep up with changes in demand (figure 33).

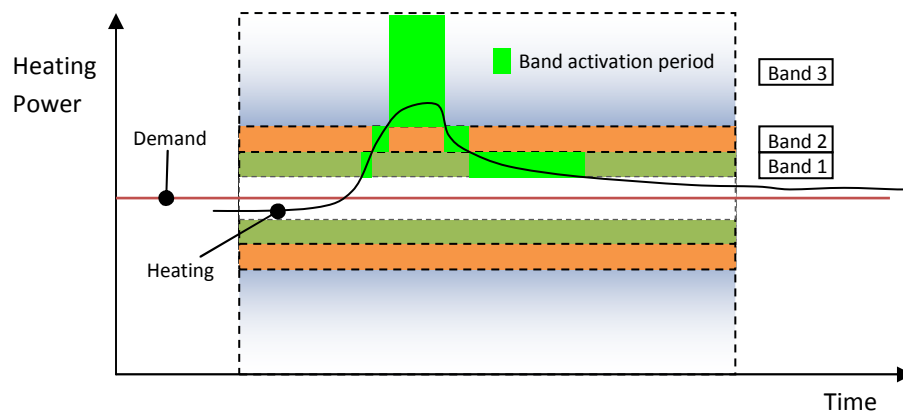


Fig. 35. An example of using the 3-band control.

From the start of the heating curve, as the error between demand and heating exceeds the Band 1 limit, Band 1 is activated as shown on the diagram. If the change in heating is too large for Band 1 to control and the demand error exceeds the Band 2 limit, Band 2 is activated and will more aggressively try to bring the heating back down to the demand level. The effect of this can be seen as the decreasing slope of the heating curve. If Band 2 is unable to bring the heating back down into Band 1, finally Band 3 is activated, as can be seen this brings down the heating very quickly. However this is too quick for the heating circuit and the heating will undershoot the demand and will also result in oscillations. This is where Band 2 and Band 1 comes in again, this time they act as damping functions reducing

the gradient as heating approaches the demand. Another enhancement to this control scheme was adding a gradient based damping function, that was shown to be more effective in bringing the heating into stability.

Underneath the 3-band scheme is a table look up control scheme to pre-determine roughly the position of V2 before the 3-band scheme takes over. The table lookup scheme uses an experimentally obtained table connecting heating, $T17$ and $T18$, and cooling tank temperature (Table 6). This is valid because of the physics of heat exchanger heat transfer; in this case it was based on a linear radiator model. The reason that the look up table was needed rather than using the 3-band scheme alone is because of the long delay in the finned coil and the overshoot effect of the heating circuit. If 3-band scheme is used alone Band 3 will begin controlling very rapidly to reach the demand, this will overshoot and undershoot the bypassed loop temperature causing instability. Further, the long delay of the finned coil will mean that although the 3-band control tracks the demand, change in heating will occur again after flow delay of the finned coil due to delayed change in $T18$. The reason that the control is able to reach the demand in the first place is due to the bypass branch of the heating circuit, this has no delay and controls the proportion of bypassed flow at temperature $T17$, which rejoins with the cooler flow from the finned coil.

Table 6. An example of the table lookup control.

Heating Demand (W)	$T17-T18$ ($^{\circ}\text{C}$)	Cooling Tank Temperature ($T13$) $^{\circ}\text{C}$	Valve Position (2-10 Vdc)
...
...

Another control issue is that there exists a variable amount of noise in the heating. There are two types of noise, one increases as the heating level increases, the other exists when the valve V2 is adjusted repeatedly. The first noise could have component of temperature probe error, this tends to increase with water temperature. However, it is thought that the main reason is due to turbulence in pipe flow. The second noise is either due to turbulence in pipe flow or flow delay in finned coil.

An experiment on turbulence in pipe flow was carried out in [40]. Here, turbulence in pipe flow is formed by an injection or suction of liquid into or out of the laminar flow, this acts as perturbation to the laminar flow, and is often found in practical pipes. The experiment was to investigate the amount of injection and suction have on the length the turbulence travel before decaying. Fig. 36 shows the results for this experiment.

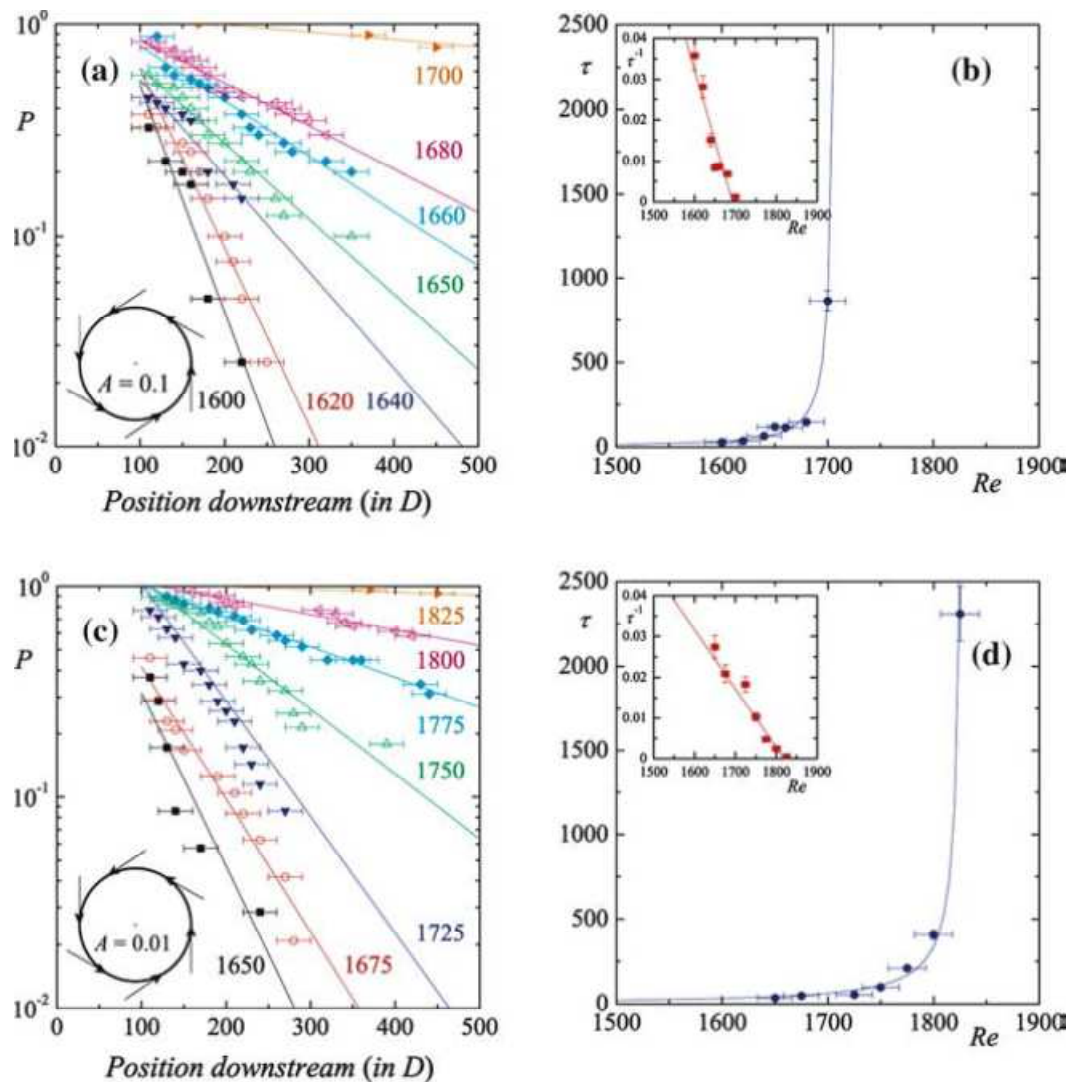


Fig. 36. (a) and (c) shows how far the turbulence travel in pipe diameters for injection amplitudes of 0.1 and 0.01 respectively. P is the probability of a particular travel length happening. The coloured lines are for different Reynolds numbers. (b) and (d) shows the half life of the turbulences for different Reynolds numbers for the two injection amplitudes [40].

Fig. 36 (a) and (c) shows that for similar Reynolds numbers a higher injection amplitude will increase probability of producing turbulences that travel a lot longer. In the heating circuit, when V2 is opened more forward flow will be sucked from the total flow into the finned coil and more return flow from the finned coil will join with the bypassed flow. This is similar to the injection and suction in the experiment, and is likely to cause turbulence in the bypass loop. As the amount of return flow from the finned coil increases, this is similar to increasing the amplitude of injection in the experiment, and will increase the probability of the turbulences to travel further. Given the length of the bypass loop, as the turbulences travels further, many will rejoin with other turbulences created, this could potentially increase the level of noise observed. Also presented in [40] is another phenomenon that could help to explain the increase of noise. The increase in injection amplitude appears to also increase the kinetic energy of the turbulences created, as observed in Fig. 37.

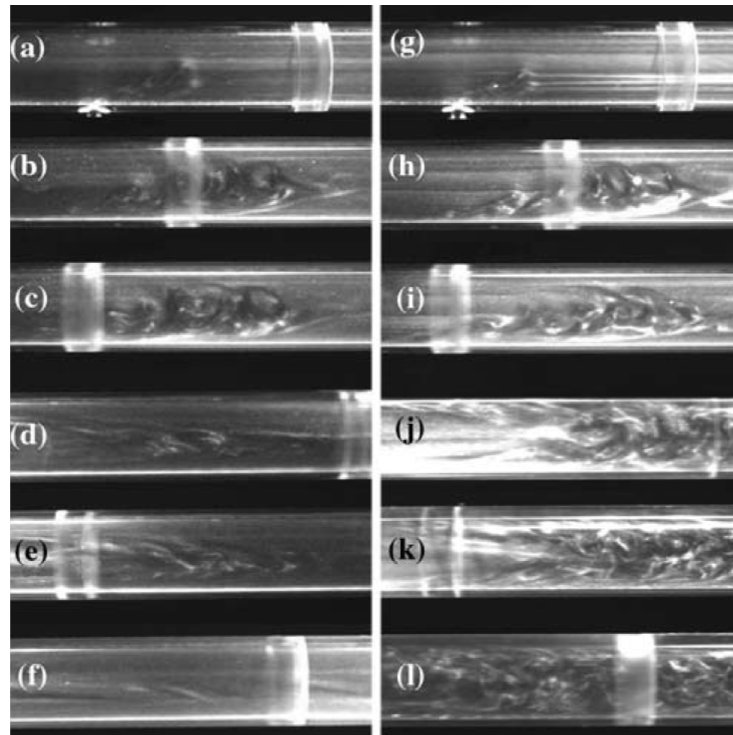


Fig. 37. (a) to (f) shows the onset of turbulence when a small amount of fluid was injected into the laminar flow. (g) to (l) shows that a 'puff' was created when a larger amount of liquid was injected [40].

It can be seen from Fig. 37 the difference in the turbulence structure when a larger amount of fluid was injected. The turbulence appear to be more violent and has more kinetic energy. This could explain the increase in heating noise when V2 is opened, as the amount of suction and injection increases for the total flow the kinetic energy of the turbulences increase causing higher noise. Most importantly however, one major difference between the experiment in [40] and the heating circuit has not been accounted, and that is the joining of warmer and cooler fluid at the heating circuit bypass, where as in [40] the injection is at the same temperature as the main flow. This means that as V2 is increased more cooler fluid from the finned coil will mix with the less warmer fluid from the bypass, this results in increased temperature gradient across the turbulences, which will result in more fluctuations in T_{17} and T_{18} and in turn leads to more heating noise. Combined with the phenomenon in Fig. 36 and Fig. 37, more heating noise will be seen as V2 is opened.

Going back to the two types of noise, the formation of turbulence in pipe flow explains why heating noise increases as the level of heating is increased. The formation of pipe turbulence also explains the creation of noise when V2 is perturbed repeatedly. It was observed that after V2 was perturbed, the noise pattern reappeared after a delay. This could be due to turbulence in the finned coil emerging after its delay, or due to turbulences travelling many times in the buffer tank side bypass loop. However, due to the slow flow in

the finned coil and the long length of the coil it is unlikely that turbulence will survive after travelling through the finned coil.

5.3 Cooling Tank dynamics

To further understand the control issues, an experimental and theoretical investigation into the cooling tank physical dynamics was performed by logging vertical tank temperatures for different heating levels of heating circuit 1.

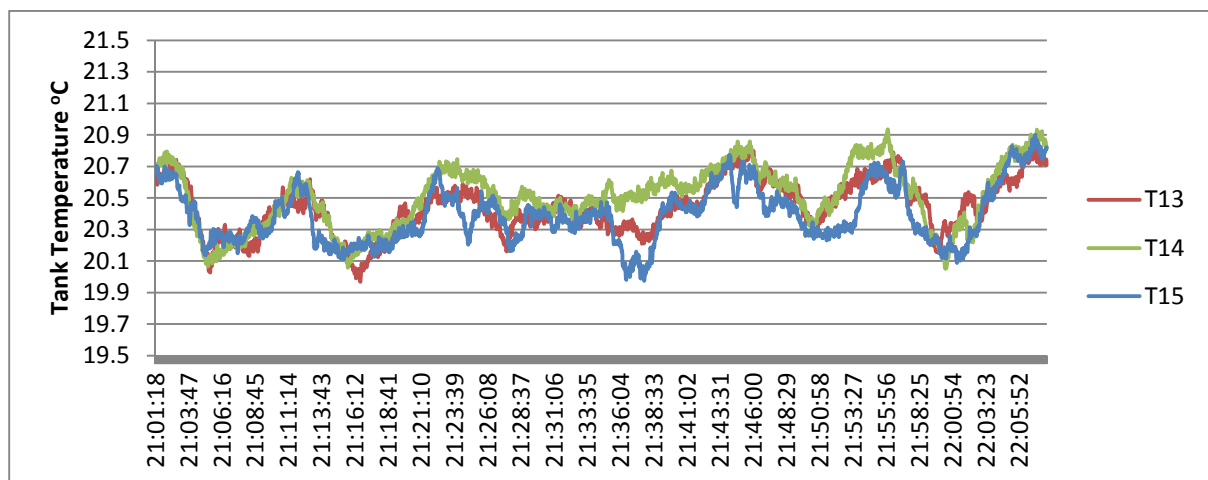


Fig. 38. Cooling Tank Vertical Temperatures for 3kW heating.

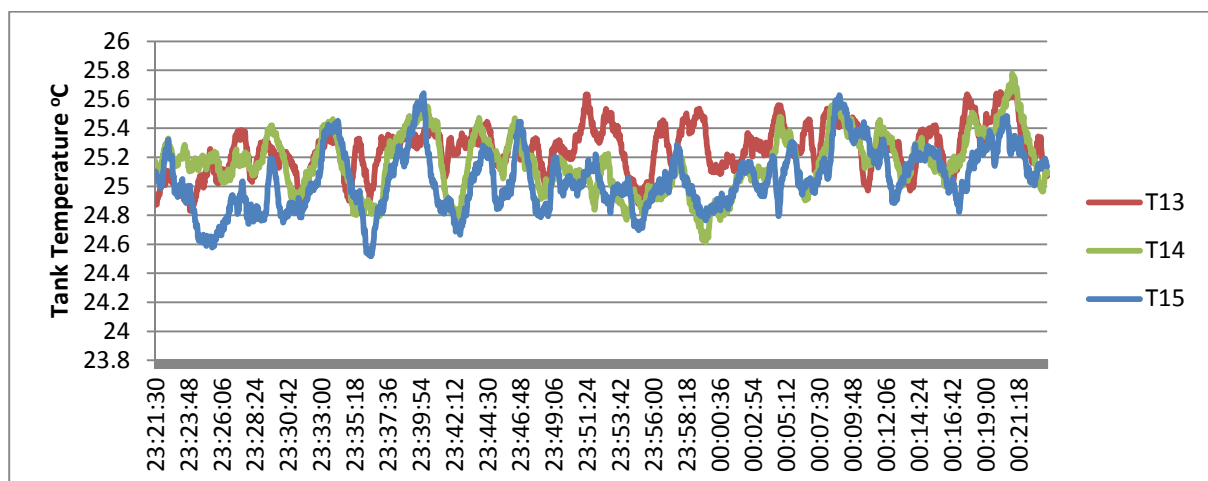


Fig. 39. Cooling Tank Vertical Temperatures for 7-8kW heating.

Figures 38 and 39 shows the vertical temperature logs of the cooling tank over a 1 hour period, please refer to Figure 27 for the position of the temperature sensors T13-T15. T12 and T16 are not used as they were not calibrated. The aim of this data collection is to aid

understanding of the physical and dynamic nature occurring inside the tank. The data are presented in two conditions, Fig. 38 is for lower heating and heat input to the tank i.e. 3kW and Fig. 39 for higher 7-8kW heating input.

Fig. 38 shows the repeated pattern of heat building up inside the tank and then removed by the upper coil when the chiller comes on. In this respect Fig. 39 shows that there is increased high amplitude temperature fluctuations as significantly more heat was input to the tank, and the tank is now operating at a higher average temperature of 25°C and rising compared to 20°C average temperature in Fig. 38.

The main process of heat transfer inside the tank is natural convection. There are two types of natural convection, laminar convection and turbulent convection. The condition of which type occurs depends on the tank dimension, position and shape of the coils, and the temperature gradients inside the tank. In this measurement method, turbulent convection or formation of turbulence would be seen as high frequency temperature fluctuations of exceeding 1°C [41]. This is neither observed in Fig. 38 or 39, which can conclude that large scale turbulence doesn't occur inside the tank. This also means that small turbulences near the finned coils are less likely to occur, as according to [41] their formation is caused by the large scale turbulence hitting rough surfaces. So the mechanism of heat transfer inside the cooling tank is hypothesised to be predominantly the formation of laminar plumes. Although the effect of plumes generated from lower turns of the finned coil hitting higher turns is unknown, and this can result in turbulence for the higher turns. More details of this will be given next.

The theoretical work concentrates on the physics inside the cooling tank as just introduced in experimental work. Since the results in the previous section indicate that the convection process is laminar, further literature research went into laminar plumes. Details of the formation of laminar plumes are given in [42] via theory and experiments. The plume cap spreads out as it rises up and the plume temperature decreases with height. The velocity at which the plume rises depends on the source power, in this case heating input to the tank. Single plumes will join to form larger plumes if close together and the combined upward speed will increase proportional to $\sqrt{2}$ multiplied by the power of each plume. This is applicable to the cooling tank finned coil, if each fin creates a single plume, then they will join up forming a cylindrical plume that has a large surface area. The mechanism of the formation of the plume cap and stem and their growth in steady state is of diffusive in nature. Contrary to the low heat transfer of the thermal diffusion, plumes have enhanced heat transfer via entrainment – the circulation of cold water at the boundary layer of the plume – and this gives 17.5 times more heat transfer than thermal diffusion alone [42].

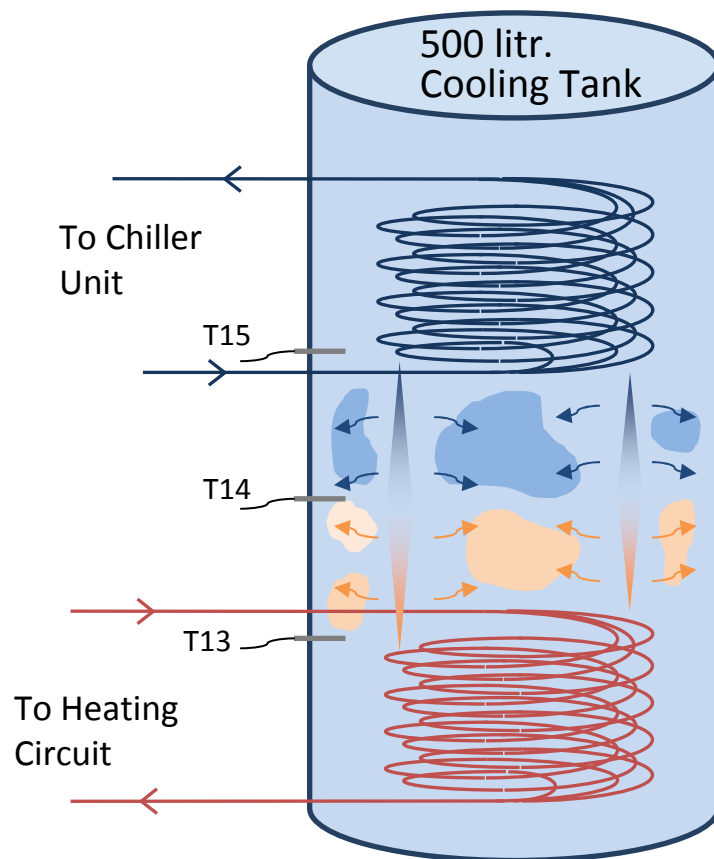


Fig. 40. Illustrating instances of the temperature and width of the plumes and the warming up of surrounding liquid. The patches show the resulting secondary plumes formed.

Returning to the results, Fig. 38 shows that the temperatures at the 3 levels of the tank vary together at an average value of 20 °C, this is no way near the heat source temperature of 29°C. This is probably due to the temperature probes are at a distance away from the path of the plumes, and plumes should be quite thin at such high heat power output [42]. Occasionally the three tank temperatures separate out, this is probably due to the cold water surrounding the plumes warms up by the plumes forming larger secondary very slow moving plumes. This is illustrated by Fig. 40 where the patches represent the secondary plumes formed. These will then begin to move around; some may join, and cool and warm plumes may interact. These are very slow moving because temperature differential against rest of the cold water is very small. Fig. 39 shows that the three tank temperatures differ greater and more frequently, implicating that the surrounding cold water cannot maintain an equilibrium heat transfer state and secondary plumes form more frequently at higher temperature differentials, these have more frequent movement and hence more temperature fluctuations. This however does create an environment that increases the probability for the creation of turbulent convections from the coils [41].

Given sufficient heating it is possible that the rising hot plume and the falling cold plumes will collide [42]. Fig. 41 shows how hot and cold plumes interact, they don't mix, instead they form a front and then slide past each other.

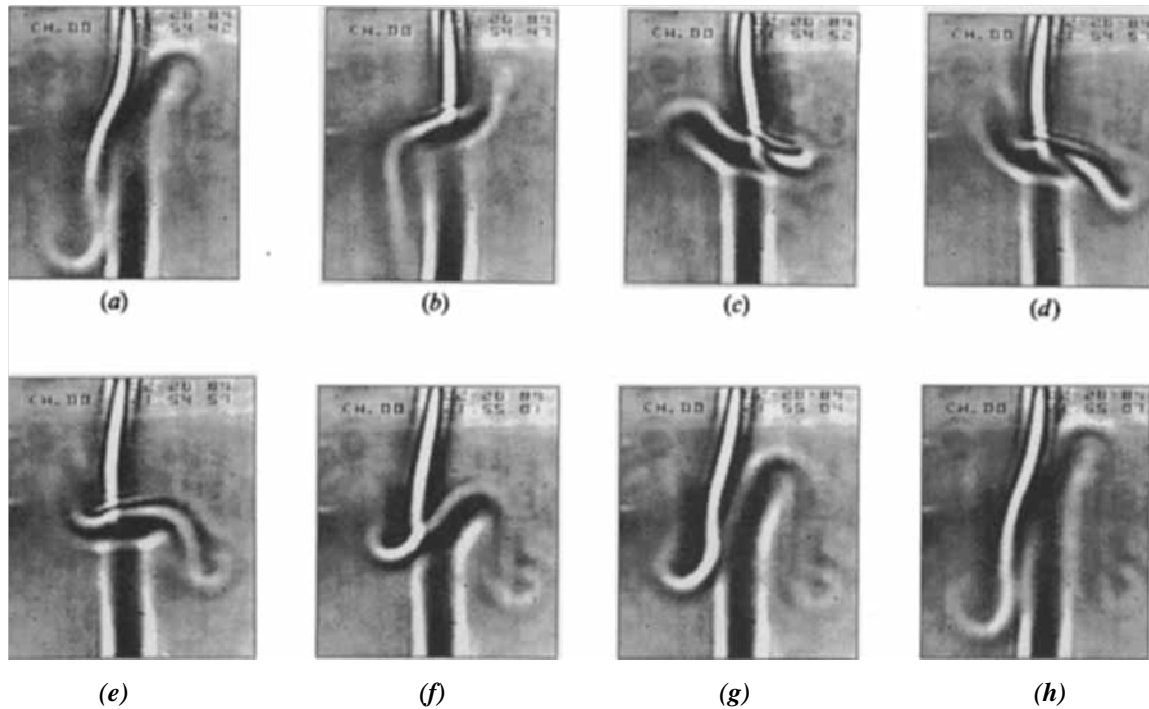


Fig. 41. The photographs from show the collision of hot and cold plumes. Time frame is: (a) 0s, (b) 5s, (c) 10s, (d) 15s, (e) 17s, (f) 19s, (g) 22s, (h) 25s [42].

However the strength of cold plumes in the cooling tank varies since the chiller operates in on/off mode. This cycling will introduce unstable dynamics to the cooling tank not allowing the heat transfer dynamics to reach a possible steady state. This in turn may contribute to the temperature fluctuations in T13-T15 in Fig. 38 and 39. At higher levels of heating this becomes significant and may add noise to the heating. This could form another reason to consider for the increase of noise in heating as heating level increases. A potential solution would be either changing for a larger buffer tank to the chiller or adding a circulation pump to the cooling tank.

6. Heating Circuit 2 and Control

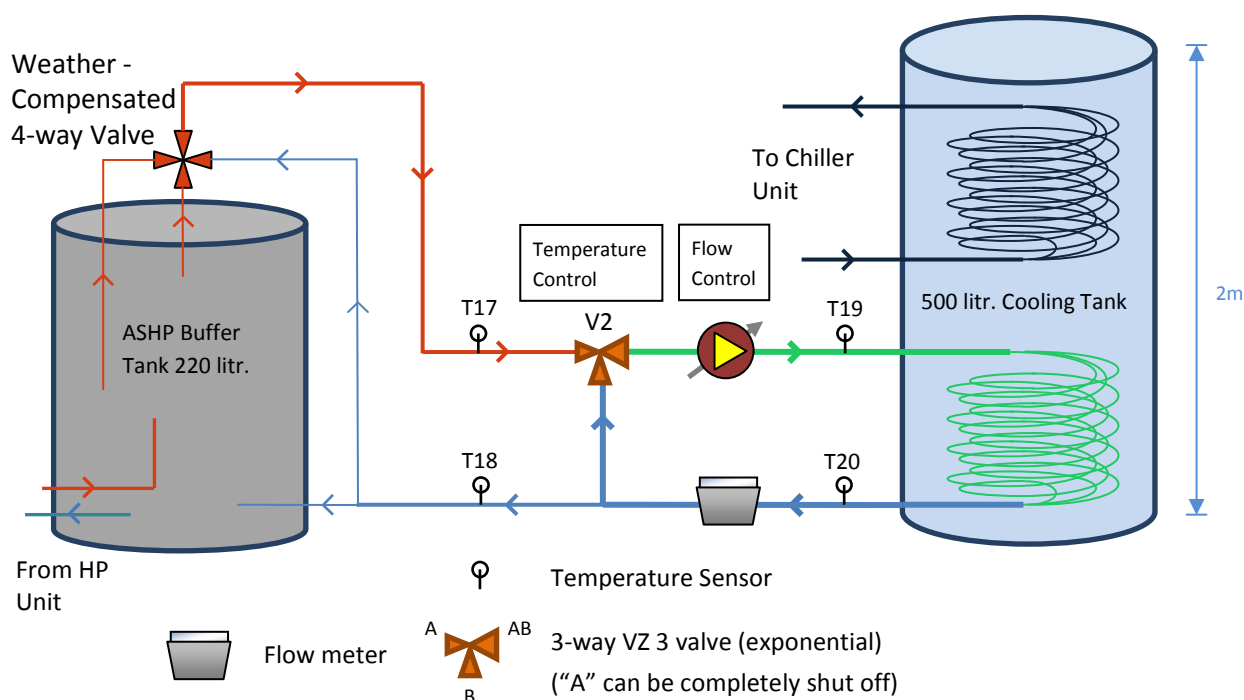


Fig. 42. Heating Circuit 2.

Fig. 42 illustrates heating circuit 2. There are several motivations to designing this heating circuit. Heating circuit 2 adopts simultaneous flow and temperature control, and moves the high flow loop to the cooling tank side. In comparison to heating circuit 1, this is able to output lower levels of heat between 0 to 2kW, whereas heating circuit 1 struggled to do this. This owes to the addition of temperature control, and the ability to output low temperature flow with good flow rate (> 7 litre/min). Heating circuit 1 only uses flow control, and given the large temperature difference between T17 and the cooling tank, the flow would have to be very slow to achieve heating of 0 to 2kW. It was hard to achieve such low flow with heating circuit 1, and it gave unstable heating, not to mention the extremely long flow delay through the finned coil as a result.

Heating circuit 2 takes into account the flow delay in the finned coil, this enables more accurate heating measurement when the heating varies continuously. The flow delay is taken into account by logging T19 and then calculating the flow delay using the flow rate and the finned coil length. The finned coil length was measured experimentally by significantly perturbing T19 and then timing the delay for the perturbation to arrive at T20. The exact coil length was found to be 6.9m or approaching 7m. The flow delay was then

calculated in real-time and used to select the historical T19 value corresponding to this delay.

The flow delay and flow speed are separated in heating circuit 2. In heating circuit 1 if V2 is varied to change the flow rate through the finned coil, the heating measurement using T18 would have to wait for this effect to take place and therefore results in inaccurate heating measurements if V2 is adjusted frequently. However, in heating circuit 2 this is avoided. The change of flow through the finned coil using the variable speed pump result in instantaneous change in heating. This means heating circuit 2 offers much more responsive flow control over heating circuit 1, and results in better control of heating.

Another significant advantage of heating circuit 2 is the reduction of the overshoot/undershoot effect in heating circuit 1. A change in V2 in heating circuit 2 will not cause much overshoot as the flow in the buffer tank side loop now increases with opening of V2 and generally has much lower flow rate than the buffer tank side loop of heating circuit 1. The flow rate in the buffer tank side loop now only increases with higher heating requirement when more heat is taken away. Similarly the loop flow rate decreases when less heat is taken away and so no excess heat energy is built up or lost in the loop.

Similar to heating circuit 1, as heating is increased in heating circuit 2 the heating noise level increases. In-pipe turbulence can occur in heating circuit 2 as flows from the heat pump buffer tank and bypass join at V2 very much the same way as heating circuit 1.

Previously in heating circuit 1 the table look up scheme uses a table of values that are based on the assumption that the return temperature of the finned coil does not vary greatly. However now that a temperature sensor (T20) is mounted on the finned coil return, it was observed that this is not the case and the return temperature of the finned coil does vary in step with the forward temperature (T19). This may explain uncertainties observed when obtaining table lookup values. It was also observed that T20 contains significantly more noise than T19. This supports the theoretical work on the cooling tank that it can also contribute to heating noise. However this may be due to the finned coil itself as it splits up into 3 parallel pipes and rejoins near the exit. However given the long length of the finned coil and the addition of higher amplitude noise this suggests that new temperature gradient was added to the flow, and this can only be caused by the heat transfer to the cooling tank.

The main disadvantage of heating circuit 2 is that it may not be suitable for the radiator model, since this installation does not follow a standard installation. However based on energy equivalence T17 and T18 may remain similar to that in heating circuit 1. Even if heating circuit 2 is not suitable for a radiator model, it is better suited to a computer model as it potentially offers better control of heating.

The control algorithm for heating circuit 2 was simpler than that of heating circuit 1, and this was another advantage of heating circuit 2. The control scheme adopts simultaneous flow

and temperature control. V2 controls the temperature of T19 and T20 and the variable speed pump controls the flow rate. The idea was to adjust V2 so that for the given heating demand the required flow rate sits within the flow control range of the variable speed pump. This is necessary as the flow range of the variable speed pump is affected by the position of V2. To achieve this a lookup table was created for positions of V2 (0-10 Vdc) and the flow range for each position. For lower voltage values of V2 the flow range leans towards lower flow rates and for higher voltages the flow range reaches higher flow rates. However, many of the flow ranges overlap as V2 is varied, and because of this the control algorithm can be simplified further. For a given heating demand, the control program calculates the flow required using T19 (historical) and T20. An upper and lower bound is set based on the lookup table. If the required flow falls below the lower bound, then V2 will open to move the required flow into one of the lower flow ranges. On the other hand if the required flow goes above the upper bound, V2 will open moving the required flow into the higher ranges. The idea here is to also attempt to move the required flow into the middle of the ranges, although experiments show that this is not necessary for slower control rate. Figure 43 shows a flow diagram of the control scheme.

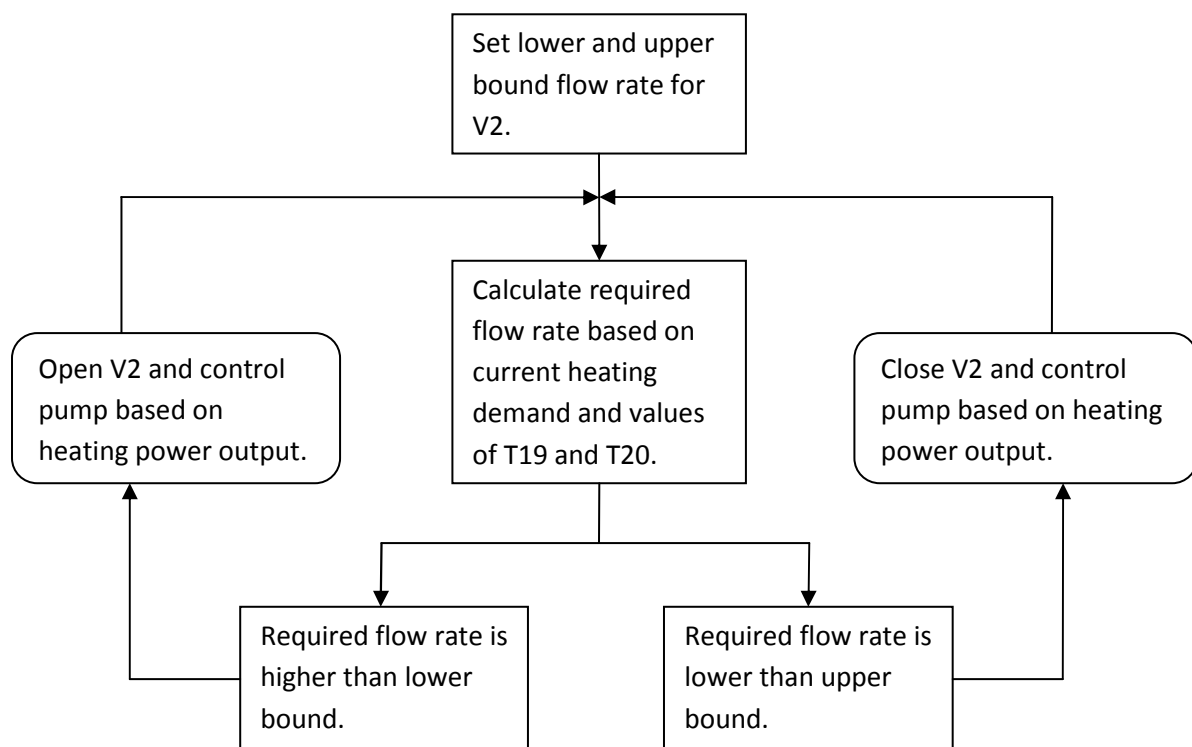


Fig. 43. Flow diagram for the combined temperature and flow control scheme.

Experiments also showed that in order for the pump control and V2 control to work together, V2 needs to adjust more slowly than the pump control. Once this is set the pump

can be controlled quite quickly achieving fast control. The pump adopts fixed step control for the entire heating range. This works well for all the heating levels, even though for higher values of V2 voltage each fix step of the pump control causes bigger change in the flow compared with lower values of V2 voltage.

7. Results 2

7.1 Chapter Introduction

This section presents results that focus on investigating the COP characteristic of the CO₂ transcritical heat pump under test, with description of the experimental method. Daily and night-time COPs were obtained for continuous operation of the heat pump for a month. A strong positive correlation between heating and COP was found for Daily COPs. However there was no obvious correlation of the COPs with outdoor temperatures. To this end the discrepancy in outdoor temperature readings were identified by logging ambient temperature at two outdoor locations, one at a wall in the area of where the heat pump is installed and one at the weather station up on the roof. Finally COPs for heat pump buffer tank heat up test by the heat pump from cold were included.

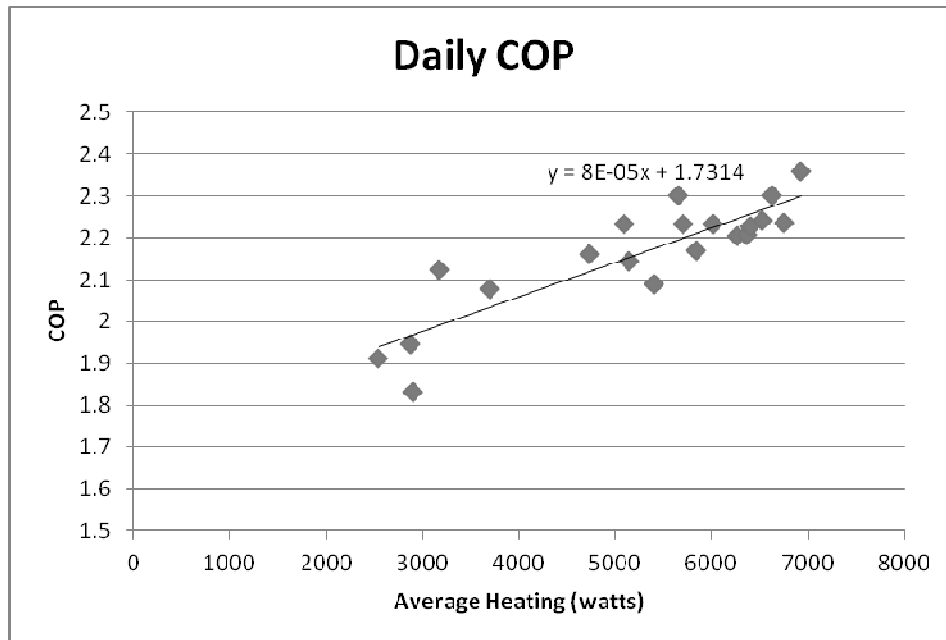
7.2 Daily and Night-time operating COPs

COPs were obtained for heating only with all auxiliary heaters switched off using heating circuit 2 with V2 fixed at either 5 or 10V. Heating was therefore varied only by the weather compensated control of the heat pump buffer tank. The average heating was much higher if V2 was set at 10V. Based on observation of the heat pump electrical power consumption, which varies around 3kW, the COP is expected to increase with the heating level if the variable capacity of the inverter driven heat pump goes up to the manufacture quoted 9kW assuming it's under the same weather conditions. To test if this is the case, heating were logged side by side with COP to see if there is any correlation. Results of which is shown in Fig. 44. The data points were obtained from the 16th of March to 24th April 2012. The daily COPs were calculated by subtracting kWh values for both heating and electricity for 0:00 this day from 0:00 the next day. Night time COPs are similar but were calculated from 7pm to 7am of the next day. Average heating were calculated by summing up all the 1 second step heating powers for that day and then divide by the number of entries. There were occasions where the automated test were interrupted due to an hardware error and in reset the kWh counters in Labview would restart from 0, in those cases the new accumulated kWh values were added to the previously accumulated kWh difference values, provided that the stop gap is small otherwise the daily or night time COP for a day was omitted.

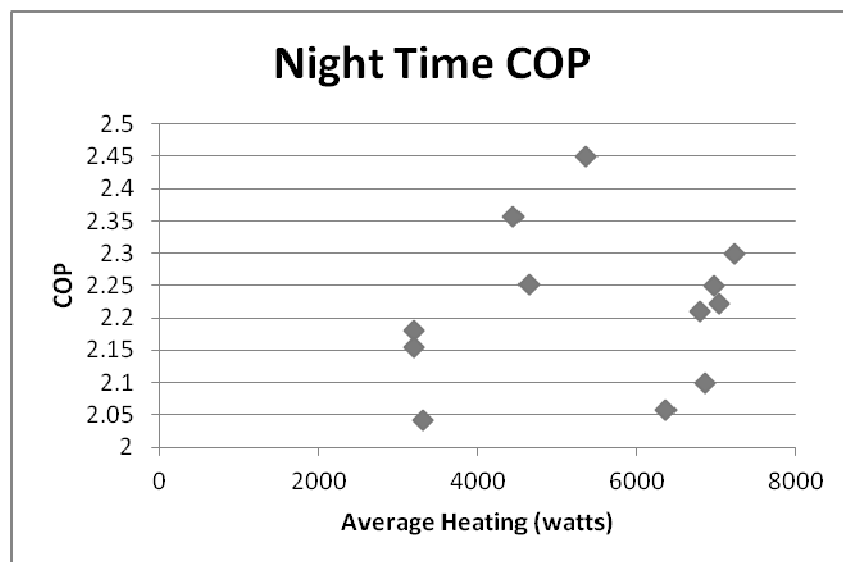
$$\chi^2 = \sum_{i=1}^n \frac{(O_i - E_i)^2}{E_i} \quad (15)$$

A linear fit to the data in Fig. 44 yields a Pearson's chi Squared value (equation 15) of 0.0415 indicating a strong correlation between COP and heating level. In equation 15, O_i is the observed data point (the daily COP), and E_i is the expected data point (trend-line data point). To reduce the uncertainties in the daily COPs the test would be repeated by fixing the heating at predefined levels using the heating control algorithm and recording the corresponding COPs. The highest COP were 2.6 near full load of 9kW, which agrees with calculated value based on observed heat pump average electrical power at outdoor temperature of around 13°C (9/3.3 kW = 2.7). This is not included in the result as it was done differently by fixing the weather compensated 4-way valve at a fixed high output level. This is an interesting characteristic of an inverter driven heat pump. It suggests that it would be best to select a heat pump with a capacity close to the likely average heating demand of the house. If an over capacity heat pump is selected the COP will be unfavourable for the owner. However this is also an issue for the manufacturer as it may be more favourable to manufacture one size for all heat pumps.

Fig. 44 (b) shows the night time COP values against average heating. It is interesting to see there is far less correlation than the daily COP graph. This is mainly due to the heating variations and the on / off operation of the heat pump, which means that it would need longer than 12 hours for the COP to converge to a steady value.



(a)



(b)

Fig. 44. (a) is daily 24 hour COP against heating for month in April. (b) is corresponding night time COPs from 7pm to 7am.

It was surprising to discover that the COP values do not correlate strongly with the weather conditions for those days with similar average heating. This could be due to the effect of

weather on this inverter driven heat pump is small compared to the heating effect, or that the weather temperature is away from the heat pump and does not reflect the outdoor temperature of the heat pump at the point of installation. To investigate this possibility further, Fig. 45 shows a temperature log in 2010 of outdoor temperatures at two locations near the heat pump unit. The weather station sensor is at the roof above the heat pump unit, and the wall sensor is a TinyTag remote compact temperature logger located at one of the walls where the heat pump weather compensation outdoor temperature sensor is located. As can be seen the temperature differences are quite large ranging from 1°C to 5°C owing to differences between the two sensor locations, the weather station sensor is on an open roof exposed to direct sunlight, the heat pump sensor is in a fenced location with other air conditioner units and is not reachable by direct sunlight.

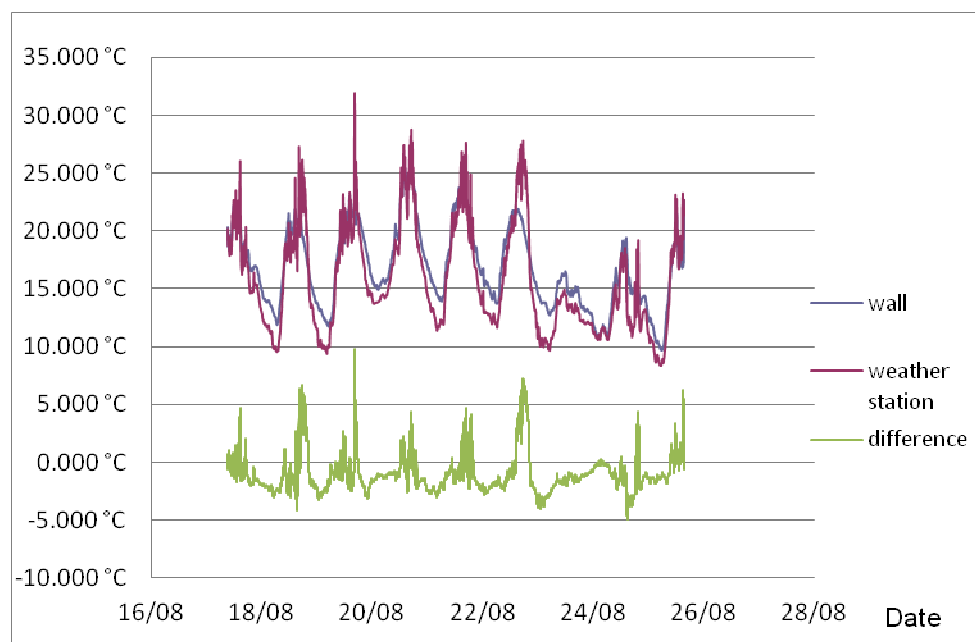


Fig. 45. Logged outdoor temperatures for sensor at different locations in the vicinity of the heat pump unit.

7.3 Heat pump Buffer Tank heat up test

A buffer tank warm up test was carried out to characterise the heat pump's performance with respect to tank water temperature. The heat pump buffer tank was cooled to 19°C with the heat pump switched off, and then heated up to 58°C with the heat pump switched back on. The COPs were calculated for every 5°C of water temperature rise. The result is shown in Fig. 46.

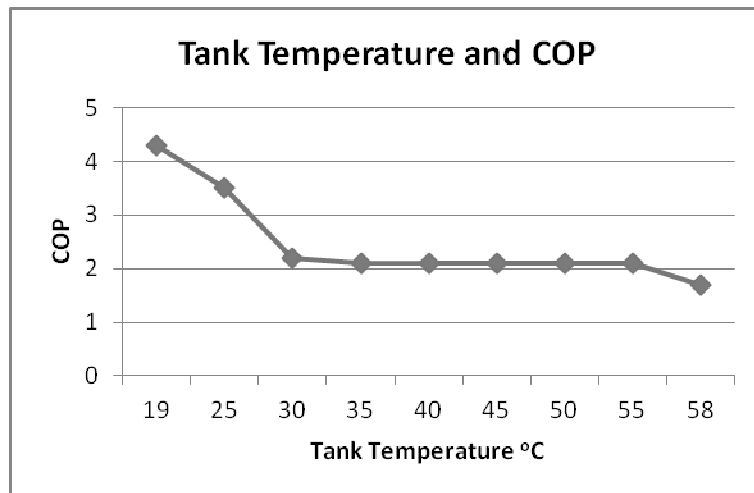


Fig. 46. COP against Tank Temperature.

8. Discussion and Analysis

This section focuses on attempting to explain why the COP in Fig. 44 (a) is such that it increases with the amount of heating load. This is unusual as most literatures cite COP decreases with increasing heating load.

However, the CO₂ transcritical heat pump tested by the test platform showed a heat load performance characteristic that contradicts with the literature survey on variable speed control and heat load in section 3.7. First the COP of the CO₂ transcritical heat pump increases with heat load, whereas the literatures all point to an increase in performance at part load. Secondly the cycling losses only accounts for 5-7%, but in Fig. 44 (a) the COP improvement from the lowest heating is about 35%, which cannot be due to cycling losses alone. It is important at this point to stress that the CO₂ transcritical heat pump operates in a particular way. Although it has an inverter driven variable speed compressor, the speed of the compressor is often constant at around 59-60Hz, perhaps when the weather changes greatly this would alter more. With this the heat pump operates in an on/off mode, the increase in heat load will lead to the heat pump unit running longer and more frequent.

The COP characteristic can be explained starting with a previous experimental study on an inverter heat pump with HFC125 operating near the critical point [43]. A result of which is shown in Fig. 47. It is interesting that for the highest water temperature the COP increases with compressor speed or heat load, recalling that in section 3.7 COP is expected to decrease with heat load, such as when the water temperature was at the lowest in Fig. 47. This is explained in [43] as could be due to as the hot water temperature increases, the refrigerant pressure increases, and this increases the heat transfer coefficient of the refrigerant, overcoming the decrease in performance when the compressor frequency increases.

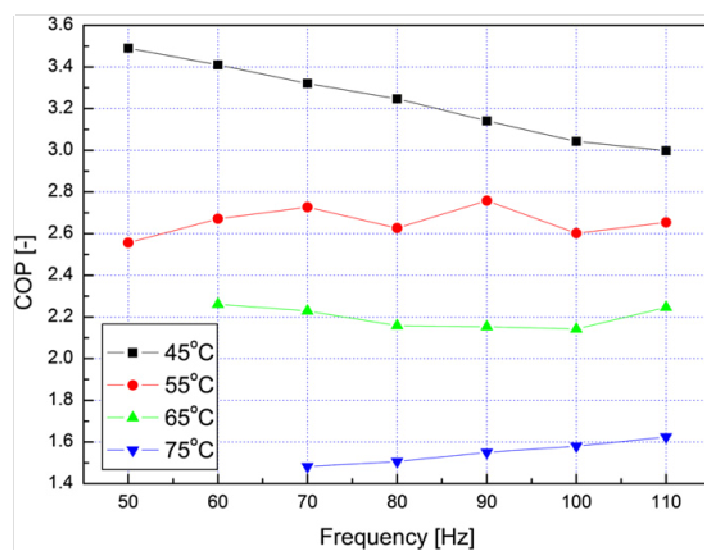


Fig. 47. COP against compressor frequency at different water temperatures [43].

Although the CO₂ heat pump under test does not vary much in compressor frequency, the rise of refrigerant pressure could partly explain the increase in COP with heat load. Prior to the COP tests it was observed that the compressor power consumption would rise slowly as the heat pump runs, the longer the heat pump runs the higher the compressor power would reach. It varies from approximately 2.7kW to a maximum recorded of 3.7kW. The duration of this increase in power consumption takes about 2.5 hours or more. Along with this increase is the steady rise in compressor discharge temperature.

It is stated in [32] that a rise in CO₂ refrigerant pressure of 5 bar would cause increase in compressor consumption of 10%. Scaling this for the CO₂ heat pump compressor of 35% in consumption variation would result in around 15 bar of pressure increase. Fig. 48 shows a graph from [32] that show how the COP varies for change in pressure of CO₂ as a transcritical refrigerant. It can be seen that for a 15 bar of pressure increase in the gas cooler, the COP could rise by 0.85, which is similar to the COP variation in Fig. 44 (a) taking 2.6 as the maximum: $2.6 - 1.8 = 0.8$. This forms a good average estimate for the heat pump's overall performance variation. The reason for the pressure increase in the CO₂ heat pump for a compressor at constant speed may be due to the increase in compressor pressure as it runs continuously, caused by the rise in heat pump inlet temperature. The rise in compressor discharge temperature over time supports this.

However the actual performance of the heat pump is higher than that in Fig.48. This is due to the high efficiency of the 2 stage rotary compressor at high pressure differentials. The rise in discharge temperature enhances the gas cooler heat transfer and therefore the COP, which forms another major factor in performance gain.

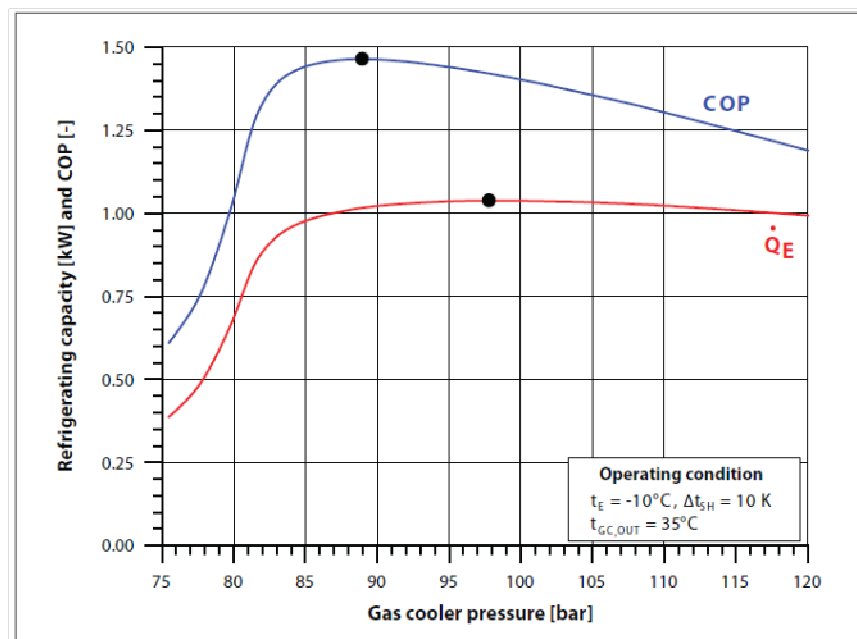


Fig. 48. Effect of gas cooler pressure on refrigerating capacity and COP [32].

This explanation of COP increase over time for each heat pump running time would also explain why Fig. 44 (b) show a much less correlation between COP and heating level. This is because for a given heating output the heat pump comes on at different duty cycles and the COP for each cycle is different, and this would require a large amount of data to converge at an average value, this is more the case if the heating varies continuously such as in the test.

It is interesting here to recall that in section 2.8 , the result for the second field trial in Sweden (Fig. 16) exhibited similar trend between SPF and heat load. Investigation into studies like this could help explain the phenomenon between COP and heat load.

On a note of the outdoor temperature sensor locations, Fig. 45 shows there are significant discrepancies between the heat pump's weather compensation outdoor temperature sensor and the weather station sensor. This has implication for the heat pump performance as many air source heat pumps in the UK are installed in a sheltered location like the one in the test platform. Therefore the air source heat pump performance will depend on local temperature of the heat pump rather than global weather temperature, and it is yet to investigate how sensitive this effect may be.

In the heat pump buffer tank warm up test (Fig. 46), initially the COP was high, and then it quickly drops to a constant value of 2.1. This agrees with most literatures which cite a linear decreasing relationship between COP and hot water temperature. However the drop in this case is quite sharp and hits a bottom COP of around 2.1 starting from 35°C. This probably owes to space heating being turned off leading to faster rise in inlet temperature to the heat pump; or that the internal pressure control of the heat pump readjusted to operate at normal tank temperatures after first switch on. Normal operation should see further improvements to COP for long running times.

9. Conclusions and Recommendations for Future Work

To support the fulfilment of the renewable energy target in the UK by heat pumps, there needs to be ways of measuring the performance of air source heat pumps and understand new technologies as they arrive to market. This project set out to investigate a possible testing platform of testing air source heat pumps by testing a new CO₂ transcritical air source heat pump product. The investigation began by working out how to control heating using heating circuit 1, as the use of simple control was met with difficulties in controlling heating to follow heating demands. This then gave rise to an interest in the inclusion of a radiator model to generate heating demands and interfacing with the Simulink model. In turn this led to investigation into the heating of real radiators and how this differs to heating by the test platform cooling tank and finned coil. The comparison resulted in the belief that their difference will affect the heating behaviour and hence the performance of the heat pump. To cope with this the heating demand was generated by a radiator model based on the forward and return flow temperatures from the heat pump buffer tank.

The control algorithm for heating circuit 1 was designed with the radiator model in mind. The difficulties that were overcome in order to successfully control the heating were: the overshoot and undershoot of the forward flow temperature due to the high flow rate of the buffer tank side of the heating circuit; the freedom of the heat pump buffer tank weather compensation control; the slow traverse rate of the control valve to keep up with changes in demand; the resonance in heating output as a result of these factors; and the noises present in the heating power due to in-pipe turbulence. Along with the radiator model a three band variable step control scheme with gradient based damping at each band were designed to successfully overcome these issues.

In order to better understand the processes of heating by the test platform, a theoretical and experimental investigation was carried out on the cooling tank. Vertical tank temperatures were logged for heating circuit 2 for two different heating levels, a low level of 3kW and a high level of 7-8 kW. For low level heating of 3kW, long duration (12 minutes) temperature fluctuations were observed due to on/off cycling of chiller. Short duration (1-2 minutes) temperature fluctuations were also observed and this attributed to natural convection process. At high levels of heating around 7-8 kW, only short duration (1-3 minutes) temperature fluctuations with significantly larger amplitudes were seen. The pattern due to chiller cycling were masked by these larger fluctuations. The above observations along with theoretical and published experimental work on turbulence and natural convection point to the dominance of laminar convections as the main process of heat transfer inside the cooling tank. The role of the cooling tank may indeed have an effect on the heating noise and possibly control stability since at different levels of heating output the temperature fluctuations inside the cooling tank have a different pattern.

The investigation into heating circuit 1 has provided insight into the possible implementations of the radiator model. The radiator model can be implemented either as an interface between Labview and Simulink model, or as a standalone heat demand generator. Both offer the benefit of improving the natural behaviour of the heat pump under test, and hence would result in COPs that better reflect the operating performance of the heat pump. A standalone radiator model would offer the added benefit of generating real time demand, as opposed to the current Simulink model producing a demand every 15 minutes.

The drawbacks of heating circuit 1 were identified and the possibility of improving heating control led to the development of heating circuit 2. The drawbacks that have been overcome by the design of heating circuit 2 are: the high flow rate on the left side of heating circuit 1 that led to overshoot and undershoot of forward flow temperature; the long delay of flow through the finned coil that led to heating measurement error and control difficulty; and the inability to output and control heating at low heating levels. The combination of flow temperature and flow rate control instead of only flow rate control in heating circuit 1 offered heating circuit 2 the improvements of a much simpler control algorithm and a more responsive heating control.

Using heating circuit 2 without any heating control obtained Daily COPs for a month for heating only. The results discovered a positive linear correlation between heating and COP. The COP ranged from 1.8 to 2.6 for heating variations of between 3 and 7kW. Using theory of CO₂ as a heat pump refrigerant and published experimental work, a possible explanation were offered to be the rise in refrigerant pressure as the heat pump comes on for longer. The unusual result of the heat pump buffer tank warm up test may also point to a similar cause of pressure variations within the heat pump. The CO₂ transcritical heat pump is possibly designed to optimise electricity consumption by having the maximum efficiency at higher heat loads.

The strong dependence of COP on heating justifies the importance of the investigations carried out on heating control. This is because how the heating is controlled will affect the heat output behaviour of the heat pump and ultimately the seasonal COP.

The results of daily COPs also demonstrated the usefulness of the test platform as a 'black box' method of testing the operating performance of whole systems of air source heat pumps. The test platform has characterised a new and unique air source heat pump product and highlighted the uniqueness of the testing method. Effective heating control methods are developed that maybe used with other test platforms to fully characterise air source heat pumps including effect of weather.

Future works will focus on gathering more COP data using the test platform in various ways. This will include testing the heat pump by using the heating control of heating circuit 2 to fix the heating at certain levels; testing the heat pump with domestic hot water, solar preheat, auxiliary heaters and so on; and testing the heat pump with realistic heating demands generated by Simulink and radiator model. Future tests will also include gathering COPs for longer durations, from months to seasons to a year, and hence resulting in SPFs. More investigations will be needed to confirm explanation for the correlation between COP and heat load. Heat pump buffer tank warm up test will be repeated to see if result varies and seek further evidence for explanations for the dependency of COP on heat load. In following these steps the test platform will be developed into a fully automated test platform capable carrying out a range of useful tests on air source heat pumps with high reliability. In the investigatory process there may emerge ways of accelerating the longer duration tests, and these pathways will form part of the automated test platform.

References:

- [1] "Types of Heat Pumps", Internet:
<http://www.heatpumps.org.uk/TypesOfHeatPumpSystems.htm> [June, 2012].
- [2] Cantor, J., "Air Source Heat Pumps – Friend or Foe", AECB, 2011.
- [3] Barker, G., "Renewable Heat Incentive", Department of Energy and Climate Change, UK, 2011.
- [4] Fawcett, T., "The future role of heat pumps in the domestic sector", ECEEE 2011 Summer Study, Environmental Change Institute, University of Oxford, 2011.
- [5] DEFRA and DECC, "2010 Guidelines to Defra/DECC's GHG conversion factors for company reporting", AEA Technology for the Department of Energy and Climate Change and the Department for Environment, Food and Rural Affairs., London, 2010.
- [6] Spicer, S., "Heat pumps: Prospects for the UK industry", Environmental Change Institute, University of Oxford, 2010.
- [7] Spiers, J., Gross, R., et al., "Building a roadmap for heat: 2050 scenarios and heat delivery in the UK", London, 2010.
- [8] Ofgem, "Decision letter: Revision of typical domestic consumption values", [Online], Available: <http://www.ofgem.gov.uk>, Office of Gas and Electricity Markets, 2010.
- [9] Baker, W., "Off-gas consumers: Information on households without mains gas heating", Consumer Focus, 2011.
- [10] Committee on Climate Change, "The fourth climate budget: Reducing emissions through the 2020s", Committee on Climate Change, London, 2010.
- [11] Zottl, A., Nordman, R., et al., "Concept for evaluation of SPF: A defined methodology of calculation of the seasonal performance factor and a definition which devices of the system have to be included in this calculation", SEPAMO, 2011.
- [12] DECC, "Phase 2: Household Voucher Scheme", Internet:
http://www.decc.gov.uk/en/content/cms/meeting_energy/renewable_ener/premium_pay/rhpp_voucher/rhpp_voucher.aspx [August, 2012].
- [13] Carbon Trust, "Micro CHP Accelerator", Interim Report, Carbon Trust, 2007.
- [14] Savidis, A., "An introduction to installing and maintaining air source heat pumps", Narec, 2010.

[15] Energy Saving Trust, "Measurement of Domestic Hot Water Consumption in Dwellings", Energy Saving Trust, 2008.

[16] The Energy Saving Trust, "Getting Warmer: A Field Trial of Heat Pumps", The Energy Saving Trust, 2009.

[17] Roy, R., "The UK heat pump field trial: user experiences, behaviour & heat pump performance", University of Edinburgh symposium, The Open University, 2012.

[18] Huchtemann, K., Müller, D., "Evaluation of a field test with retro-fit heat pumps", Building and Environment, Elsevier, 53 (2007) 100-106.

[19] Tiljander, P., Axell, M., Stignor, C. H., "Field measurements to demonstrate new technology for heat pump systems", SP Report 2011, Energy, SP Technical Research Institute of Sweden, 2011.

[20] Staffell, I., "A Review of Domestic Heat Pump Coefficient of Performance", 2009.

[21] Yamamoto, T., "System Efficiency Analysis of a CO₂ Heat Pump Water Heater by Numerical Simulation Using Thermal Network Models", Matsushita Electric Industrial Co.,Ltd., 2007.

[22] Nagano, K., "Field test of ground-coupled heat pump for cold climate region of Japan: First and Second demonstration project heat pump system in the Low Energy House", Hokkaido University, Japan, 2008.

[23] ISO, "ISO 9459-5: System Performance Characterization by Means of Whole System Tests and Computer Simulation", ISO, 1997.

[24] BSi, "Heating systems in buildings – Method for calculation of system energy requirements and system efficiencies – Part 4-2: Space heating generation systems, heat pump systems", British Standards, 2008.

[25] CEN, "EN 14511-2: Air conditioners, liquid chilling packages and heat pumps with electrically driven compressors for space heating and cooling – Part 2: Test conditions", CEN, 2004.

[26] Morrison, G. L., Anderson, T., Behnia, M., "Seasonal Performance Rating of Heat Pump Water Heaters", Solar Energy, Elsevier, 76 (2004) 147-152.

[27] Hawlader, M. N. A., Chou, S. K., Jahangeer, J. A., et al., "Solar-assisted heat pump dryer and water heater", Applied Energy, Elsevier, 74 (2003) 185-193.

[28] Zhang, J., Wang, R. Z., Wu, J. Y., "System optimization and experimental research on air source heat pump water heater", Applied Thermal Engineering, Elsevier, 27 (2007) 1029-1035.

- [29] Anderson, T. N., Morrison, G. L., "Effect of load pattern on solar-boosted heat pump water heater performance", *Solar Energy*, Elsevier, 81 (2007) 1386-1395.
- [30] Xu, G., Zhang, X., Deng, S., "A simulation study on the operating performance of a solar-air source heat pump water heater", *Applied Thermal Engineering*, Elsevier, 26 (2006) 1257-1265.
- [31] EST, DECC, et al., "Heat Emitter Guide for Domestic Heat Pumps", EST, DECC, et al.
- [32] Danfoss, "Transcritical Refrigeration Systems with Carbon Dioxide (CO₂): How to design and operate a small-capacity (< 10kW) transcritical CO₂ system", Refrigeration and Air Conditioning Division, Danfoss, 2008.
- [33] Qureshi, T. Q., Tassou, S. A., "Variable speed capacity control in refrigeration systems", *Applied Thermal Engineering*, Pergamon, Vol. 16, No. 2, pp 103-113, 1996.
- [34] Cohen, R., Hamilton, J. F., and Pearson, J. T., "Possible energy conservation through the use of variable-capacity Compressor", *Proc. Purdue Compressor Technology Conf.*, Purdue, USA, 1974, pp. 50-54.
- [35] Lida, K., Yamamoto, T., Kuroda, T. and Hibi, H., "Development of an energy-saving-oriented variable-capacity system heat-pump", *ASHRAE Trans.*, 88 (1982) 441-449.
- [36] Tassou, S. A., Marquand, C. J. and Wilson, D. R., "Comparison of the performance of capacity-controlled and conventional-controlled heat-pumps", *Appl. Energy*, 14 (1988) 241-256.
- [37] Omega Engineering, "omegaWeb Technical Reference", Internet: <http://www.omega.com/techref/> [June, 2012].
- [38] Myhren, J. A., Holmberg, S., "Design considerations with ventilation-radiators: Comparisons for traditional two panel radiators", *Energy and Buildings*, Elsevier, 41 (2009) 92-100.
- [39] Bradley, T., "A Simulink house model", Narec, 2010.
- [40] Mullin, T., Peixinho, J., "Transition to Turbulence in Pipe Flow", *Journal of Low Temperature Physics*, 145 (2006) 75-88.
- [41] Tong, P. and Du, Y. B., "Turbulent thermal convection in a cell with ordered rough boundaries", *J. Fluid Mech.*, 407 (2000) 57-84.
- [42] Moses, E., Zocchi, G., Libchaber, A., "An experimental study of laminar plumes", *J. Fluid Mech.*, Cambridge University Press, 251 (1993) 581-601.

[43] Wang, F., Wang, F., Fan, X., Lian, Z., “Experimental study on an inverter heat pump with HFC125 operating near the refrigerant critical point”, *Applied Thermal Engineering*, Elsevier, 39 (2012) 1-7.